Tikrit Journal of Engineering Sciences

TJES Tikrit Journal of Engineering Sciences

Open Access

Article

A Review on Lanthanum-Nickel-Based Perovskite Catalysts for Catalytic Dry Reforming of Methane

Halah A. Ramadhan [1]*, Maha Al-Ali [2]

[1] Department of Chemical Engineering, College of Engineering, Tikrit University, Tikrit, Iraq.
[2] Department of Oil and Gas Refining, College of Petroleum Process Engineering, Tikrit University, Tikrit, Iraq.

Emails:
Halah A. Ramadhana: halah.a.ramadhan42116@st.tu.edu.iq, Maha Al-Ali: maha.al.ali@tu.edu.iq

Abstract:

Climate change and the depletion of fossil fuels are the main motives for hydrogen production. Hydrogen is considered a potential form of sustainable energy for daily energy use, and many processes, such as catalytic dry reforming of methane, can produce it. Catalytic dry reforming of methane is essential to hydrogen energy production, and many Ni-based catalysts are highly active in the reforming reaction but deactivate within hours due to carbon deposition and metal sintering. Among all the catalysts studied for catalytic dry reforming of methane, Lanthanum-Nickel-based perovskite catalysts have been considered particularly promising due to their good performance under reaction conditions. Different preparation methods for Lanthanum-Nickel-based perovskite catalysts can influence their surface area and porosity. Partial substitution of their cations also enhances catalytic activity and stability, while reducing coke formation. In addition, it enhances metal-support interactions, leading to smaller particle sizes, greater surface area, and improved crystallinity and dispersion. The support addition for this type of catalyst can produce an active perovskite catalyst with a high surface area and carbon resistance. As a result, this review provides a comprehensive overview of current developments and key future directions in Lanthanum-Nickel-based perovskite catalysts for the catalytic dry reforming of methane. The main components discuss catalyst synthesis methods, their structural characteristics, catalytic performance, mechanistic insights, and strategies to improve catalytic activity and stability. The effects of multiple parameters, including composition, morphology, and surface characteristics, on catalytic performance are critically assessed. In addition, challenges and future directions in the design and application of Lanthanum-Nickel-based perovskite catalysts for CDRM are outlined to provide a comprehensive overview and guidance for researchers and engineers working in catalysis and renewable energy.

Keywords:

Perovskite catalyst; lanthanum-nickel catalysts; methane dry reforming; partial substitution.

Highlights:

- La-Ni-based perovskite catalysts show promising performance for CDRM.
- Preparation with solution-based methods gives better performance for La-Ni-based perovskites than preparation with solid-based methods.
- Perovskite dispersing on certain supports, like (MCM-41, SBA-15, and MCF), leads to smaller perovskite particles and, thus, higher surface area.
- Partial substitution of B-site cations has more difficulty than that of A-site cations.

Citation:

Ramadhan HA, Al-Ali M. **A Review on Lanthanum-Nickel-Based Perovskite Catalysts for Catalytic Dry Reforming of Methane**. *Tikrit Journal of Engineering Sciences* 2026; **33**(1): 2294.

Article History:

Received:	30	Jul.	2024
Received in revised form:	06	Sep.	2024
Accepted:	05	Jan.	2025
Final Proofreading:	15	Mar.	2026
Available online:	26	Apr.	2026

https://doi.org/10.25130/tjes.33.1.5

Corresponding Author*:

Halah A. Ramadhan
Department of Chemical Engineering, College of Engineering, Tikrit University, Tikrit, Iraq.
Email: halah.a.ramadhan42116@st.tu.edu.iq

© This Is an Open Access Article Under the cc by License. http://creativecommons.org/licenses/by/4.0/
©All rights reserved to Tikrit Journal of Engineering Sciences

1.INTRODUCTION

Global population growth and industrialization can raise energy demand [1, 2]. For the past few centuries, humans have primarily relied on fossil fuels. The daily consumption of fossil fuels has resulted in significant amounts of methane [3] and carbon dioxide [4, 5], both of which are considered greenhouse gases (GHGs). These gases harm the global environment and ecology. Methane (CH_4), a significant component of shale and natural gas, has a more noticeable warming effect than CO_2, up to 120 times higher [3]. The energy outlook of consumption in 12 years, from 2012 to 2023, of fossil fuels such as oil, natural gas, and coal, which are considered non-renewable energy sources, is evaluated as shown in Fig. 1. Oil had the highest rate of consumption among coal and natural gas (NG) [6-8]. Global energy consumption in 2018 was approximately 13,864 million tons of oil equivalent and is anticipated to reach 20,805 million tons of oil equivalent in 2040 [9]. The release of greenhouse gases from burning fossil fuels caused natural disasters, unexpected global surface temperature differences, animal extinction, blizzards, floods, and droughts that have received great attention this decade [10, 11].

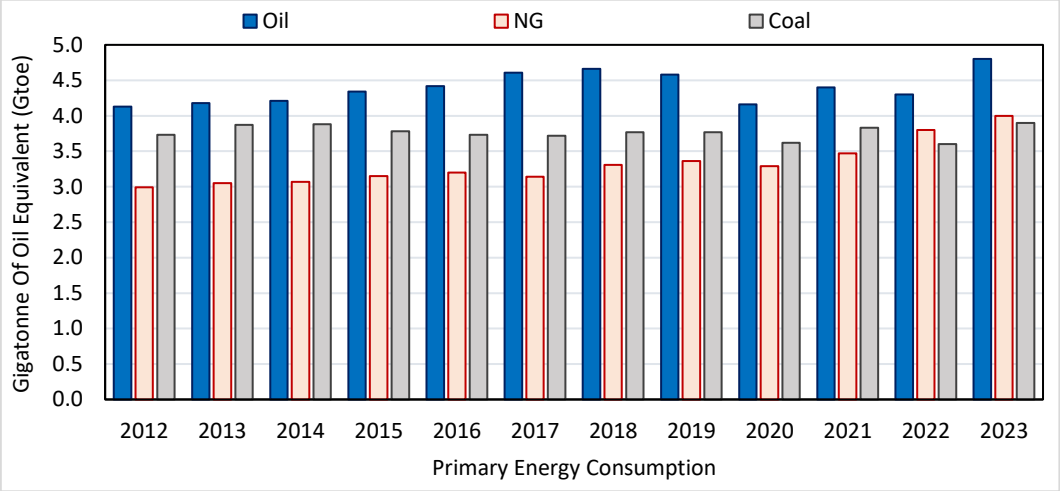

Fig. 1 Primary Energy Consumption in 12 Years Around the World [6-8].

Given the escalating demand for energy and the diminishing supply of fossil fuels, coupled with the imperative to protect the environment, exploring alternative energy sources has become crucial. Efforts should be made to investigate more advanced technologies and approaches for effectively utilizing natural gas and other byproducts of fossil fuels [12]. Synthesis gas, also known as syngas, is a versatile feedstock with extensive applications in the chemical industry. It serves as the primary component in producing liquid energy carriers and valuable chemicals. One environmentally friendly method for producing syngas is the catalytic dry reforming of methane (CDRM) [13, 14], as shown in Eq. (1) [15].

$$(\mathbf{CDRM}):\ \mathbf{CH_4 + CO_2 \rightarrow 2CO + 2H_2} \qquad \Delta H^0{}_{\mathbf{298k}} = \mathbf{247\ kJ/mol}\ \ (1)$$

CDRM is a chemical process that converts carbon dioxide and methane, known as the world's largest source of greenhouse gases (GHG), to the synthesis gas hydrogen and carbon monoxide, with an H_2/CO molar ratio approximately equal to one [16]. Employing abundant resources, such as methane, the primary component of natural gas, which is often referred to as a transition fuel for converting from fossil fuels like oil and coal to renewable energy, is one of the reasons the CDRM process is essential [17]. Furthermore, CO_2 is the most common greenhouse gas and a primary cause of global warming [18-21]. CDRM provides a method for transforming greenhouse gases into valuable chemical feedstocks by using readily available methane and CO_2 to produce hydrogen and syngas [22]. Since hydrogen is expected to be critical for reducing greenhouse gas emissions in industries, power plants, and transportation, its production is essential to the worldwide energy transition [23]. CDRM uses CO_2 and CH_4 as feedstocks, eliminating the need for additional carbon sources and producing hydrogen with a lower environmental impact than other technologies, such as methane steam reforming, which emits considerable CO_2 [24]. Using CO_2 as a reactant to generate valuable products (hydrogen, syngas) enables CDRM to efficiently recycle CO_2 and reduce the accumulation of GHGs in the environment [25]. Transforming excess CO_2 into energy or chemicals with higher value, thus supporting an adaptive carbon economy [26, 27]. CDRM is therefore a crucial procedure for reducing total carbon emissions worldwide [28]. Syngas generated by the CDRM process can be converted into chemicals (e.g., methanol, ammonia) [28] and fuels in liquid form (e.g., synthetic propane or diesel) [22]. In recent

years, there has been a focus on using such products as an energy transporter to connect renewable energy sources to demand regions worldwide [29]. CDRM-generated syngas from methane and CO_2 can help create more environmentally friendly fuel options. In addition, syngas can be used to generate electricity in gas turbines or fuel cells, providing another form of sustainable energy [30]. To conclude, CDRM promotes sustainable natural gas use, reduces CO_2 emissions, and generates valuable hydrogen and syngas. It supports the global energy transition by promoting environmentally friendly energy systems, reducing the carbon impact of fossil fuels, and advancing alternative energy sources such as hydrogen. In the CDRM process, the catalyst plays a crucial role, modifying reaction rates and increasing syngas production without consuming it. Catalysts reduce the activation energy (EA), making it easier to reach the conversion state [31]. The CDRM is highly endothermic; therefore, high temperatures are required to achieve the desired conversion levels. This causes particle sintering and/or coking, finally leading to catalyst deactivation. As a result, employing the appropriate catalyst to mitigate these problems is highly desirable [32]. Numerous catalytic materials have been designed for the CDRM process. Many precious metals, including Pt, Pd, Rh, Ru, and Ir, as well as their alloys, have outstanding stability, high catalytic activity, and low carbon deposition [33]. Noble metal catalysts are very active and stable in this process [34], but they have some limitations for use in CDRM processes, such as their high cost, which makes them unsuitable for large-scale industrial applications [34]. Also, their restricted availability and use in commercial applications will be unsustainable in the future; hence, their use will be challenging at a large industrial scale [35]. In addition, they exhibit high-temperature sensitivity: while noble metals typically remain stable at high temperatures, they can undergo sintering, reducing surface area and catalytic efficiency. Besides, the noble metals can aggregate at high temperatures, resulting in reduced surface area and catalytic efficiency [36]. Noble metals are often supported on or reinforced by support materials such as Al_2O_3 or SiO_2 [37]; however, these supports can potentially deactivate or undergo phase transitions at CDRM reaction conditions [38]. The interaction between the metal and the support can affect the catalyst's long-term stability, and poor selection can lower efficiency [39]. Although noble metal catalysts have excellent catalytic activity and selectivity, they are not as suitable for general application in CDRM due to their high cost, susceptibility to deactivation, and other drawbacks [40]. To address those challenges and make CDRM a more profitable process, other catalyst designs or approaches, such as the use of base-metal catalysts or the development of stronger supports, are being investigated [41]. Nickel-based catalysts are the most effective for CDRM due to their high activity, abundant deposits, and low cost. Ni-based catalysts typically experience significant deactivation [42]. The biggest challenge in the CDRM process is catalyst deactivation due to carbon deposition on the catalyst surface [22]. These carbon deposits form during the reaction and may block active sites, reducing the catalyst's capacity to sustain the process [43]. In addition, poisoning by sulfur present in natural gas or CO_2 feedstocks can deactivate the catalyst and significantly reduce activity [44]. This is a major concern for many CDRM catalysts, as they are sensitive to poisons and require complex purification steps [45]. As a result, deactivation reduces catalyst life, requiring frequent regeneration or replacement [46]. Thus, this condition requires the development of Ni-based catalysts with enhanced activity and stability. This can be achieved by placing the active metal within a well-defined structure, such as a perovskite-type oxide with the general formula ABO_3. Fig. 2 shows the ABO_3 structure, which is arranged in a cubic lattice, with a single B-ion at the center and A-cations at the corners. Each oxygen atom is shared by the next unit cells at the face sites. A-site cations are generally substantially bigger than B-site cations, and this size variation significantly impacts the material's characteristics [47]. This condition needs the development of Ni-based catalysts with enhanced activity and stability. This can be achieved by placing the active metal within a well-defined structure, such as a perovskite-type oxide with the general formula ABO_3. Fig. 2 shows the ABO_3 structure [47], where A is often alkaline-earth, rare-earth, or other large ions, while B sites are occupied with transition-metal cations [48].

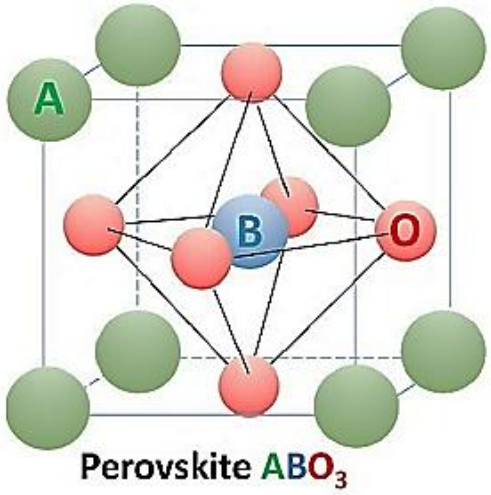

Fig. 2 The Perovskite Structure, where (A) Represents Alkaline-Earth, Rare-Earth, or other Large Ions, while (B) Transition-Metal Cations [47].

After the reduction process, this structure yields very small metal particles (on the nanometer scale) that are highly dispersed throughout the solid matrix, thereby favoring carbon-free operation while increasing catalytic activity and stability [49]. The B-site is the active site in perovskite oxide, whereas the A-site metal affects the perovskite's stability. The appropriate interaction between A and B-site metals improves catalytic activity [50]. There are many types of ABO_3 perovskite catalysts; among them, $LaNiO_3$ and its derivatives are most widely used in the CDRM reaction due to their unique properties. La-Ni-based perovskites are substantially more resistant to carbon deposition than common nickel-based catalysts [51]. The perovskite structure can better resist the creation of carbon deposits, allowing the catalyst to sustain its activity over time. This is critical for increasing the lifetime and economic feasibility of the CDRM process [52]. La-Ni perovskites have greater catalytic activity in CDRM processes, activating both CH_4 and CO_2 gases more effectively. Nickel promotes CH_4 activation, while lanthanum assists in activating CO_2. This behavior increases hydrogen output and syngas generation while improving selectivity and activity [53]. The perovskite structure of La-Ni-perovskite catalysts provides excellent thermal stability and, consequently, excellent thermal properties [54]. This stability decreases the likelihood of metal sintering, a major problem with conventional catalysts that reduces their effectiveness at high temperatures [55]. Also, these oxides have better resistance to contaminants such as sulfur in natural gas feedstocks, which can cause poisoning problems. The catalyst's durability is further increased, requiring less regeneration or purification [56]. An exciting characteristic of these oxides is their ability to enhance catalytic activity by partially substituting the A-site and/or B-site, with little change to their overall structure [57]. Many types of CDRM catalysts have been reported in the literature, but few papers have reviewed the use of perovskite-type oxide catalysts in the catalytic dry reforming of methane. Therefore, we wrote this review to provide researchers with a comprehensive description of perovskites and related materials. In this review, we focused on La-Ni-based perovskite catalysts, and we presented the fundamentals and characteristics of these catalysts, synthesis methods, catalytic performance, factors affecting the catalytic activity, such as the possibility of partial substitution of its cations and support addition, and challenges facing this kind of catalyst in the catalytic dry reforming of methane. Lastly, the conclusion from this review is presented. This review aims to comprehensively examine La-Ni-based perovskite catalysts, focusing on identifying optimal conditions for their performance. The study explores the most effective preparation methods and investigates the potential advantages of introducing a third element to enhance perovskite activity, as well as suitable supporting materials to achieve better performance. Moreover, the review seeks to develop strategies to address the long-term challenge of efficiency weakening and to propose future solutions.

2.PEROVSKITE CATALYSTS: FUNDAMENTALS AND CHARACTERISTICS

The main challenge to implementing CDRM in industry is the lack of commercial catalysts that can operate at high temperatures up to 1000 ℃, required for CH4 and CO2 activation, without suffering catalytic deactivation due to carbon deposition [58]. Perovskite-type oxides have the potential to serve as precursors for catalysts, enabling the synthesis of stable, highly active transition-metal catalysts supported by lanthanide oxides. Several investigations have shown that $LaNiO_3$-derived catalysts exhibit improved catalytic performance when employed during CDRM compared to other materials [59]. In recent years, there has been significant interest in perovskite catalysts due to their strong Lewis basicity, which can facilitate various catalytic reactions [60]. Several types of perovskites have already been utilized as catalysts for the CDRM process. For example, Ahmad et al. [61] synthesized $BaNiO_3$ by the co-precipitation method and used it to produce synthesis gas via the CDRM process. The catalyst remained active and stable for 24 hours on stream, as the Ni/BaO catalyst formed under hydrogen reduction is considered the active phase. The reduction of $BaNiO_3$ catalysts led to higher CO_2 conversion than CH_4 due to the reverse water-gas shift reaction (RWGS). However, no deactivation was observed in the stream after 5 or 24 hours [61]. In another study by Ahmad et al. [62], they prepared two perovskite structures, $SrNiO_3$ and $CeNiO_3$, and compared their performance in the CDRM reaction. $CeNiO_3$ showed superior specific surface area, pore volume, number of reducible species, and nickel dispersion. The catalytic activity data showed that $CeNiO_3$ had higher conversion rates for CH_4 (54.3%) and CO_2 (64.8%) than $SrNiO_3$, which had 22% CH_4 conversion and 34.7% CO_2 conversion. The stability analysis indicated that both catalysts ($SrNiO_3$ and $CeNiO_3$) deactivated due to carbon formation, with $SrNiO_3$ exhibiting greater deactivation than $CeNiO_3$ [62]. Osazuwa et al. [63] synthesized a $SmCoO_3$ perovskite catalyst via the sol-gel citrate method and used it to generate syngas (H_2 and CO) via the CDRM process for the first time. They also studied the effect of $SmCoO_3$ reduction by H_2 and found that, compared to the unreduced catalyst, the reduced catalyst showed no notable difference

in the conversions of CH_4 and CO_2 after 4 hr of reaction. The catalytic activity resulted in a maximum conversion of 93% for both reactants (CH_4 and CO_2), and the syngas had maximum yields of 67% for H_2 and 65% for CO [63]. Johansson et al. [64] studied the characterization of $LaRhO_3$ perovskite catalyst for the CDRM process. They aimed to investigate the structural modifications of $LaRhO_3$ perovskite induced by redox processes and to analyze its catalytic performance in promoting the CDRM reaction under relevant conditions. The XRD results indicated that pattern of the calcined $LaRhO_3$ perovskites showed the presence of highly crystalline $LaRhO_3$ and La_2O_3 phases and the H_2-TPR analysis reveals a wide peak with a peak at 448℃, indicating the steady reduction of Rh^{3+} to Rh^o, and this matches CH_4-TPR data, which indicated a broad peak with CO, CO_2, and H_2 maximum generation at)455-460)℃ [64]. An interesting work on synthesizing "$LnFe_{0.7}Ni_{0.3}O_{3-\delta}$" perovskite was reported by Kapokova et al. [65]. They prepared $LnFe_{0.7}Ni_{0.3}O_{3-\delta}$ (Ln = La, Pr, Sm) perovskites by the pechini method and used them as catalysts for the CDRM reaction. They observed that these perovskites transformed into Ni-Fe alloy composites, with LnOx directly attached to Ln-Fe-O perovskite particles. The Ln type affected the Fe content in the alloy particles and oxygen mobility. The active samples obtained due to Ni-Fe formation, which were released from the perovskite lattice and stabilized on the perovskite surface $PrFe_{0.7}Ni_{0.3}O_{3-\delta}$, showed the highest activity and stability since Ni-Fe alloy was formed and the redox properties [65]. More studies on the use of ABO_3 were conducted by several researchers, for instance, Gallego et al. [66]. The authors prepared $LaNiO_3$ and La_2NiO_4 perovskites using the self-combustion method and used them as catalyst precursors for the CDRM reaction. They got good catalytic performance toward CH_4 and CO_2 conversions with good coke resistance. La_2NiO_4 conversions were higher than $LaNiO_3$ after reduction treatment due to smaller nickel particle formation (7 nm) [66]. In another study reported by Choudhary et al. [67], a $NdCoO_3$ perovskite-type oxide catalyst was prepared, and its catalytic performance was compared with that of NiMgOx, CoOx–Y_2O_3, CoOx–ZrO_2, CoCeOx, and (Rh or Ru)/Al_2O_3 catalysts. $NdCoO_3$ exhibited high carbon resistance at several operating conditions, high catalytic activity, and selectivity with 92.3% CH_4 conversion and 95.5% selectivity at a high space velocity of about 20,000 $cm^3.g^{-1}.h^{-1}$. The high carbon resistance was attributed to strong metal-support interactions between Co and Nd_2O_3, which increased the support's basicity [67]. Another study was conducted by Batiot-Dupeyrat et al. [68] to prepare $LaNiO_3$ by the auto-ignition method and to employ it in the CDRM reaction. The catalyst showed high activity and stability, as well as a high resistance to carbon formation, due to the presence of Ni^o and $La_2O_2CO_3$ phases [68]. The literature indicates that perovskite oxides are the most commonly used catalysts for the CDRM reaction due to their unique properties and robust performance under severe reaction conditions. Among these many types of perovskite catalysts, La-Ni-containing perovskite oxides are the most used catalysts in CDRM studies due to their excellent catalytic activity in the CDRM process. La-Ni-based perovskites have a special crystal structure that allows the dispersion of active nickel sites, hence increasing catalytic activity [51]. In more detail, Ni sites promote C-H bond activation, whereas La_2O_3 combines with CO_2 to create $La_2O_2CO_3$, resulting in an active Ni-$La_2O_2CO_3$ interface [69]. In which the Lanthanum stabilizes the perovskite structure and promotes Ni particle dispersion. This provides for a higher number of active sites in the catalytic reaction [70]. The incorporation of rare-earth elements or alkali metals into the $LaNiO_3$ structure has been observed to mitigate carbon deposition. In contrast, adding a second metal, such as Mn, Fe, Cu, or Al, to the metallic particles reduces the Ni concentration, thereby inhibiting sintering [71]. $LaNiO_3$ undergoes complete decomposition upon reduction, forming Ni and La_2O_3. The resulting Ni particles have a size range of approximately 2-50 nm, and they are uniformly distributed on the La_2O_3 support. A robust metal-support interaction accompanies this distribution. Moreover, the reaction ($La_2O_3+CO_2 \rightarrow La_2O_2CO_3$) enhances the activity of the lattice oxygen and facilitates the removal of carbon species adsorbed on the Ni surface due to $La_2O_2CO_3$ formation. This review will focus on $LaNiO_3$ and its derivatives, which exhibit robust catalytic reforming properties. Table 1 summarizes a selection of perovskite-type oxides recognized for their notable catalytic capabilities, including the amount of carbon deposition, surface area, conversion rates, and the operating conditions applied.

Table 1 Summary of Perovskite Catalysts Used for CDRM Reaction:

Catalyst	Carbon deposits	Surface area (m^2/g)	$\%CH_4$	$\%CO_2$	Operating conditions	Ref.
$GdCoO_3$ $((NH_4)_2CO_3)$	_	6.9	97	99	T= 1173 K CO_2:CH_4 =1	[72]
$GdCoO_3$ $(NaOH)$	_	6.6	96	98		
$CeNi_{0.9}Zr_{0.1}O_3$	_	9.35	73	86	T= 800 °C	[73]
$CeNi_{0.9}Zr_{0.07}Y_{0.03}O_3$	_	1.27	61	75	GHSV= 42 $L.g^{-1}.h^{-1}$	
$CeNi_{0.9}Zr_{0.05}Y_{0.05}O_3$	_	1.62	73	85	CH_4:CO_2:N_2=3:3:1	
$CeNi_{0.9}Zr_{0.03}Y_{0.07}O_3$	_	1.85	87	90		
$CeNi_{0.9}Zr_{0.01}Y_{0.09}O_3$	_	2.66	90	91		
$CeNiO_3$	_	44.042	89	_	T= 700 °C	[74]
$CeCo_{0.2}Ni_{0.8}O_{3.066}$	_	38.764	55		CH_4:CO_2=1:2	
$CeCo_{0.6}Ni_{0.4}O_{3.2}$	_	37.125	27			
$CeCo_{0.8}Ni_{0.2}O_{3.266}$	_	36.610	21			
$LaAlO_3$	_	16	0	15	T= 800 °C	[75]
$LaAl_{0.98}Ru_{0.02}O_{3-\delta}$	_	4	86	100	GHSV= 48000 h^{-1}	
$LaAl_{0.98}Pt_{0.02}O_{3-\delta}$	_	8.6	60	100	CH_4:CO_2:N_2=1:1:8	
$LaAl_{0.98}Pd_{0.02}O_{3-\delta}$	_	8	65	80		
$GdFeO_3$	_	9.9	45	60	T= 950 °C	[76]
$GdMn_{0.2}Fe_{0.8}O_3$	_	7.7	22	58	GHSV = 1 $L.h^{-1}$	
$GdMn_{0.5}Fe_{0.5}O_3$	_	7.8	43	45	CH_4:CO_2 = 1:1	
$GdMn_{0.8}Fe_{0.2}O_3$	_	8.1	20	57		
$GdMnO_3$	_	8.5	30	28		
$LaCr_{0.95}Co_{0.05}O_{3-\delta}$	_	_	0	0	T=750 °C	[77]
$LaCr_{0.95}Rh_{0.05}O_{3-\delta}$	_	_	75	86	GHSV=4000 h^{-1}	
$LaCr_{0.95}Ir_{0.05}O_{3-\delta}$	_	_	81	82	CH_4:CO_2:N_2=1:1:2	
$GdFeO_3$	_	3	44.6	60.4	T= 950 °C	[78]
$GdFe_{0.8}Co_{0.2}O_3$	_	7.24	97.7	100	CH_4:CO_2=1:1	
$GdFe_{0.5}Co_{0.5}O_3$	_	7.4	84.2	96.2		
$GdFe_{0.2}Co_{0.8}O_3$	_	6.3	95.3	99.4		
$GdCoO_3$	_	_	96.1	99.5		
$BaZr_{0.8649}Rh_{0.1351}O_3$	0.0019 $g.g^{-1}$ cat.	11.7	99	98	T=850-1150 K	[79]
$BaZr_{0.8649}Ru_{0.1351}O_3$	0.0027 $g.g^{-1}$ cat.	12.8	96	92	CH_4:CO_2= 0.8; 1.0; 1.2;1.4	
$BaZr_{0.9272}Pt_{0.0728}O_3$	0.0094 $g.g^{-1}$ cat.	10.3	89	87	N_2 ($L.min^{-1}$)=0.3	
$SrTi_{0.92}Ru_{0.08}O_{3-\delta}$	_	13	91	95	T= 1073 K	[80]
$SrTi_{0.85}Ru_{0.15}O_{3-\delta}$	_	17	94	95.5	GHSV = 28800 h^{-1}	
$SrTi_{0.69}Ru_{0.31}O_{3-\delta}$	_	15	92	95	CH_4:CO_2:N_2= 1:1:1	
$Ca_{0.2}La_{0.8}Ni_{0.3}Al_{0.7}O_{2.9}$	_	3.5-9.5	96		T= 500-800 °C	[81]
$Ca_{0.5}La_{0.5}Ni_{0.3}Al_{0.7}O_{2.75}$	_	3.5-9.5	96		CH_4:CO_2:N_2 = 1:1:8	
$Ca_{0.8}La_{0.2}Ni_{0.3}Al_{0.7}O_2$	0.71%	3.5-9.5	96			
$Sr_{0.2}La_{0.8}Ni_{0.3}Al_{0.7}O_{2.9}$	8.31%	3.5-9.5	99	_		
$Sr_{0.5}La_{0.5}Ni_{0.3}Al_{0.7}O_{2.75}$	_	3.5-9.5	97	_		
$Sr_{0.8}La_{0.2}Ni_{0.3}Al_{0.7}O_{2.6}$	3.21%	3.5-9.5	98	_		

3.SYNTHESIS METHODS FOR La-Ni-BASED PEROVSKITE CATALYSTS

The physicochemical characteristics of the catalyst, such as its porosity and surface area, redox potential, reducibility, size and dispersion of active metals, oxygen vacancies, metal-support interactions, etc., all impact how effectively the catalyst works in the CDRM process. Several techniques, such as optimizing synthesis processes, can improve the physicochemical characteristics of catalysts [82]. Thus, the catalytic efficacy of methane reforming catalysts is significantly influenced by the synthesis process employed. Different catalyst preparation methods yield catalysts with distinct textural and structural properties, which in turn affect their behavior. Consequently, many methods, such as co-precipitation, spray pyrolysis, surfactant-assisted method, freeze-drying, and sol-gel techniques, have been developed to improve the specific surface area of perovskite-type oxide catalysts [83]. Solution-based methods of perovskite synthesis, such as co-precipitation, complexation, sol-gel, and freeze/spray drying, compared with solid-based synthesis methods, produce perovskite-type oxides that decompose at lower temperatures, have higher specific surface area, and exhibit lower grain dispersion [84]. Many researchers used different preparation methods for La-Ni-based perovskites. For instance, Omari et al. [85] prepared $LaNi_{1-x}Co_xO_3$ ($0 \le x \le 0.6$) oxides by the sol-gel method, and characterization results showed that the perovskite oxides were successfully synthesized, with pure crystalline phases obtained and uniform morphologies [85]. Another study used the hydrothermal method conducted by Ozbay et al. [86], which successfully prepared $LaNiO_3$ and $LaMnO_3$ perovskite catalysts by the hydrothermal method, due to the distinctive properties that this method provides for the prepared catalyst, such as crystallization, greater yields, a cleaner synthetic process, and shorter crystallization time compared with other conventional methods of preparation. Nevertheless, the characterization results indicated that the preparation method gave the desired crystalline phases with small crystal sizes and a surface area of up to 19 m^2/g [86]. Several studies were conducted using comparative preparation methods. Touahra et al. [87], for example, prepared $LaCuO_3$ and $LaCu_{0.53}Ni_{0.47}O_3$ and

studied the effect of preparation methods of perovskite oxides using the sol-gel citrate technique, whereas 5% NiO/$LaCuO_3$ using the impregnation method. The BET results revealed that the impregnated sample (5% NiO/$LaCuO_3$) exhibited a higher surface area than the sol-gel sample [87]. Sagar et al. [88] prepared $LaNi_xCe_{1-x}O_3$ ($0 \leq x \leq 1$) by the sol-gel method and compared their activity with that of samples prepared by the hydrothermal method. They found that the sol-gel method had advantages over the hydrothermal method in terms of higher surface area and higher activity, as shown in Fig. 3. The catalyst prepared by the sol-gel method exhibited a 95% CO_2 conversion rate, while the one prepared by the hydrothermal method was 87% after one hour of reaction, and the same for CH_4 conversion. As well as showing better coke resistance and Ni dispersion. The catalysts have higher surface areas, greater Ni dispersion, and are less prone to coking. $LaNi_{0.4}Ce_{0.6}O_3$ catalyst has the highest activity. It maintains reasonable stability during the reaction [88]. Chawla et al. [89] prepared $LaNiO_3$ and $LaCoO_3$ by sol-gel and co-precipitation methods. $LaNiO_3$ prepared by the two methods showed higher conversions than LaCoO3; this can be attributed to the smaller Ni particles, which provide abundant active sites on the catalyst surface, and to $LaCoO_3$'s lower reducibility. In addition, the results showed that $LaNiO_3$ prepared by the co-precipitation method had a higher conversion than that prepared by the sol-gel method [89]. Another important study was conducted by Pereniguez et al. [90] to synthesize $LaNiO_3$ samples using four preparation methods. These methods were hydrothermal (HT), combustion (CM), spray pyrolysis (SP), and spray pyrolysis-combustion (SPCM) methods. This study examined the physicochemical and catalytic properties of Ni/La_2O_3 catalysts prepared by reducing four $LaNiO_3$ samples and found that the physicochemical properties varied with the preparation method. A crystalline $LaNiO_3$ rhombohedral phase and a significant amount of amorphous NiO were observed in XAS and TPR measurements; the amount of NiO varied depending on the preparation technique. However, following oxidative treatment can reduce the NiO proportion. The lower amount of amorphous NiO phase resulted in a higher CDRM conversion, which made the Ni/La_2O_3 samples perform effectively during the CDRM process [90]. Rivas et al. [91] prepared a series of $LaNiO_3$ perovskite oxides and studied the effect of different preparation methods and nickel substitution with rhodium on $LaNiO_3$ performance in the CDRM reaction. They used sol-gel and co-precipitation methods for preparing the perovskites, the surface area for both catalysts obtained by the co-precipitation method was higher than those obtained by the sol-gel method, this difference proportional to crystal and grain sizes, large sizes result in smaller surface area. In addition the modification by Rh addition, resulted in improving the catalytic performance and this can be related to nickel dispersion and reduction enhancement [91]. As such, catalysts synthesized using various methods have varying Ni particle sizes, rates of Ni particle dispersion, and interactions between the Ni atoms and the support, thus exhibit different catalytic activity, sintering resistances, and performance stabilities [92].

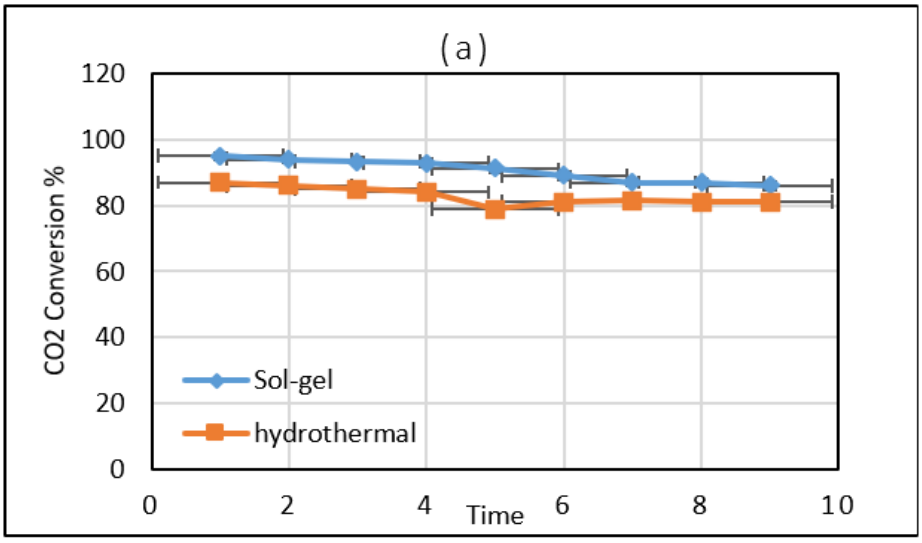

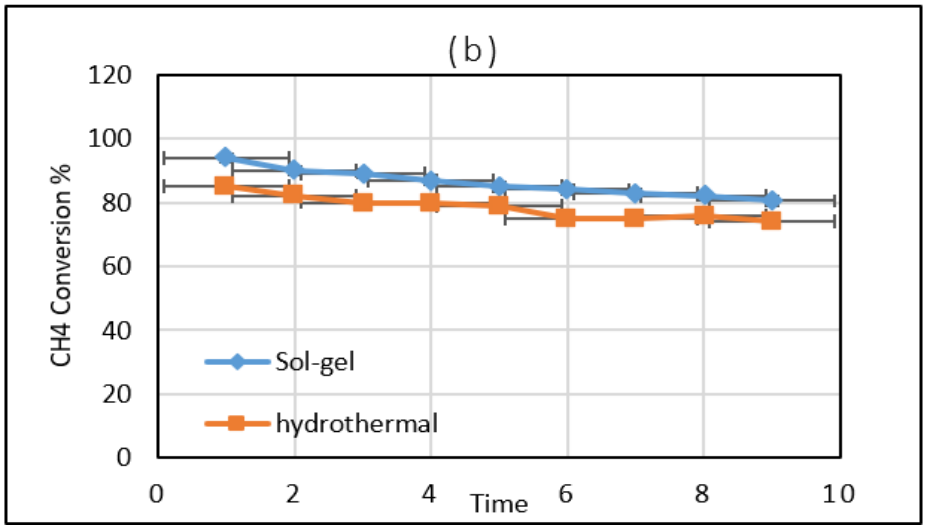

Fig. 3 Conversion Profiles of the $LaNi_{0.4}Ce_{0.6}O_3$ Prepared by Sol-Gel and Hydrothermal Methods, (a) CO_2 Conversion and (b) CH_4 Conversion [88].

Although these preparation methods are efficient, applying them has some limitations. For example, sol-gel is efficient for preparing La-Ni-based perovskite catalysts, but the process is complex. It involves many steps, such as gel production, aging, drying, and calcination, which can take a long time. In addition, controlling particle size can make it difficult to achieve uniformity, consequently affecting catalytic efficiency [93]. The same applies to the hydrothermal method, which improves the catalyst's performance [94]; however, it has certain drawbacks. The resulting catalysts have a low surface area, which may restrict both catalytic activity and profitability [51]. Also, the solid-phase crystallization and resultant catalytic characteristics can be strongly influenced by the form and structure of the parent nanoparticles created by hydrothermal synthesis [95]. While wet impregnation is easy and efficient for loading large amounts of metal, it often produces larger particles and less dispersion than other methods. According to literature [96], the citrate complex approach produced Ni particles that were one-third the size of those produced via impregnation. Additionally, impregnation may result in partial development of the required perovskite structure, potentially impacting the catalyst's performance [97]. The co-precipitation method has several drawbacks for producing La-Ni-based perovskite catalysts. Although it is capable of creating catalysts with large surface areas (33–44 m^2/g) [98], compared to other methods, the process may produce large particles. Co-precipitation favors the production of the $La(OH)_3$ phase, which is less beneficial for anti-coking [99]. For the other method, combustion, there are benefits and drawbacks to the process for creating La-Ni-based perovskite catalysts. In dry methane reforming, this method may yield highly dispersed nickel nanoparticles with superior anti-coking properties [99]. However, the fuel used and the heat released during combustion significantly affect the crystal structure and particle size of the resulting powders [100]. However, synthesis parameters, such as pH and the citric acid-to-metal cation ratio, can significantly affect the final physicochemical and catalytic properties [101]. In addition, although the spray pyrolysis method is a versatile technique, it has drawbacks for the production of perovskite catalysts for the dry reforming of methane. The method's efficacy depends on several variables. However, it can yield high-surface-area catalysts with enhanced shape and performance [102]. The precursor feed rate during spray pyrolysis also influences support properties, which in turn affect nickel dispersion and catalytic activity [103]. Several synthesis parameters affect the physicochemical properties and catalytic performance of perovskite catalysts (e.g., precursor stoichiometry, calcination temperature, oxygen content, and solvent type), and many studies have reported their effects on catalyst performance. For example, Sagar et al. [104] investigated the incorporation of Zr in the $LaNiO_3$ catalyst with different stoichiometric amounts ($LaNi_xZr_{1-x}O_3$: $0 \le x \le 1$). They found that at x = 0.2, the pyrochlore phase ($La_2Zr_2O_7$) was formed, and at x = 0.8, the pyrochlore phase disappeared as the Ni concentration increased, and the $LaNiO_3$ perovskite oxide phase formed. During reduction, the catalyst with a high x value (x = 0.8) produced well-dispersed Ni metal species supported by La_2O_3. The catalyst with x = 0.8 exhibited better performance than other $LaNi_xZr_{1-x}O_3$ catalysts in terms of CH_4 and CO_2 conversion efficiency, as well as higher surface area [104]. Jahangiri et al. [105] synthesized a series of Sm-doped $LaNiO_3$ perovskites using a modified citrate sol-gel method. They used different stoichiometric

amounts of La and Sm, and the samples were denoted as La1-xSmxNiOx-δ (x = 0, 0.1, 0.3, 0.5, 0.7, 0.9, and 1). According to the characterization results, the XRD patterns shown in Fig. 4 revealed that, as the Sm content increased, the intensities of the crystalline phase diffraction lines (La_2NiO_4 and NiO) increased. Also, TPR results, as shown in Fig. 5, proved that with increasing Sm content the surface area increased thereby improving the catalytic performance, in which the $LaNiO_3$ sample is reduced in two stages. The first reduction area appears at low temperatures (573-723 K), indicating the reduction of Ni^{3+} to Ni^{2+} and the formation of $La_2Ni_2O_5$. The second peak area appears above 723 K, indicating the reduction of Ni^{2+} to Ni^0 and the deposition of metal nickel on lanthanum oxide [105]. These results verified the catalytic nature of $LaNiO_3$ in CH_4 reforming, as reported by Rivas et al. [106] and Provendier et al. [107]. Another study reported by Gallego et al. [108] prepared $La_{1-x}A_xNiO_{3-\delta}$ (A = Pr, Ce) perovskites by the auto-combustion method with different stoichiometric ratios and investigated their performance as catalyst precursors in the CDRM reaction. The incorporation of Pr and Ce in the $LaNiO_3$ structure showed an increment in the surface area as well as the catalytic activity and stability, and a decrease in the carbon deposition [108]. As a result, varying the stoichiometric amounts can enhance the catalyst's properties and their performance. Lima and Assaf reported that varying the calcination temperature and studying its effect were also important [109]. The authors synthesized $LaNiO_3$, $LaNi_{1-x}Fe_xO_3$, and $LaNi_{1-x}Co_xO_3$ (x = 0.4 and 0.7) by precipitation and employed these materials for methane reforming. They investigated the effect of different calcination conditions (800 °C for 5 h, 900 °C for 5 h, 10 h, and 15 h). They showed that the ideal structure developed at calcination temperatures as low as 800 °C. However, with increasing calcination times and temperatures, the structure became slightly more crystalline and more similar to the standard phase. These results demonstrated that oxides with the required structure and significant features for application in heterogeneous catalysis could be produced by appropriately combining the preparation process with calcination conditions (time and temperature) [109].

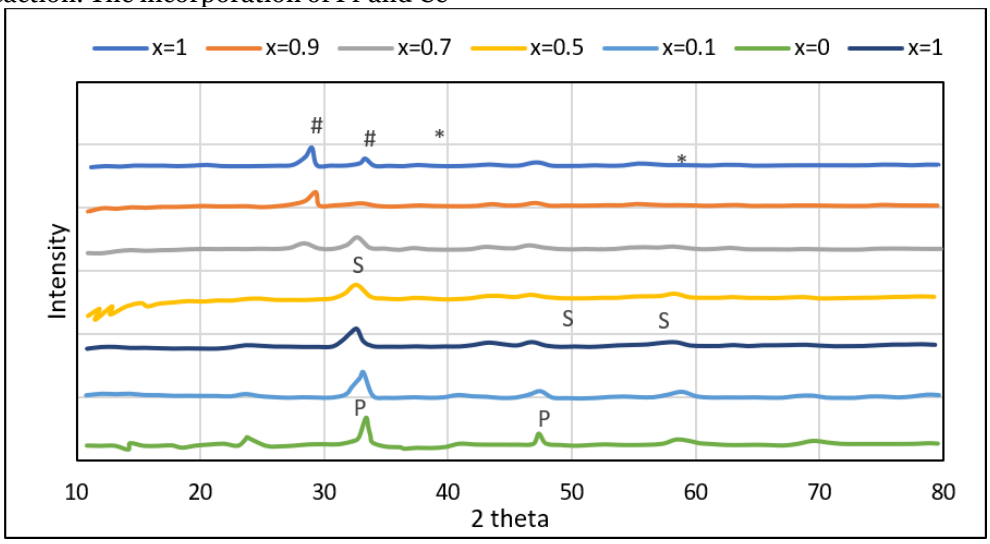

Fig. 4 XRD Patterns of $La_{1-x}Sm_xNiO_{3-\delta}$ Samples after Calcination at 800 °C. (Perovskite (P), Spinel (S), NiO (*), and Sm_2O_3 (#)) [105].

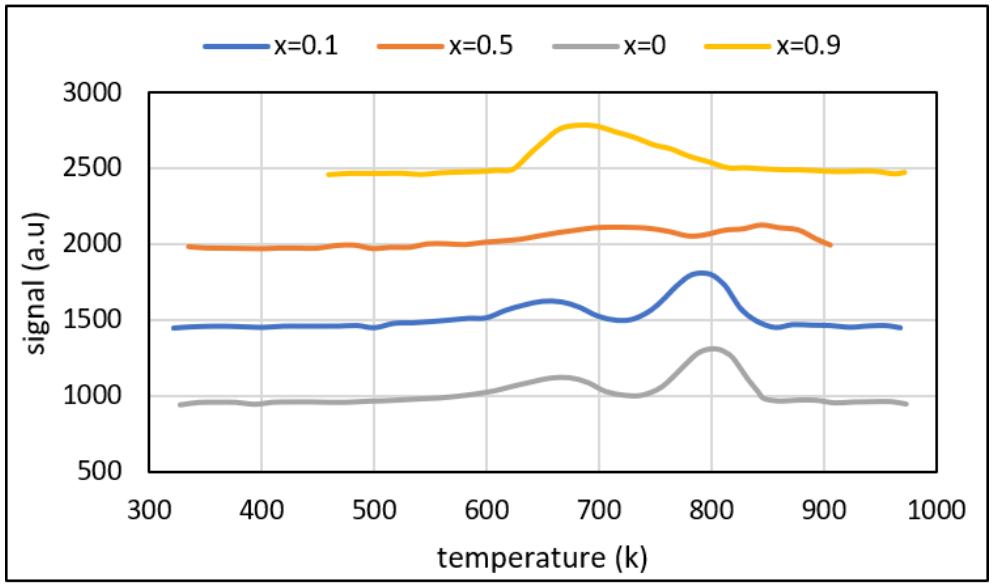

Fig. 5 TPR Profiles of Different $La_{1-x}Sm_xNiO_{3-\delta}$ Catalysts Calcined in Air at 800 ℃ [105]

Another preparation variable was investigated by Blasco et al. [110]. The authors studied the oxygen current flow during calcination to investigate the influence of oxygen content on the properties of LaNi1-xMnxO_3. The characterization showed that the crystal structure of the samples depended on the oxygen content, and that preparing mixed oxides with Ni^{+3} ions required strong oxidation conditions, high oxygen pressure, and low temperature. On the other hand, preparing the $LaMnO_3$ phase required an inert atmosphere. In this instance, the use of an oxidative atmosphere resulted in the production of non-stoichiometric $LaMnO_3$. Also, the Mn substitution affected cell volume; as Mn content increased, cell volume decreased [110]. The type of solvent used in the preparation procedures also has an effect on the textural properties of La-Ni-based perovskite catalysts. For example, Mousavi and Pour [111] synthesized $LaNiO_3$ and $LaNi_{0.5}Co_{0.5}O_3$ by the co-precipitation method using distilled water (W) and magnetized distilled water (MW). From the results they got, the amount of carbon deposited on the catalysts' surfaces was in this order: $LaNiO_3$ (W) >$LaNiO_3$ (MW) > $LaNiCoO_3$ (W) > $LaNiCoO_3$ (MW). Also, the surface area of the samples prepared with MW was lower. In addition, the XRD results indicated that the crystalline phases of NiO and La2O3 in the MW-prepared samples were lower than those in other samples [111]. Moradi et al. [112] prepared catalysts $LaNiO_3$/c-Al_2O_3 with 10, 15, 20, and 25 weight percent Ni, using a combination of the sol-gel method, with ethanol as a solvent and the addition of acetic acid (LNA-eth), as well as propionic acid as a solvent and an impregnation process (LNA-acid). They found that impregnating $LaNiO_3$ on a c-Al_2O_3 support with ethanol solvent resulted in significant Ni dispersion on the catalyst surface. They found that the 20LNA-eth catalyst, prepared by impregnation with ethanol as solvent, exhibited better catalytic activity for methane at all reaction temperatures and a higher H_2/CO ratio than the 20LNA-acid catalyst, prepared by sol-gel with propionic acid as solvent. On the other hand, the 20LNA-acid catalyst provided a higher CO_2 conversion than 20LNA-eth. This results can be atributed due to better dispersion of Ni on *c*-Al_2O_3 for 20LNA-eth thanoLNA-acid [112]. Another report was established by Moradi and Parvati [113]; the researchers developed $LaNi_xAl_{1-x}O_3$ (0.1<x<0.9) perovskite systems by the sol-gel method using propionic acid as solvent. Their catalysts showed good resistance to carbon deposition and strong interactions with the reactants. Also, they achieved good performance, with 98% methane conversion and 95% CO yield [113]. The literature indicates that the solvent type used in the preparation step can be a critical parameter for the desired perovskite. In summary, synthesis methods such as sol-gel, hydrothermal, and co-precipitation significantly affect the catalytic performance of La-Ni-based perovskite catalysts by controlling surface area and porosity, with high surface area and porosity providing a large number of active sites. The stoichiometry of perovskite compositions can also be controlled during preparation to achieve the desired stoichiometry and optimal performance. In addition, calcination temperature, oxygen content, and solvent type can all be controlled by choosing the appropriate synthesis method for La-Ni-based perovskite catalysts.

4.CATALYTIC PERFORMANCE OF La-Ni BASED PEROVSKITE CATALYSTS IN CDRM:

Nowadays, there is significant interest in catalytic precursors with perovskite structures, particularly La-Ni-based perovskite catalysts. Unlike other perovskite-type oxides,

lanthanum nickelates exhibit high reducibility and oxygen storage/release capacity [114]. Also, during the reforming reaction, CO_2 interacts with La_2O_3 to produce $La_2O_2CO_3$. The oxycarbonate interacts with carbon-containing molecules at the nickel contact, producing carbon monoxide. In which $La_2O_2CO_3$ is primarily responsible for the stable and carbon-resistant properties, hence good catalytic performance [115]. As a result, using the $LaNiO_3$ structure improves the activity and long-term stability of the Ni-based catalysts [116, 117]. La-Ni-based perovskite catalyst's surface adsorbs CH_4 and CO_2, in which the Ni site activates the (C-H) bond in CH4, leading to the formation of CO and H_2, and the dissociation of CO_2 forms CO and oxygen [69]. In more detail, La-Ni-perovskite catalysts activate CH_4 and CO_2 via the nickel redox cycle, in which Ni is oxidized and reduced during the reaction, enabling efficient charge transfer and reaction promotion. While the La component stabilizes oxygen vacancies to enhance transport and catalyst stability, the vacancies maintain a constant redox activity of Ni^{2+}/Ni^{3+}. The cooperation between metal and oxide components promotes high catalytic efficiency in producing syngas (CO and H_2) [118]. Several researchers studied La-Ni-based catalysts due to their high activity and stability at high reaction temperatures. For example, Da Silva et al. [119] synthesized $LaNiO_3$ and evaluated its activity and stability in oxy-CO_2 reforming of methane. The catalyst showed good catalytic activity with low carbon deposition [119]. Another study reported by Li et al. [120] presented the formation of a $LaNiO_3$ phase on a Ni/La_2O_3 catalyst. They showed high catalytic activity with 50 hr of time-on-stream stability. The prepared catalyst exhibited a high surface area and a large pore volume, providing more catalytically active Ni sites for reactants and thereby increasing reforming activity. Carbon deposition and Ni metal sintering were substantially decreased on the mesoporous Ni/La_2O_3 catalyst with La_2O_3-m support [120]. Oliveira et al. [121] synthesized the $LaNiO_3$ catalyst via a one-step method and evaluated its performance in the CDRM reaction. The catalyst showed good catalytic stability and high CH_4 and CO_2 conversions to about 95% and 90% at 800 ℃, respectively, with good levels of H_2 and CO yields, as shown in Fig. 6. The catalysts showed high stability for a long time at different temperatures and good products yield percentages, as well as good resistance to carbon formation due to the presence of the $La_2O_2CO_3$ [121]. Dacquin et al. [122] used SBA-15 as a support for $LaNiO_3$ to prepare 20LaNi-SBA(10) nanocomposite, which exhibited high CH_4 and CO_2 conversions at about 75% and 85%, respectively. They showed that the catalyst remained stable during 48 hr of reaction, and the product syngas CO and H_2 also remained stable with a CO/H_2 ratio of less than 1. They also observed low-carbon deposition on the catalyst surface due to the presence of LaOx species, which can reduce carbon poisoning and the restriction effect of the mesoporous SBA-15 material, thereby reducing metallic particle sintering [122]. De Araujo et al. [123] prepared perovskite-type oxides $LaRu_xNi_{1-x}O_3$ ($0.0 < x < 1.0$) and tested their catalytic performance in the CDRM process. The results indicated that the $LaNiO_3$ catalyst showed high activity and stability for 14 hr time on stream, as well as, the selectivity, and were stable for the 14 hr as shown in Fig. 7. The catalytic activity curves indicate that all catalysts were active in methane dry reforming, but they had various performances. The $LaNiO_3$ demonstrated significant activity and stability. However, when partly modified catalysts were activated under identical conditions (at 750 ℃ for 3 h), no activity was found. Increasing the activation temperature to 800 ℃ activated the catalysts, resulting in a greater than 50% rise in conversion during the first 4 hours of the reaction followed by stable values. The rapid increase in conversion suggests that active sites formed during the process rather than during activation with hydrogen. Because the ruthenium had stronger Ru–O–La bond strength made the metal reduction more difficult in comparison to the Ni–O–La bond. Anothor advantageous of this catalysts, the formed coke was filamentous that is not harmful to the catalysts [123]. A study reported by Lima et al. [124] aimed to investigate the addition of cerium at the A-site of $LaNiO_3$. They prepared $La_{1-x}Ce_xNiO_3$ (x = 0, 0.05, 0.4, and 0.7) by the citrate method and used them in the CDRM reaction. The activity results showed an increase in catalytic activity and stability, which exhibited a stable performance during (15-20) hr time on stream. Also, they observed an increase in the inhibition of coke formation. This good performance was due to the reverse water-gas shift (RWGS) reaction, which was enhanced by catalyst surface enrichment with Ce [124]. Batiot-Dupeyrat et al. [68] prepared a $LaNiO_3$ catalyst using the auto-ignition method. The catalyst demonstrated high activity, stability, and resistance to carbon deposition during the CDRM reaction. Due to the formation of $La_2O_2CO_3$, which can inhibit the carbon deposits in the nickel phase. The CH_4 and CO_2 conversions were 90% and 87%, respectively, with a H_2/CO molar ratio of 1, and the catalyst remained stable for more than 100 hr [68]. Other nickel and lanthanum-based catalysts showed lower catalytic performance in comparison to La-Ni-based perovskite catalysts. For example, Dhillon et al. [125] synthesized $NiFe/TiO_2$ and investigated its catalytic performance in the CDRM reaction. The catalyst exhibited unstable performance, with conversion decreasing over time on

stream, and low CH4 and CO2 conversions of 34% and 37%, respectively, after 6 h on stream. The decrease in conversions may be related to the Fe metal, despite its ability to reduce carbon deposition [125]. Gonzalez-Delacruz et al. [126] prepared a Ni–CeO_2 catalyst with a Ni wt% loading of 13% and employed it in the CDRM reaction. The catalyst showed decreases in activity, stability, and selectivity for H2 and CO over 12 hrs of reaction due to the formation of carbon nanofibers [126]. Another important study reported by Zhang et al. [127] compared LaNiO3 perovskite with conventional nickel-based catalysts (Ni/γ-Al_2O_3, Ni/CaO/γ-Al_2O_3, and Ni/CaO). They observed that the conventional Ni-based catalysts suffered from constant deactivation with time on stream. On the other hand, the $LaNiO_3$ catalyst showed stable performance with time on stream. The enhancement in the rate of reaction over the Ni/La_2O_3 catalyst during the reaction is positively correlated with the concentrations of formate and $La_2O_2CO_3$ on the support, indicating that these species could be involved in the surface chemistry that generates synthesis gas. A novel kind of synergetic sites in the Ni-La_2O_3 interfacial area is suggested to be created by the interaction of nickel and lanthanum species, providing a stable and active carbon dioxide reforming of methane to synthesis gas across the specified catalyst [127].

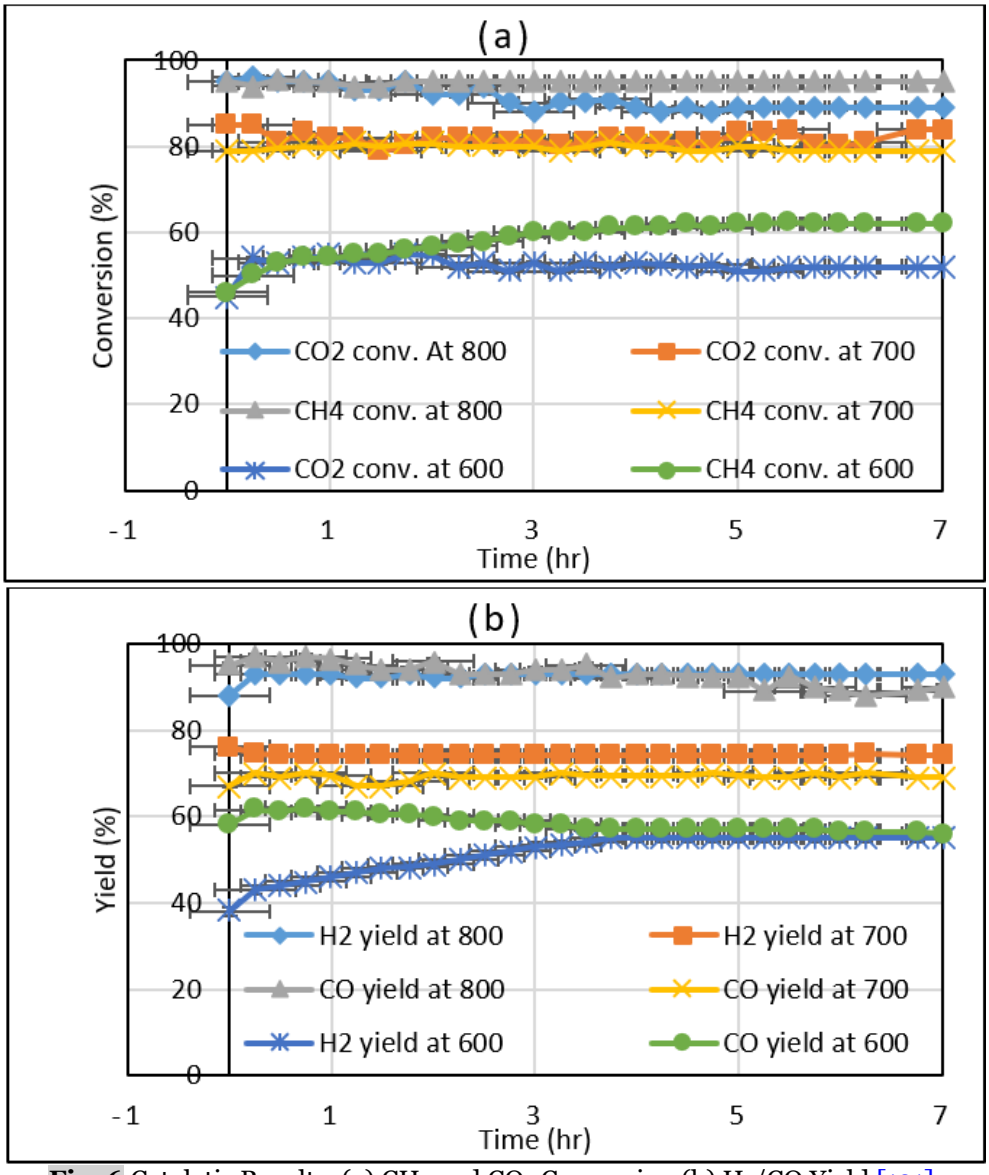

Fig. 6 Catalytic Results: (a) CH_4 and CO_2 Conversion (b) H_2/CO Yield [121].

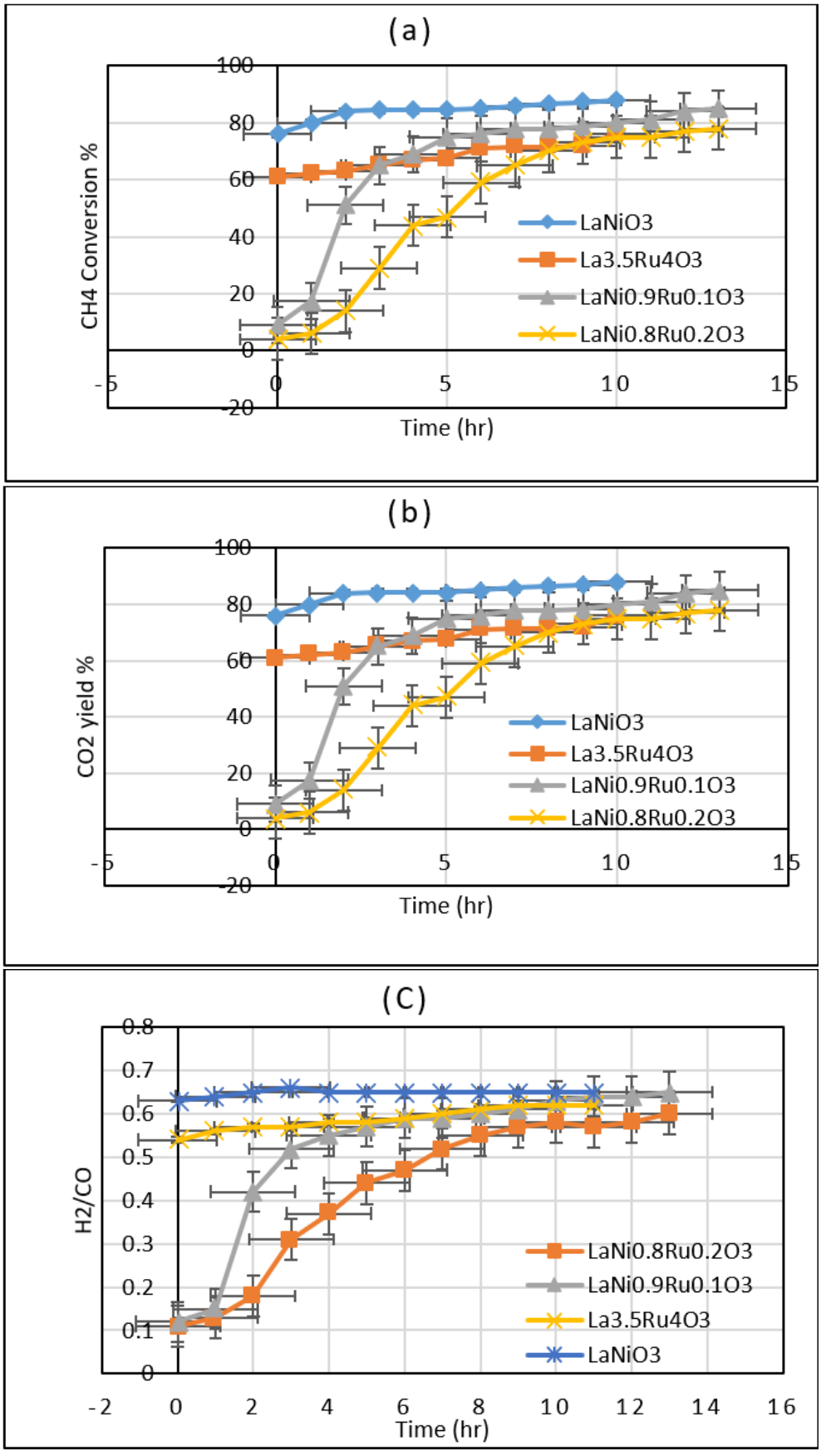

Fig. 7 (a) Methane Conversion, (b) Carbon Dioxide Yield, and (c) Hydrogen to Carbon Monoxide Molar Ratio Produced, as a Function of Time Over the Catalysts: (□) $LaNiO_3$, (▼) $LaNi_{0.9}Ru_{0.1}O_3$, (●) $LaNi_{0.8}Ru_{0.2}O_3$, and (Δ) $La_{3.5}Ru_4O_3$ [68].

5.FACTORS AFFECTING THE CATALYTIC ACTIVITY

A number of factors influence the catalytic activity of La-Ni-based perovskite catalysts. Each factor plays a significant role in determining its efficacy in catalyzing CDRM reactions. This section discusses the effects of partial substitution at the A^-, B^-, and both A^- and B^-sites, and the influence and importance of support addition for La-Ni-based perovskite catalysts. Understanding and studying these factors is important for optimizing catalyst design and performance. Substituting the A and/or B sites of the $LaNiO_3$ structure can modify the electronic properties. This alteration influences the distribution of charge carriers, as well as the band structure and catalyst stability. Partial substitution can improve catalytic activity by enhancing synergistic interactions between the catalyst's active sites and the substituted elements. The other factor we discussed in this section is the support addition. Support materials can improve and stabilize the structure of La-Ni-derived perovskite catalysts and protect them from deactivation, such as sintering, during the CDRM reaction. These materials provide better dispersion of the active sites on the catalyst surface, thereby enhancing catalytic activity and stability. In addition, the high surface area of supports can increase the catalyst's surface area, enhancing the dispersion of active sites and thereby improving catalytic activity.

5.1.Effect of Partial Substitution

The catalytic performance can be significantly influenced by the partial substitution of each A & B site [128]. Plenty of studies have been conducted on the impact of partially substituting elements in either the A-site (such as Pr, Ce, Na, Ba, and Sr) or the B-site (such as Mn, Cu, Mg, Zr, Zn, and Co) of the $LaNiO_3$ perovskite structure as a catalyst for methane reforming. Partial substitution is used to improve catalytic activity, increase specific surface area, or enhance resistance to carbon deposition [83, 129], which is an additional advantage of perovskite-type structures, as they provide a more dispersed active phase with higher coke resistance [130]. This modification affects the catalytic activity and stability of the components [131]. Furthermore, the catalyst's stability can be enhanced by the synergistic effect of nickel and the metal at the B site of the $LaNiO_3$ perovskite structure [111].

5.1.1.A-Site Partial Substitution

Partial substitution at the A-site of La-Ni-based perovskite with rare-earth metals, alkaline-earth metals, and transition metals can improve catalyst properties and enhance catalytic performance during reactions. Several studies investigated the effect of partial A-site substitution on the catalytic properties of $LaNiO_3$. For instance, Su et al. [132] studied the influence of the partial substitution of Ni by Ce. The $LaNiO_3$ and $La_{1-x}Ce_xNiO_3$ ($x \leq 0.5$) were prepared by the Pechini method to inhibit the accumulation of carbon and the agglomeration of nickel species. The presence of lattice oxygen vacancies in Ce facilitated the activation of Ce-H bonds, resulting in an enhanced selectivity of H_2 as shown in Fig. 8. This figure indicates that the H_2 selectivity over the $La_{0.9}Ce_{0.1}NiO_3$ catalyst improves from 57 to 61% at 600 °C (x=0, 0.1). $La_{0.9}Ce_{0.1}NiO_3$ may increase the progressive breakdown of CH_4 into surface CH ($CH_4 \rightarrow CH_3 \rightarrow CH_2 \rightarrow CH$) and hydrogen while also providing extra oxygen atoms for CHO formation. Then, CHO dissociates into CO and H_2. CO selectivity rises with Ce replacement. They also obtained $LaNiO_3$ and $La_{1-x}Ce_xNiO_3$ ($x \leq 0.5$) catalysts in fiber form, and the formation of carbon structures was observed after the reforming reaction. With a carbon whisker structure, the carbon structures had a greater diameter than the catalyst fibers LaNiO3 and La1-xCexNiO3. Fortunately, the reactant gases were not prevented from reaching this whisker's catalytic surface, preserving stability and high activity [132]. Similar results were observed by Lima et al. [133], indicating that the addition of Ce improved the stability and selectivity of the catalysts. As a result, partial substitution with rare-earth metals, such as Ce, yielded good results. Partial substitution with alkaline earth metals (Ba, Sr, Mg, and Ca) improved the perovskite structure, leading to better catalytic activity and stability, along with lower coke deposition; this improvement was attributed to the presence of oxygen vacancies. For instance, Trevisani and Batista [117] conducted a study on the substitution of the three alkaline-earth elements (Ca, Ba, Sr) in $M_xLa_{1-x}NiO_3$ (x = 0.0, 0.3, and 0.5) doped perovskites. They were successfully synthesized by the citrate method as catalyst precursors to get high catalytic activity and stability in the CDRM process. The Ca, Ba, and Sr partial substitutions had a major effect on the reduction behavior of (Ca, Ba, Sr)$_x$La$_{1-x}$NiO$_3$ perovskites (x = 0.3 and 0.5). Doping with (Ca, Ba, Sr) yielded a more stable $LaNiO_3$ perovskite with broad peaks of H_2 consumption at higher temperatures, as shown in Fig. 9. The figure displays all H_2-TPR patterns of (Ca, Ba, Sr)$_x$La$_{1-x}$NiO$_3$ perovskites. The $LaNiO_3$ perovskite (x = 0.0) experienced Ni^{3+} reduction to Ni^{2+} at 460 °C, and converted $LaNiO_3$ to La_2NiO_4 or $La_2Ni_2O_5$. Ni^{2+} is then reduced to Ni^0 at 640 °C, while the remaining was supported by lanthanum oxide. However, increasing the content of these elements above 0.5 decreases activity [117]. The same observations were reported by Dezvareh et al. [134], who applied $La_{1-x}Ce_xNi_{1-y}Zr_yO_3$ perovskite catalysts in the CDRM reaction. The TPR test indicated a reduction of Ni3+ to Ni2+, which was related to $La_2Ni_2O_5$ formation. Another study reported by Gomes et al. [135] aimed to

evaluate the impact of Barium substitution in the A-site of $LaNiO_3$ perovskite catalyst. It appeared that an activity decay occurred, attributed to Ba substitution due to structural changes. Also, as shown in Fig. 10, the presence of $BaCO_3$ at temperatures above 610 ◦C induced an orthorhombic-to-hexagonal phase transition. This led to reduced coverage of the active sites and restrained interactions between the reactants and the active sites. Nevertheless, Ba substitution showed a stable behavior, with higher resistance to carbon formation, sintering, and poisoning [135]. De Lima et al. [136] examined the effect of La substitution with Ca when preparing $La_{1-x}Ca_xNiO_3$ (x = 0.0, 0.05, 0.1, 0.3, 0.5, and 0.8). After substitution, the catalytic activity increased during the reaction period, and the conversion of CO_2 and CH_4 for most catalysts began to increase and approached a steady state. However, only the unsubstituted sample ($LaNiO_3$) and the sample with x = 0.3 showed a little decline in methane conversion with time. The slight decrease in activity is most likely due to the buildup of carbon that forms on the surface from the impact. It was also observed that CO_2 conversion was consistently higher than CH_4 conversion due to the occurrence of the reverse water-gas shift reaction. However, better coke resistance was observed for the Ca-substituted samples, with resistance dependent on Ca content [136]. As a result, alkaline earth metals showed enhanced catalytic activity, stability, and resistance to carbon deposition.

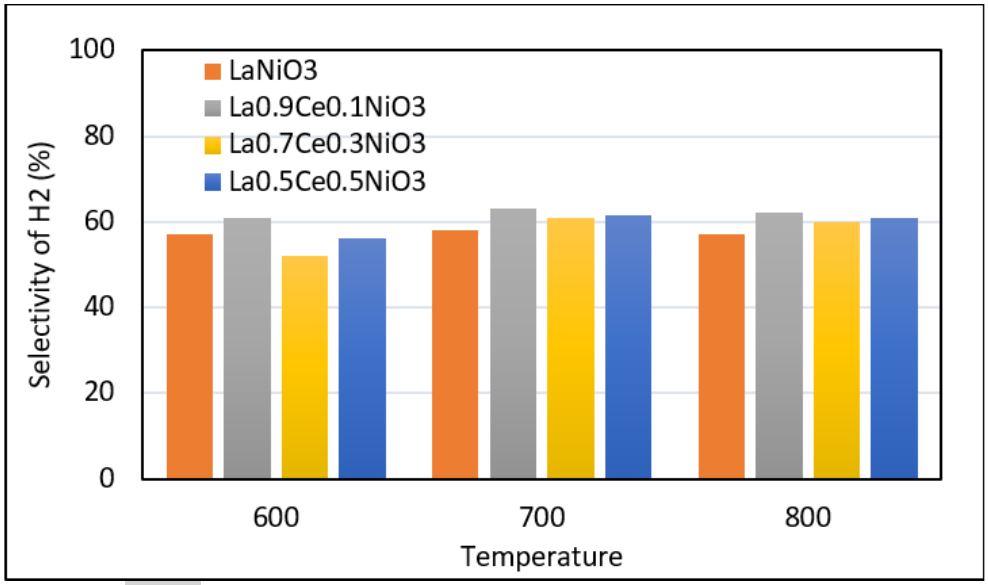

Fig. 8 Selectivity of H_2 of $La_{1-x}Ce_xNiO_3$ Catalyst (x ≤ 0.5) [132].

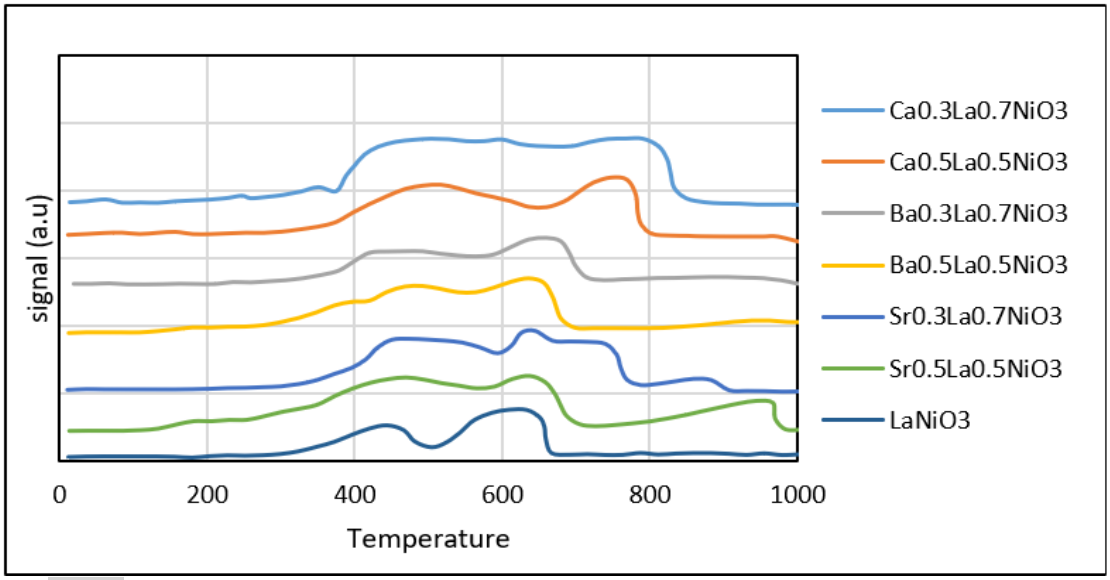

Fig. 9 H_2-TPR Profiles of $M(Ca, Ba, Sr)_xLa_{1-x}NiO_3$ (x = 0.0, 0.3, 0.5) Perovskites [117].

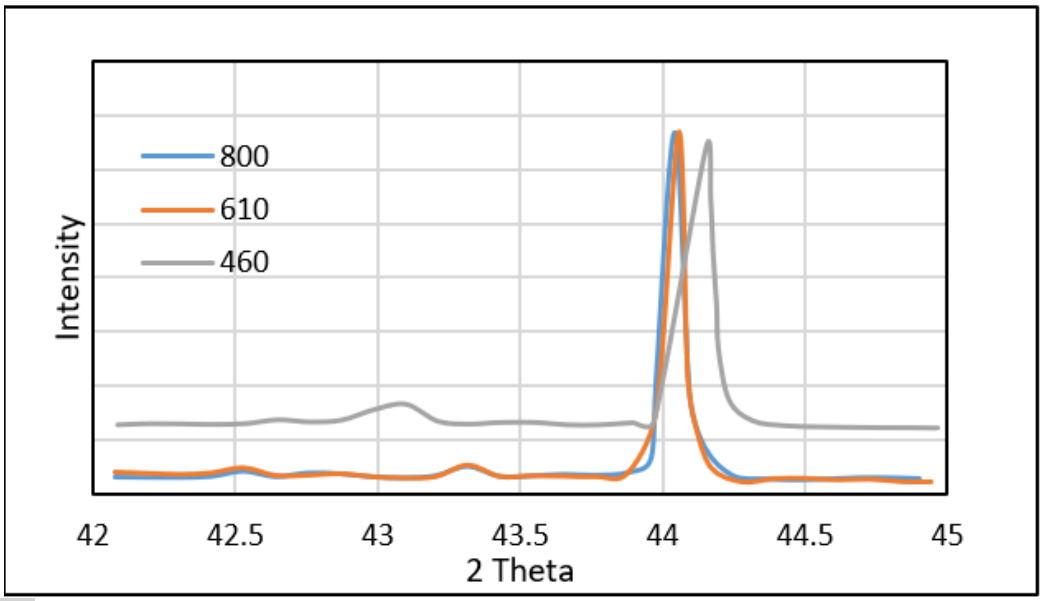

Fig. 10 X-ray Diffractograms for the Catalysts under the Reaction Atmosphere of $La_{0.8}Ba_{0.2}NiO_3$ at Different Oxidation Temperatures (800, 610, and 460) [135].

A-site substitution with some transition metals was also investigated. The influence of zirconium-substituted perovskite reported by Talaie et al. [137] gained undesirable effects since the partial substitution of La^{3+} by Zr^{4+} in the $La_{1-x}Zr_xNiO_3$ structure reduced the mobility of oxygen towards the solid's surface, and the yield of H_2 and CO is decreased. Also, CH_4 and CO_2 conversions were higher with pure perovskite than with multi-phase catalysts, as demonstrated in Fig. 11. The research also showed that, for all catalysts, CH_4 and CO_2 conversions increase with temperature. Nevertheless, compared to CO_2, CH_4 conversions are lower. This might be the result of a reverse water gas shift reaction. In addition, as the reaction temperature increases, the yields of CO and H_2 both increase [137], and the results are comparable to those of Aghabozorg et al. [105]. Table 2 summarizes the recent studies, including the amount of carbon deposition, surface area, conversion rates, and the operating conditions applied.

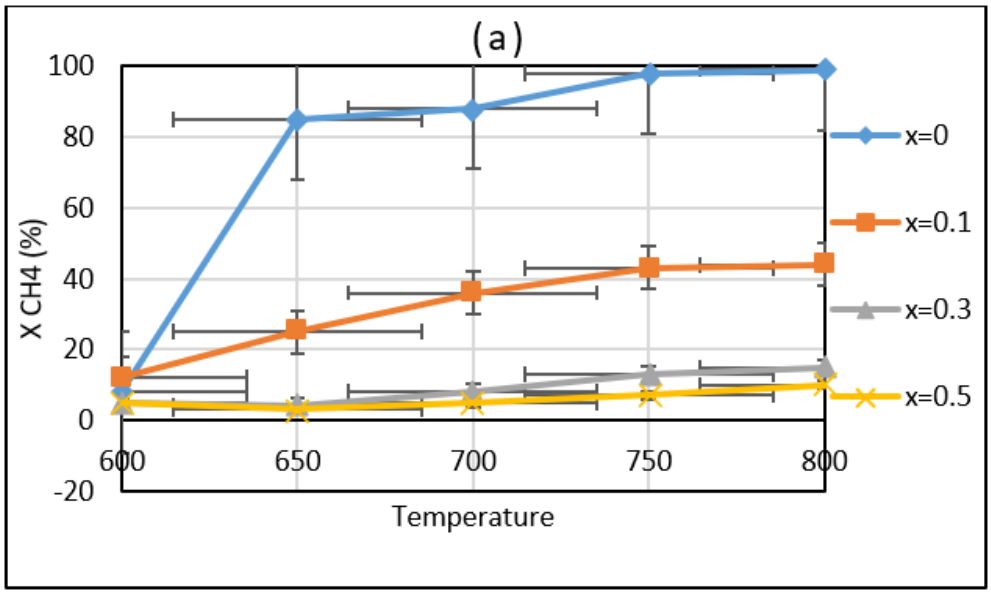

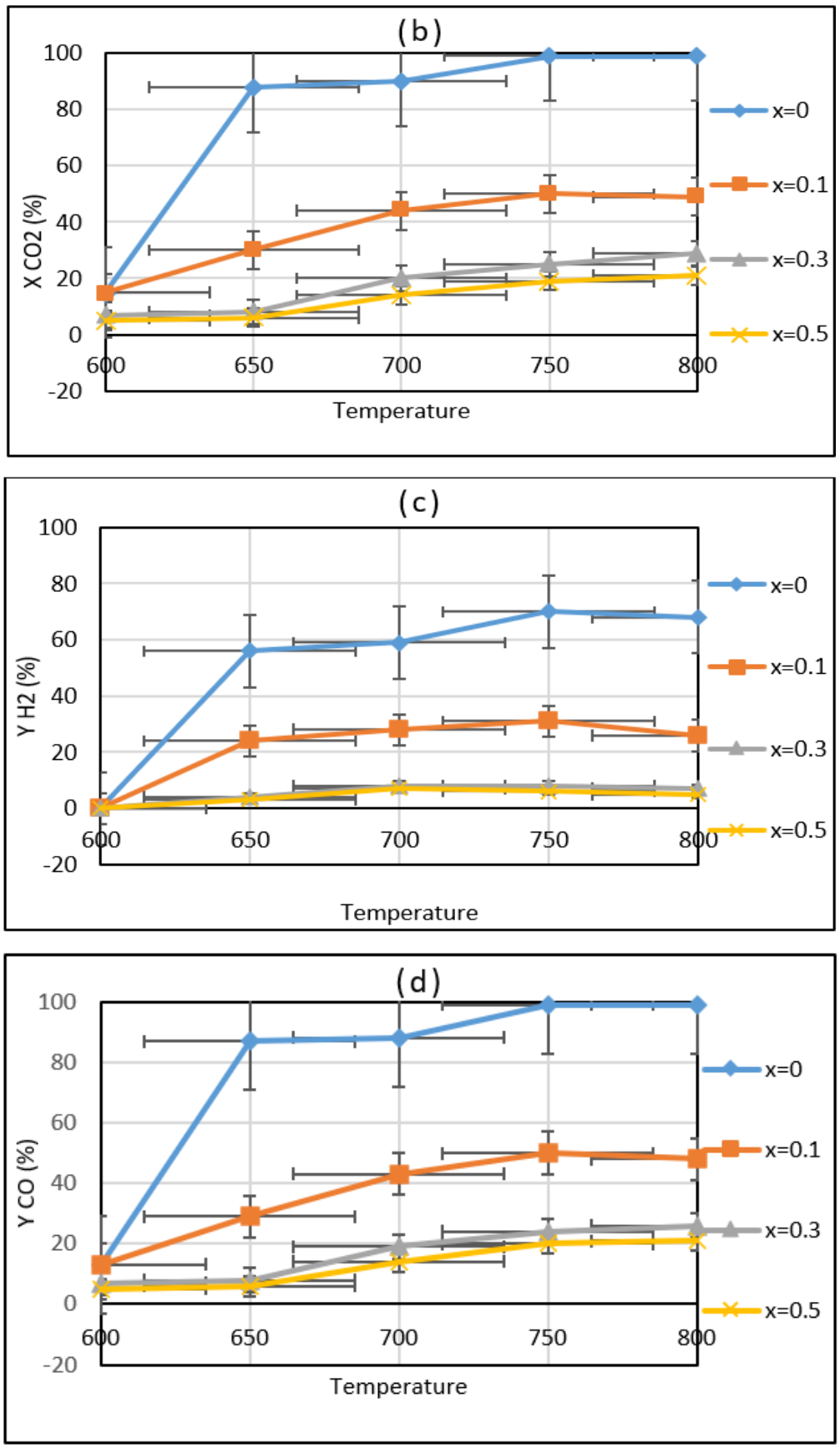

Fig. 11 CH_4 and CO_2 Conversions, and H_2 and CO Yields for $La_{1-x}Zr_xNiO_3$ Samples, as a Function of Reaction Temperature [137].

Table 2 La-substituted Based Perovskite Catalysts for CDRM Reaction:

Catalyst	Carbon deposits	Surface area (m^2/g)	$\%CH_4$	$\%CO_2$	Operating Conditions	Ref.
$LaNiO_3$	4.5 mg. g^{-1} cat.	_	31	33		[117]
$Ca_{0.3}La_{0.7}NiO_3$	0.37 mg. g^{-1} cat.	_	73	81	T= 700 °C	
$Ca_{0.5}La_{0.5}NiO_3$	0.14 mg. g^{-1} cat.	_	53	64	CH_4:CO_2= 1:1	
$Ba_{0.3}La_{0.7}NiO_3$	0.06 mg. g^{-1} cat.	_	55	66		
$Ba_{0.5}La_{0.5}NiO_3$	0.08 mg. g^{-1} cat.	_	42	50		
$Sr_{0.3}La_{0.7}NiO_3$	0.24 mg. g^{-1} cat.	_	65	67		
$Sr_{0.5}La_{0.5}NiO_3$	0.07 mg. g^{-1} cat.	_	47	60		
$LaNiO_3$	1.64 mg. g^{-1} cat.	6	48	61	T= 700 °C	[135]
$La_{0.95}Ba_{0.05}NiO_3$	0.08 mg. g^{-1} cat.	4-6	_	_	GHSV =2 *10^5 NL.h^{-1}.kg^{-1}	
$La_{0.9}Ba_{0.1}NiO_3$	0.16 mg. g^{-1} cat.	4-6	35	49	CH_4:CO_2:Ar=1:1:2	
$La_{0.8}Ba_{0.2}NiO_3$	0.03 mg. g-1 cat.	4	33	45		
$LaNiO_3$	_	3	99	100	T= 600-800 °C	[137]
$\mathbf{La_{0.9}Zr_{0.1}NiO_3}$	_	5	47	50	WHSV=15 L.g^{-1}.h^{-1}	
$\mathbf{La_{0.7}Zr_{0.3}NiO_3}$	_	3	15	30	CH_4:CO_2= 1:1	
$\mathbf{La_{0.5}Zr_{0.5}NiO_3}$	_	2	10	20		
$LaNiO_3$	_	6.9	95	93	T = 400-800 °C	[132]
$La_{0.9}Ce_{0.1}NiO_3$	_	28.6	94	94	GHSV =10,000 h^{-1}	
$La_{0.7}Ce_{0.3}NiO_3$	_	_	92	92	CO_2:CH_4=1:1	
$La_{0.5}Ce_{0.5}NiO_3$	_	_	93	93		
$LaNiO_3$	_	_	37	46	T= 650 °C, 700 °C and	[138]
$La_{0.9}Ba_{0.1}NiO_3$	_	_	64	57	750 °C. CH_4:CO_2:He=1:1:8	
$La_{0.8}Ba_{0.2}NiO_3$	_	_	51	_		
$La_{0.7}Ba_{0.3}NiO_3$	_	_	29	_		
$LaNiO_3$	65.7%	0.21	86	86	T= 750 °C	[123]
$LaNi_{0.9}Ru_{0.1}O_3$	20.3%	1.9	85	88	CH_4:CO_2= 1:1	
$LaNi_{0.8}Ru_{0.2}O_3$	6.86%	1.9	80	84		
$La_{3.5}Ru_4O_3$	0.938%	1.2	76	83		

5.1.2.B-Site Partial Substitution

Partial substitution of B-site cations is more challenging than that of A-site cations. Because, in some cases, the addition of reducible metals produces a metal-Ni alloy, making the reduction process more difficult. In contrast, because the substituted element is inert, reducing the catalyst produces nickel nanoparticles supported by a mixture of oxides [139]. The partial substitution of nickel by manganese on the B-site to produce bimetallic catalysts has been studied by Bhavani and Wani [139]. They synthesized Ni-substituted lanthanum manganite with the formula of $LaMn_{1-x}Ni_xO_3$ (x = 0.2, 0.4, 0.5, 0.6, 0.7), using the sol-gel method. This procedure produced a single-phase perovskite structure, thereby enhancing physicochemical properties, including crystallinity, surface area, pore volume, and Ni particle size. Increasing the level of Ni substitution was found to optimize surface area, pore volume, and metallic surface area, thereby enhancing stability [139]. The good results can be attributed to high nickel dispersion caused by manganese addition [84]. Nickel substitution with cobalt or copper improves carbon resistance. Several researchers studied this kind of metal. For instance, Messaoudi et al. [140] studied the effect of partial substitution in the B-site with (Co, Cu). They prepared $LaNi_{0.9}M_{0.1}O_3$ (M = Co, Cu) using the sol-gel method and found that replacing nickel with copper lowers the temperature and decreases the methane activation temperature. On the other hand, the cobalt-substituted catalyst exhibited enhanced stability and catalytic activity, and syngas generation attributed to the synergistic interaction between nickel and cobalt, as well as low carbon deposition [140]. Touahra et al. [87] synthesized perovskite oxide $LaCuO_3$ and $LaCu_{0.53}Ni_{0.47}O_3$ using the sol-gel citrate technique, while 5% $NiO/LaCuO_3$ was created using impregnation. They found that at 700°C, the amount of CH_4 consumed was at its lowest in the presence of $LaCuO_3$. At the same time, the CH_4 conversion increased to 60% with the $LaCu_{0.53}Ni_{0.47}O_3$ precursor. Also, it showed better resistance to carbon formation [87]. Valderrama et al. [141] synthesized $LaNi_{1-x}Co_xO_3$ (x= 0, 0.2, 0.4, 0.6, 0.8, 1) perovskite-type oxides by the sol-gel resin method. The catalysts showed high activity, with conversions and selectivities approaching 100%. As shown in Fig. 12, the Ni ($x \leq 0.6$) rich solids have strong selectivity for forming syngas, with CH_4 conversions somewhat greater than CO_2 and H_2 selectivities a little higher than CO. This performance can be attributed to the Ni^0-Co^0 particle formation, which was highly dispersed on $La_2O_2CO_3$ and inhibited the coke formation. Doping with Co stabilizes Ni^0 particles, reducing coke formation, whereas tiny amounts of Ni promote Co reduction and accelerate solid activation [141]. From the literature above, we can say that cobalt doped catalysts showed similar results to copper doped catalysts in terms of catalytic activity. Partial substitution of the B-site with Fe produces a bimetallic catalyst that enhances catalytic activity and stability. Song et al. [142] conducted a study on the partial substitution of Fe in $LaNiO_3$ and La_2NiO_4 perovskite precursors, as these structures were unstable and reduced completely in the CDRM reaction, forming Ni particles as the active metal and La_2O_3 as the

support. They prepared ($La_2Ni_{0.5}Fe_{0.5}O_4$ and $LaNi_{0.5}Fe_{0.5}O_3$) using the wet impregnation method, and the results showed an improvement in the stability and carbon resistance of these catalysts. The increased metal-support interaction led to smaller particle sizes and improved Ni dispersion [142]. Similarly, to investigate the impact of Fe loading on the perovskite catalyst, Jahangiri et al. [143] prepared $LaNiO_3$ and $LaNi_{1-x}Fe_xO_3$ (x = 0.2, 0.4, 0.6, 0.8, and 1) perovskites by the citrate sol-gel method. Their results showed that as x increased, a NiFe2O4 phase formed at high temperatures, delaying the atomic nickel synthesis. The order of activity was $LaNiO_3$ > $LaNi_{0.4}Fe_{0.6}O_3$ > $LaNi_{0.6}Fe_{0.4}O_3$ > $LaNi_{0.8}Fe_{0.2}O_3$ > $LaNi_{0.2}Fe_{0.8}O_3$ > $LaFeO_3$. The $LaNiO_3$ exhibited the highest activity and stability, and this behavior was attributed to the formation of small nickel particles [143]. Another study reported by De Lima and Assaf [144] examined $LaNi1-xFe_xO_3$ (x=0, 0.2, 0.4, and 0.7) perovskite oxides to increase the catalytic activity, stability, and coke resistance of $LaNiO_3$. The addition of Fe decreased the activity of both CH_4 and CO_2, but increased the catalyst's stability [144]. Previous literature indicates that La-Ni-perovskites with Fe incorporation exhibit improved stability during the CDRM reaction. Table 3 provides an overview of the relevant research.

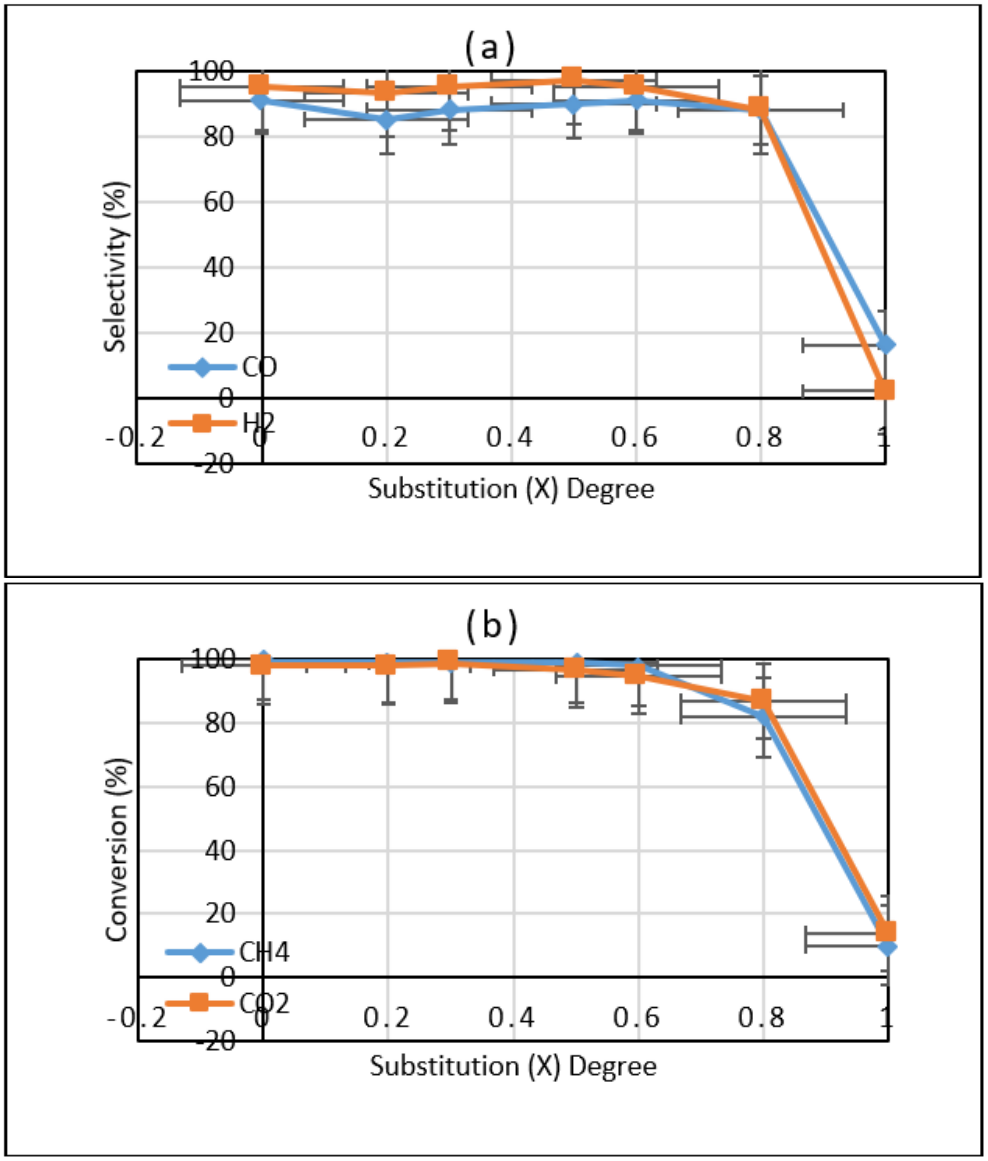

Fig. 12 (a) CH_4 and CO_2 Conversions of $LaNi_{1-x}Co_xO_3$, (b) CO and H_2 Selectivities Obtained for $LaNi_{1-x}Co_xO_3$ [141].

Table 3 Ni-Substituted Based Perovskite Catalysts for CDRM Reaction:

Catalyst	Carbon deposits	Surface area (m^2/g)	$\%CH_4$	$\%CO_2$	Operating conditions	Ref.
$LaNi_{0.2}Zr_{0.8}O_3$	13.14%	14	6	7.5	T=800 °C CH_4:CO_2:N_2=1:1:1	[104]
$LaNi_{0.3}Zr_{0.7}O_3$	7.89%	12	7.5	11.25		
$LaNi_{0.4}Zr_{0.6}O_3$	5.93%	7	16.25	21		
$LaNi_{0.6}Zr_{0.4}O_3$	3.56%	3	25	27		
$LaNi_{0.8}Zr_{0.2}O_3$	3.51%	5	37	50		
$LaNi_{0.05}Cr_{0.95}O_3$	0.02 mg. g^{-1}cat.h^{-1}	9.7	12	34	T= 750 °C GHSV=12 L.g^{-1}.h^{-1} CH_4:CO_2=1:1	[145]
$LaNi_{0.1}Cr_{0.9}O_3$	negligible	9.4	84	87		
$LaNi_{0.2}Cr_{0.8}O_3$	15 mg. g^{-1}cat.h^{-1}	7.2	84	85		
$LaNi_{0.3}Cr_{0.7}O_3$	25 mg. g^{-1}cat.h^{-1}	9.4	85	86		
$LaNi_{0.4}Cr_{0.6}O_3$	64 mg. g^{-1}cat.h^{-1}	9.9	90	79		
$LaNi_{0.5}Cr_{0.5}O_3$	76.2 mg. g^{-1}cat.h^{-1}	9.5	87	86		
$LaNiO_3$	_	7.2	89	93.5	T = 600-800 °C GHSV= 15 L.g^{-1}.h^{-1} CH_4:CO_2:N_2=1:1:2	[84]
$LaNi_{0.8}Mn_{0.2}O_3$	_	17.1	94	87.5		
$LaNi_{0.6}Mn_{0.4}O_3$	_	22.0	95	94		
$LaNi_{0.4}Mn_{0.6}O_3$	_	22.4	95	93		
$LaNi_{0.2}Mn_{0.8}O_3$	_	21.3	95	89		
$LaMnO_3$	_	19.3	93	87		
$LaNiO_3$ non-treat	23.7 g. g^{-1} cat.	4.9	68	72	T = 823-1073 K GHSV = 18 L.g^{-1}.h^{-1} CH_4:CO_2=1:1	[111]
$LaNiO_3$ treat	19.1 g. g^{-1} cat.	4.4	65	70		
$LaNi_{0.5}Co_{0.5}O_3$ non-treat	18.2 g. g^{-1} cat.	3.8	59	68		
$LaNi_{0.5}Co_{0.5}O_3$ treat	15.2 g. g^{-1} cat.	3.2	57	63		
$LaNiO_3$	_	_	61	75	T= 750 °C CH_4:CO_2:He=1:1:1	[131]
$LaNi_{0.8}Zn_{0.2}O_3$	_	_	86	93		
$LaNi_{0.6}Zn_{0.4}O_3$	_	_	76	86		
$LaNi_{0.4}Zn_{0.6}O_3$	_	_	14	16		
$LaNi_{0.2}Zn_{0.8}O_3$	_	_	13	15		
$LaZnO_3$	_	_	5	6		
$LaNi_{0.8}Fe_{0.2}O_3$	_	18	60	90	T= 800 °C GHSV=13.7 L.g^{-1}.h^{-1} CH_4:CO_2=1:1	[146]
$LaNi_{0.8}Mn_{0.2}O_3$	_	18	80	95		
$LaNi_{0.5}Co_{0.5}O_3$	_	5-9	83.7	88.5	T=800 °C GHSV=12 L.g^{-1}.h^{-1} CH_4:CO_2:N_2=1:1.05:1	[147]
$LaNi_{0.34}Co_{0.33}Mn_{0.33}O_3$	_	5-9	93.7	92.5		
$LaNi_{0.8}Ti_{0.2}O_3$	2.21%	3.4	62	57.9	T=800°C CO_2:CH_4:O_2= 0.8:1.0:0.2	[148]
$LaNi_{0.6}Ti_{0.4}O_3$	0.63%	4.4	67.4	65.4		
$LaNi_{0.5}Ti_{0.5}O_3$	0.84%	3.8	73.4	76.4		
$LaNi_{0.4}Ti_{0.6}O_3$	2.11%	9.1	69.8	71.5		
$La_2Ti_2O_7$	0.12%	4.1	47.1	41.4		
$LaNiO_3$	$0.0048\frac{\text{mol carbon}}{\text{mol }(CH_4+CO_2).\text{h}}$	3.2	85	44	T=800 °C WHSV=15 L.g^{-1}.h^{-1} CH_4:CO_2:O_2=1:1:0.5	[143]
$LaNi_{0.4}Fe_{0.6}O_3$	$0.0143\frac{\text{mol carbon}}{\text{mol }(CH_4+CO_2).\text{h}}$	5.4	80	42		
$LaNi_{0.6}Fe_{0.4}O_3$	$0.0088\frac{\text{mol carbon}}{\text{mol }(CH_4+CO_2).\text{h}}$	_	70	40		
$LaNi_{0.8}Fe_{0.2}O_3$	$0.0132\frac{\text{mol carbon}}{\text{mol }(CH_4+CO_2).\text{h}}$	7.6	30	0		
$LaNi_{0.2}Fe_{0.8}O_3$	$0.0134\frac{\text{mol carbon}}{\text{mol }(CH_4+CO_2).\text{h}}$	_	68	33		

5.1.3.Both A & B Sites Partial Substitution

As with A-site and B-site substitutions, a number of researchers studied the effects of partial substitutions at both A and B sites in the ABO_3 structure. These researchers aimed to improve the performance of the perovskite catalysts. For instance, Abasaeed et al. [118] synthesized $MNi_{0.9}Zr_{1-x}Y_xO_3$ catalysts (M = Ce, La, and $La_{0.6}Ce_{0.4}$; x = 0.00, 0.05, 0.07, and 0.09) using the sol-gel method. The study demonstrated that substituting 0.1% of Ni with Zr in the $La_{0.6}Ce_{0.4}NiO_3$ catalyst resulted in excellent catalytic activity, achieving an 83% hydrogen production at 800°C. This good performance was attributed to the presence of reducible NiO species that interacted strongly with the support (produced after reduction) and to the redox reactions, which were generated from substituting Zr and Y for Ni in the $CeNiO_3$ catalytic system results in Ni_3Y, since a stable metallic Ni for CH_4 decomposition, and cerium yttrium oxide phases, which provide significant redox input [118]. Several researchers studied the effect of strontium incorporation; for example, Das et al. [149] investigated the mechanism of CDRM reaction on $La_{0.9}Sr_{0.1}NiO_3$ and $La_{0.9}Sr_{0.1}Ni_{0.5}Fe_{0.5}O_3$. They observed that $La_{0.9}Sr_{0.1}Ni_{0.5}Fe_{0.5}O_3$ may partially retain a perovskite structure even after reduction and in a CDRM atmosphere, and that it exhibits higher coke resistance than $La_{0.9}Sr_{0.1}NiO_3$. The study showed that lanthanum oxycarbonates activated CO_2 and oxidized carbonaceous intermediates from methane on the $La_{0.9}Sr_{0.1}NiO_3$ catalyst. On the other hand, the oxidation of carbonaceous intermediates occurred only through the MvK-type redox mechanism by support lattice oxygen in $La_{0.9}Sr_{0.1}Ni_{0.5}Fe_{0.5}O_3$ [149]. Dezvareh et al. [134] prepared $La_{1-x}Ce_xNi_{1-y}Zr_yO_3$ (x=0.1, y=0.1, 0.2) by the citrate sol-gel method; according to the results of morphology investigations, particles

in the nanometer range were produced, resulting in homogeneity. In accordance with the TPR results shown in Fig. 13, the reduction of $LaNiO_3$ perovskite involved two stages. The peaks' maxima were observed at 408 and 505 °C. The first peak indicates the reduction of Ni^{3+} to Ni^{2+}, resulting in the formation of $La_2Ni_2O_5$. The second peak resulted from the reduction of Ni^{2+} to NiO. Cerium-doped perovskites ($La_{1-x}Ce_xNiO_3$) exhibit a small shift towards lower temperatures in the TPR profile2; the reduction process occurred at higher temperatures and became more difficult as the Zr doping level increased. To activate the active sites for the reforming reaction in $La_{1-x}Ce_xNi_{1-y}Zr_yO_3$ samples, they must be reduced. This results in highly scattered Ni and Zr on a matrix of La-Ce-O, resulting in the production of a metal catalyst. The catalyst $La_{0.9}Ce_{0.1}Ni_{0.8}Zr_{0.2}O_3$ perovskite exhibited the highest catalytic activity with more than 60% for CH_4 and more than 70% for CO_2 [134]. $La_{1-x}Ce_xNi_{0.4}Fe_{0.6}O_3$ (x = 0.1, 0.2, and 0.3) perovskite nanostructures were synthesized and characterized by Dezvareh et al. [150]. They obtained a well-crystallized perovskite structure at doping levels of up to x = 0.2. The catalytic activity of developed samples at temperatures ranging from 600 to 800°C was investigated through the CDRM process. The CH_4 and CO_2 conversions, as well as the H_2 and CO yields in the presence of $La_{1-x}Ce_xNi_{0.4}Fe_{0.6}O_3$ at various temperatures, are shown in Fig. 14. The figure shows that increasing temperature leads to both CH_4 and CO_2 conversions rising, with CO_2 conversions consistently exceeding CH_4 conversions. The consumption of CO_2 in the reaction may be the reason behind this behavior. Additionally, as the reaction temperature increased, the yields of both H2 and CO increased, with CO yields exceeding H2 yields when the catalyst La1-xCexNi$_{0.4}$Fe$_{0.6}$O$_3$ was present. The higher the temperature, the more prominent this behavior is. A partial doping level of x = 0.3 in $La_{1-x}Ce_xNi_{0.4}Fe_{0.6}O_3$ samples has not resulted in substantial CH_4 and CO_2 conversions or product yields at any temperature. Where Ce addition to $La_{1-x}Ce_xNi_{0.4}Fe_{0.6}O_3$ increased the catalytic activity up to x = 0.2, but decreased considerably when x > 0.2 [150]. Yang et al. [151] prepared $La_{0.9}M_{0.1}Ni_{0.5}Fe_{0.5}O_3$ (M = Sr, Ca) perovskite catalysts by the ethylene diaminetetraacetic Acid-cellulose method (EDTA) to investigate the influence of partial substitution of A- site by Sr/Ca. Partial substitution of the A site with Ca or Sr affected the basicity and crystalline phases of the catalysts, resulting in better performance. $La_{0.9}Ca_{0.1}Ni_{0.5}Fe_{0.5}O_3$ catalyst exhibited the best catalytic performance among the prepared perovskite catalysts, owing to improved carbon resistance during the reaction. The two catalysts showed good metal-support interactions due to Fe substitution, which offered high resistance to sintering and carbon deposition [151]. Sutthiumporn et al. [152] developed $La_{0.8}Sr_{0.2}Ni_{0.8}M_{0.2}O_3$ (LSNMO) perovskite precursors for the CDRM process (where M = Bi, Co, Cr, Cu, and Fe). They found that the Cu-substituted Ni catalyst precursor exhibited the highest initial catalytic activity due to the largest accessible Ni surface area and the presence of mobile lattice oxygen species capable of activating C–H bonds. However, the Fe-substituted Ni catalyst exhibited the highest catalytic stability because of strong metal-support interaction and presence of the abundant lattice oxygen species. Which reacted with CO_2 to generate $La_2O_2CO_3$ and minimized carbon production by reacting with surface carbon to form CO [152]. In conclusion, it is generally believed that oxygen vacancy formation, associated with A-site substitution, improves carbon resistance. On the contrary, B-site substitution with reducible metals frequently produces a synergistic effect that can be advantageous or disadvantageous. Further investigation would help address the issue, as the process of partial substitution of both the A and B sites and its subsequent effects on DRM remain unclear.

5.2.Effect of Support Addition

Support materials are essential for enhancing catalytic activity and preventing carbon deposition during the CDRM reaction, given the low surface area of perovskite oxides (<10 m2/g) and the high reaction temperatures required for endothermic reforming. Coke production occurs primarily through the decomposition of CH_4 at high CDRM reaction temperatures [153]. In addition to their weak mechanical strength and susceptibility to SO2 poisoning, these limitations limit their potential applications [112]. Therefore, the demand for promising techniques to overcome these challenges is significant, as they are needed to create a well-dispersed perovskite on a support with a high specific surface area and good thermal stability to prevent active metal sintering [83]. The introduction of support modifies the product distribution, increases the surface area of the active phase, and enhances thermal stability. Many types of support have been studied, including alkaline oxides (MgO and CaO), γ-Al_2O_3, oxygen-binding affinity materials (CeO_2, Fe_2O_3, MnO_X, and La_2O_3), and zeolites (ZSM-5, SBA-15, and MCM-41). Compared with other supports, zeolites are considered the best materials due to their unique properties, such as crystallinity, well-ordered micropores, and large surface area [154]. The support is an essential component of supported catalysts, as its selection plays a key role in determining catalytic performance. The kind and nature of the support significantly affect the dispersion, stability, and heat transfer performance of active components [155]. Besides, the redox characteristics of the support

can reduce carbon deposits on the catalyst surface. In addition, as dry reforming reaction requires adsorption and activation of CO_2, the basic support may enhance the activity of Ni-based catalysts [156]. Some catalysts exhibit interactions between the metal and the support [153], and several investigations have demonstrated that small nickel particles and stronger metal-support interactions improve catalytic activity and stability [153, 157].

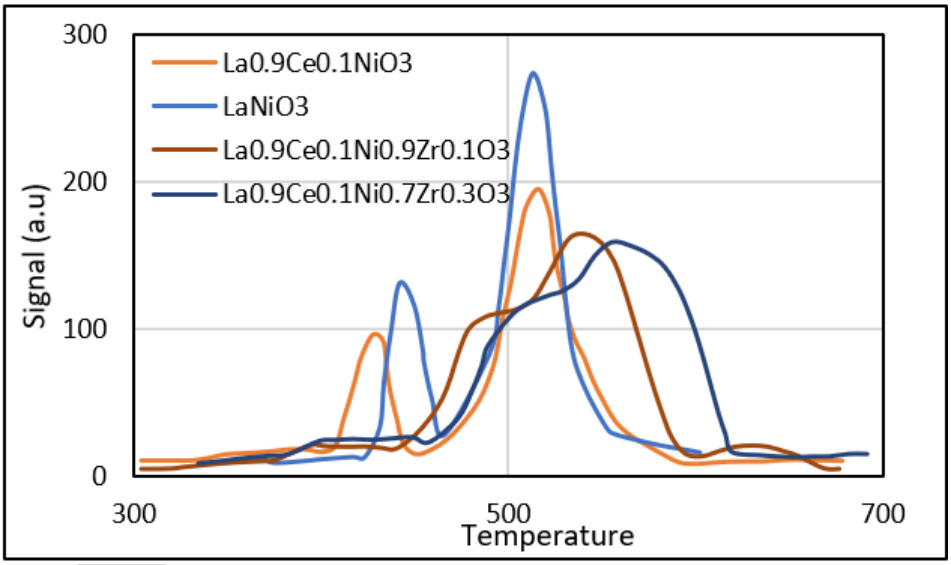

Fig. 13 TPR Profiles of $La_{0.9}Ce_{0.1}Ni_{1-y}Zr_yO_3$ Calcined at 800 ℃ [134]

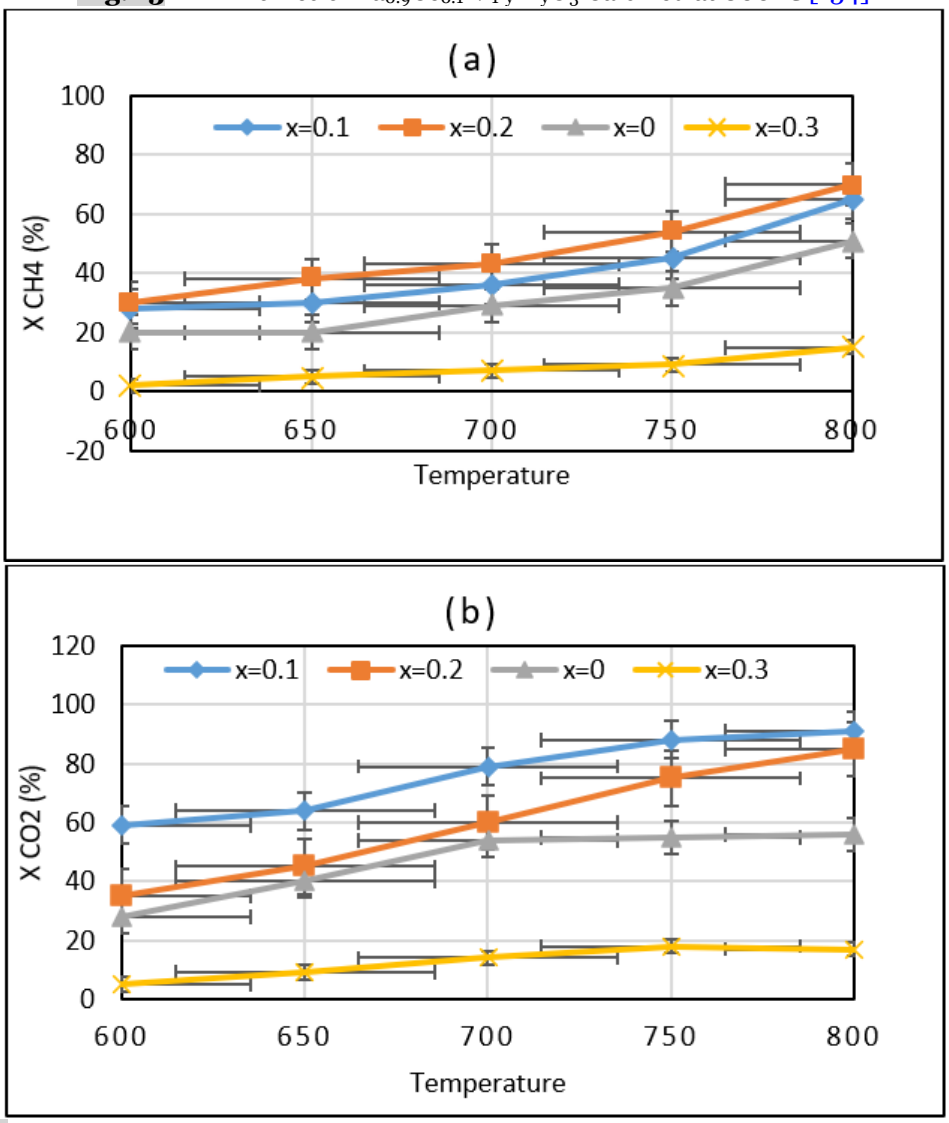

Fig. 14 Conversions of (a) CH_4 and (b) CO_2 as a Function of the Reaction Temperature for $La_{1-x}Ce_xNi_{0.4}Fe_{0.6}O_3$ Samples [150].

Several reports investigated the influence of support additions on La-Ni-based perovskite catalysts. Silica-based mesoporous materials were used as supports with different surface areas and pore diameters. For example, a monolithic silicon carbide foam (SiC-foam) structured nickel and lanthanum oxide (Ni-La_2O_3) nanocomposite catalyst is synthesized and characterized by Zhang et al. [158]. This catalyst significantly improved coke-depositing/Ni-sintering resistance compared to unmodified Ni-La_2O_3 nanocomposites, owing to their homogeneous component distribution and strong Ni-La2O3 interactions. In contrast, Ni-La2O3/alumina (Al2O3) showed better coke and sintering resistance due to enhanced interactions after support addition [158]. In another work by Zhang and Liu [159], $LaNi_{1-x}Co_xO_3$ perovskite (x = 0, 0.05, 0.1, 0.2) was inserted into mesostructured cellular foam silica structure support (MCF). The La_2O_3 and Ni-Co alloy crystallites with close contact were widely distributed throughout the MCF support's windows and cells, as shown in Fig. 15. The La_2O_3 species may serve as both a physical barrier and a CO_2 methanation promoter for the Ni-Co/MCF catalyst, enhancing its stability and catalytic activity. To study the effect of MCF support material, they found that LN0.95C0.05/M exhibits lower agglomeration and better anti-sintering efficiency during lifetime testing than the $LaNi_{1-x}Co_xO_3$ catalyst [159]. A noteworthy study conducted by Sellam et al. [160] included the preparation of $LaNiO_3$ and silica-supported $LaNiO_3$ perovskite catalysts (20$LaNiO_3/SiO_2$ and 40$LaNiO_3/SiO_2$) by the auto-combustion method. The results showed high catalytic activity for 40$LaNiO_3/SiO_2$ and a higher surface area (32 m2/g) than for unsupported $LaNiO_3$ (9 m^2/g). However, there is a considerable decrease in pore volume and size, perhaps due to partial blockage of the original pores by mixed oxides. Also, CH_4 and CO_2 conversions obtained from 40$LaNiO_3/SiO_2$ were higher. The 20$LaNiO_3/SiO_2$ catalyst has a low specific surface area and large NiO particles. This result is due to the development of well-crystallized mixed oxide $LaNiO_3$, which has a low specific surface area and contains free oxide NiO [160]. In a comparative study, Wang et al. [83] used mesoporous carrier supports (SBA-15, MCM-41, and SiO_2) for $LaNiO_3$ perovskite. The catalytic activity tests in Fig. 16 showed that the CH_4 and CO_2 conversion rates for the $LaNiO_3$/MCM-41 and $LaNiO_3$/SBA-15 catalysts were greater than 75% and 70%, respectively. They were comparatively stable at 700 ◦C for 60 hours on stream, with $LaNiO_3$/SBA-15 exhibiting greater stability than $LaNiO_3$/MCM-41. However, $LaNiO_3$/MCM-41 had higher initial catalytic activity due to higher Ni dispersion. On the other hand, $LaNiO_3$/SBA-15 surpassed $LaNiO_3$/MCM-41 in long-term stability, probably due to its stable silica matrix, which impeded nickel species agglomeration and could have been caused by the superior binding effect. In addition, the poorest stability was for bulk $LaNiO_3$ sample. Also, $LaNiO_3$/MCM-41 and $LaNiO_3$/SBA-15 showed similarly H_2 selectivity, but $LaNiO_3/SiO_2$ showed decreased selectivity comparable to the $LaNiO_3$ catalyst [83]. Rivas et al. [161] investigated the performance of $LaNiO_3$, $La_{0.8}Ca_{0.2}NiO_3$, and $La_{0.8}Ca_{0.2}Ni_{0.6}Co_{0.4}O_3$ supported on SBA-15 mesoporous silica host. They applied them as catalyst precursors in the CDRM reaction to increase surface area, inhibit carbon formation, and reduce the high energy consumption required for the reforming reaction. The result of the TPR test Fig. 17 showed a broad and low signal of the perovskite at higher temperatures (maximum at 414 and 622 ℃), revealing a strong interaction between the Ni inside the perovskite and SBA-15 silica-host, resulting in a higher temperature of reduction compared to bulk perovskite. However, a high conversion rates of CH_4 and CO_2 for the supported catalysts were higher than the unsupported ones [161]. From the reported studies we can say that silica-based support materials offer superior properties for the supported catalysts that can influence their catalytic performance.

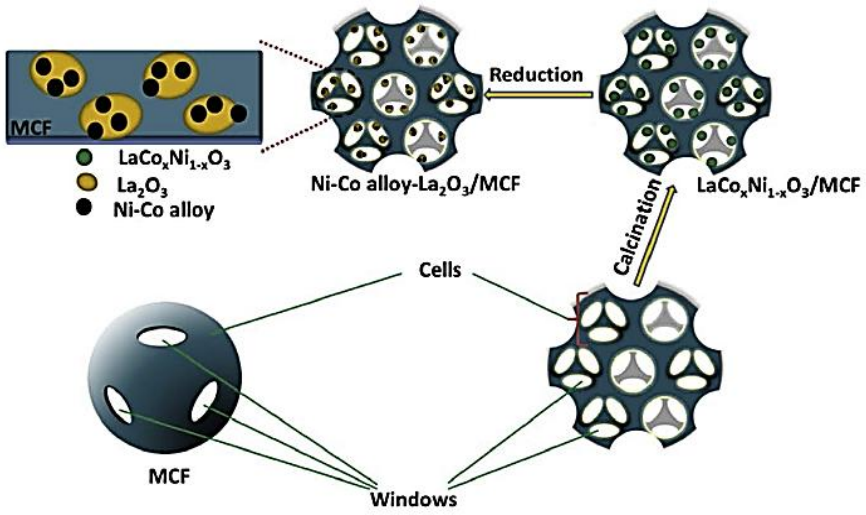

Fig. 15 Schematic Illustration of the $LaNi_{1-x}Co_xO_3$/MCF Catalyst [159].

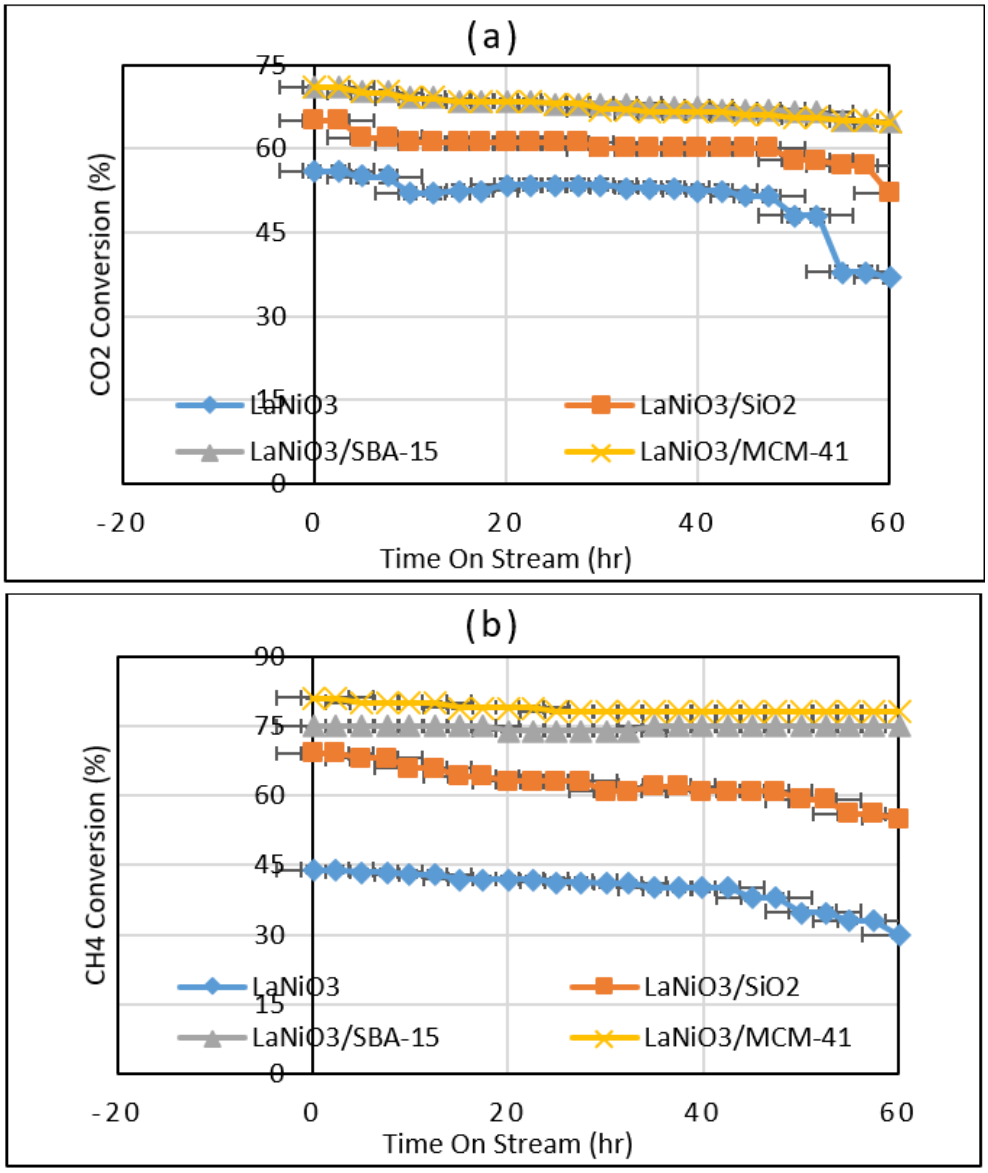

Fig. 16 Catalytic Stability of Bulk and Supported $LaNiO_3$ Catalysts for the CDRM Reaction at 700 ◦C for 60 h, (a) CO_2 Conversion%, (b) CH_4 Conversion% [83].

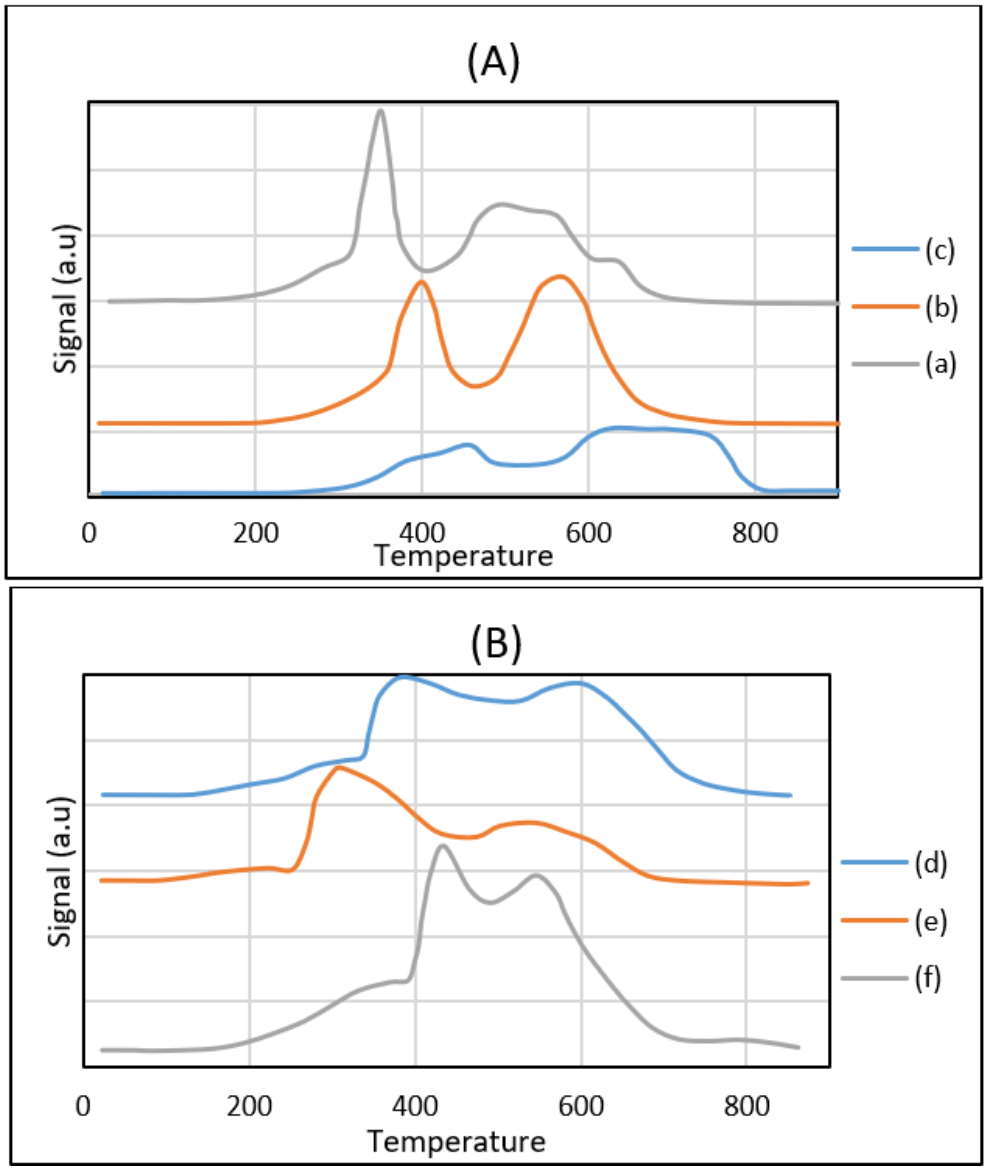

Fig. 17 TPR Profiles of Perovskite-Type Oxides: (A) Bulk and (B) Built-in SBA-15 Mesoporous Silica. (a) $LaNiO_3$; (b) $La_{0.8}Ca_{0.2}NiO_3$; (c) $La_{0.8}Ca_{0.2}Ni_{0.6}Co_{0.4}O_3$; (d) $LaNiO_3$/SBA-15. (e) $La_{0.8}Ca_{0.2}NiO_3$/SBA-15; (f) $La_{0.8}Ca_{0.2}Ni_{0.6}Co_{0.4}O_3$/SBA-15 [161].

Other oxide materials were investigated as supporting materials for La-Ni-based perovskites. Yadav et al. [162] synthesized bulk and supported $LaNi_xFe_{1-x}O_3$ catalysts by sol-gel, incipient wetness impregnation (IWI), and co-precipitation techniques. The results showed that the inclusion of supports (AL_2O_3, SiO_2, MgO) enhanced the dispersion of the perovskite phase, as well as the surface area and pore size of the bulk perovskite catalysts [162]. Messaoudi et al. [156] synthesized bulk La_xNiO_y and supported $La_xNiO_y/MgAl_2O_4$ catalysts using sol-gel and impregnation techniques, with x values of 1 or 2 and y values of 3 or 4. The supported catalysts increased specific surface areas, providing additional basic sites to activate CO2 and increasing nickel dispersion. Also, it exhibited greater activity and stability at 65 hr of reaction than bulk catalysts in the CDRM reaction, due to better nickel dispersion and smaller nickel particles, as well as the beneficial effect of the basic support [156]. A comparative study was conducted by Rabelo-Neto et al. [163], in which $LaNiO_3$, $LaNiO_3/Al_2O_3$, and $LaNiO_3/CeSiO_2$ were synthesized to compare the effect of different oxide supports. Good results were obtained for the supported catalysts, which showed higher catalytic activity and lower carbon deposition than the $LaNiO_3$ catalyst. On the other hand, a very low surface area of almost 10 m2/g was observed for the unsupported $LaNiO_3$ catalyst. The carbon content for $LaNiO_3/Al_2O_3$ was almost one-third of that of unsupported $LaNiO_3$, and $LaNiO_3/CeSiO_2$ exhibited the lowest carbon deposition. This could be attributed to ceria's increased oxygen storage capacity [163]. Moradi et al. [112] studied the effect of γ-Al_2O_3 support on the activity of $LaNiO_3$ perovskite catalyst. They used several Ni wt% (10, 15, 20, and 25) to obtain catalysts with different Ni wt%. The catalytic activities of

the prepared $LaNiO_3/\gamma\text{-}Al_2O_3$ catalysts (10, 15, 20, and 25) for CO_2 and CH_4 were examined. A high nickel crystal dispersion (14–50) nm on the $\gamma\text{-}Al_2O_3$ support for $20LaNiO_3/\ \gamma\text{-}Al_2O_3$ catalyst, since it showed high activity and high resistance to carbon deposition during 75 hours on stream, and the lowest activity was for $10LaNiO_3/\ \gamma\text{-}Al_2O_3$, which means that higher Ni content gives better activity. According to their tests, they also obtained a crystalline LaNiO3 structure well dispersed on $\gamma\text{-}Al_2O_3$, which has an amorphous structure [112]. Based on the literature, the addition of support can be a solution for many La-Ni-based perovskite catalyst problems, such as low surface area, low porosity, and rapid deactivation, since oxide-supported materials provide better catalytic performance with higher nickel dispersion and surface area.

6.CHALLENGES AND FUTURE DIRECTIONS

The primary challenges in the CDRM are considered in this section. Particularly, aspects of the reaction, such as carbon/coke deposition, sintering, and poisoning, and the examination of CDRM deactivation paths, are critical to understanding the efforts made in recent years to synthesize an effective and stable catalyst for this reaction. One of the biggest challenges in developing new, sustainable catalysts for industrial syngas synthesis via the CDRM process is catalyst deactivation. Deactivation, caused by coking, sintering, or poisoning, is a significant concern associated with using nickel-based catalysts in the CDRM reaction. Coking is a phenomenon that occurs when coke covers the catalyst surface due to side reactions. Sintering is a process of accumulation that results in a decrease in the support's surface area or in the crystallite development of the catalytic phases. Poisoning occurs due to strong chemisorption of substances on catalytic sites, which inhibits catalytic activity [164]. Generally, a CDRM reaction is highly endothermic; as a result, numerous side reactions occur, leading to catalyst deactivation. At high temperatures, Ni nanoparticles begin to sinter and expand, reducing the active surface area and leading to carbon deposition. This had a negative effect on Ni-based catalysts during gaseous reactions at high temperatures [85]. Using La-Ni-based perovskite catalysts in the catalytic dry reforming of methane (CDRM) presents several challenges despite their promising catalytic activity. Some of these challenges include:

6.1.Carbon or Coke Formation

Generally, the main challenge for Ni-based catalysts is rapid deactivation caused by coke formation resulting from side reactions during the reforming process. These side reactions include methane cracking (Eq. (a), present an elementary step of CDRM that causes carbon deposition on the surface. Therefore, methane cracking must be considered as one of the basic reactions in the formation of carbonaceous deposits, as well as the deactivation by coking and Boudouard reaction Eq. (b). The carbon produced by these reactions deposits on the metal surface, blocking the active sites. As a result, catalyst deactivation and a decrease in catalyst activity occur [53, 165].

$$CH_4 \rightarrow C_{ads} + 2H_2 \quad \Delta H^{\circ}_{298k} = 75\ kJ/mol \ \textbf{(a)}$$

$$2CO \rightarrow C_{ads} + CO_2 \quad \Delta H^{\circ}_{298} = -172\ kJ/mol \ \textbf{(b)}$$

Given the thermodynamic nature of the CDRM side reactions listed above, operating CDRM over Ni-based catalysts at high temperatures can increase syngas output while reducing carbon formation. The optimum temperature range for minimizing catalyst deactivation due to carbon (coke) production is 870-1040 ℃ [166]. There are three forms of solid carbon deposits on catalytic surfaces, depending on their oxidation temperature ranges: graphitic carbon (C_γ), amorphous carbon (C_β), and carbolic carbon (C_α). These carbonaceous types formed at the following temperature ranges: (>600) ℃, (450-550) ℃, and (300-450) ℃ as shown in Fig. 18 which illustrates the process by which carbon forms, deposits, and transforms on metal-based catalysts. Adsorbed carbon atoms are produced when CO dissociates upon coming into touch with the active metal component, and C_α interacts with its repeating units to form polymerisation into C_β. The more active C_α and C_β are changed into the less active C_γ at high temperatures [45]. Graphitic carbon, which is more difficult to remove than carbolic and amorphous carbons, forms when carbon atoms in close contact with metal nanoparticles undergo graphitization. The distance between a carbon atom and a metal nanoparticle has a significant effect on the degree of graphitization [167].

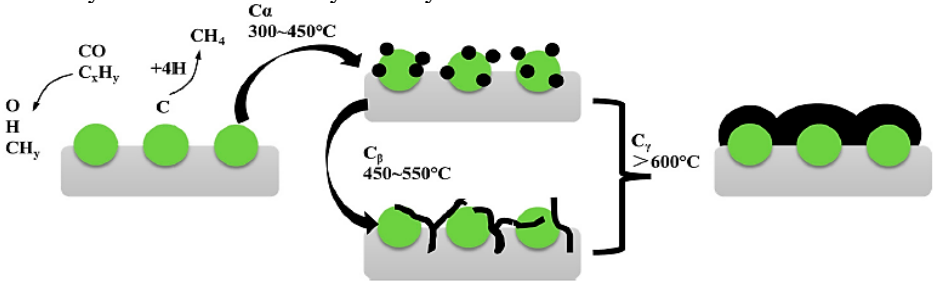

Fig. 18 Forms of Solid Carbon Deposits on Catalytic Surfaces [45].

The coking process in catalyst particles can be extremely complex and follows three mechanisms. First, the coke covers the active sites, isolating them from reactants; second, due to the large concentration gradients of coke precursors in the particle, coke frequently covers the inner surface non-uniformly. Then, as coke agglomerates on the pore surface, it narrows the pores and increases diffusion resistance, further lowering the catalyst particles' activity. Finally, coke can block pores, leading to their complete deactivation [168]. The adsorption of carbonaceous deposits covers the catalyst's active sites on the surface or in the pore channels, making them difficult to access. On the other hand, pore blockage stops reactants from entering the pores and may reduce the amount of carbonaceous deposits on the catalyst [169]. Moreover, the composition of carbonaceous deposits is greatly influenced by the characteristics of the active sites, which dictate the catalyzed reaction steps. In addition, the size of coke molecules, a phenomenon referred to as the confinement effect, is also restricted by the pore size of porous materials, since pore size is an essential property that affects the physicochemical properties of porous materials and the behavior of chemical species within their pores. It can also significantly impact diffusion, phase transitions, catalytic properties, and related phenomena [170]. La-Ni-based perovskite catalysts under the CDRM harsh conditions lead to carbon formation, in which nickel, particularly in its reduced state, assists in the decomposition of methane into carbon atoms [69]. These carbon particles can then settle on the catalyst surface, forming carbonaceous molecules such as graphitic carbon, carbide species, and amorphous carbon [171]. According to some studies, CDRM employed catalysts derived from perovskites to produce hydrogen, but these catalysts also produced filamentous carbon (also known as carbon nanotubes). These studies also provided important and pertinent information because methane decomposition is one of the main drivers of carbon production during methane reforming. For example, in a study reported by De Araujo et al. [172], the $LaNiO_3$ catalyst was prepared by thermal decomposition and used in the CDRM process. The catalyst showed the deposition of filamentous carbon, with 65.7% carbon and a low surface area. However, there was no decrease in activity, even though carbon encapsulation would be expected to reduce it. Nevertheless, the authors suggested incorporating noble metals, such as Ru, to prevent carbon formation. In which $LaNi_{0.8}Ru_{0.2}O_3$ exhibited high resistance to carbon deposition, the carbon percentage was 6.86% [172]. Another study, belonging to Messaoudi et al. [140], examined the effect of partial substitution of Co on the B-site. $LaNi0.9Co0.1O3$ was prepared by the sol-gel method, and the cobalt-substituted catalyst showed enhanced resistance to carbon formation, resulting in improved stability over time and better catalytic activity. This effect is attributed to the synergistic interaction between nickel and cobalt [140]. As with Ni-based catalysts, the incorporation of a second metal enhances carbon-deposition resistance, as reported by Károlyi et al. [173]. They prepared 3wt%Ni/SiO_2 and bimetallic 3wt%Ni-2wt%In/SiO_2 catalysts. Their goal was to modify the Ni/SiO_2 surface area and the carbon-deposition resistance, and this could be achieved by introducing a second metal (indium (In)), known for its resistance to carbon deposition, into the Ni/SiO_2 structure. They found that the 3 wt% Ni-2 wt% In/SiO2 catalyst showed no carbon deposits on its surface compared with Ni/SiO2, due to indium incorporation, which enhanced resistance to carbon deposition by strengthening metal-support interactions [173]. As a result, altering the perovskite structure by substituting A or B sites is an approach to improve catalytic performance [51]. Although the deactivation mechanism involves the accumulation of carbon, it can be reduced in various ways. One method exploits the reversed segregation of Ni into the perovskite lattice, enabling catalyst regeneration via reoxidation [174]. Adding promoters might enhance the coke resistance and catalytic characteristics of Ni-based catalysts. Furthermore, the addition and selection of support materials can improve oxygen mobility while reducing carbon deposition [175]. Employing support materials with an appropriate pore size can confine active metal sites within a restricted structure, thereby inhibiting the formation of many aromatic carbon rings on the catalyst's surface [170]. Since the coke formation depends on the stability of the catalyst's active phase and particle size, it is a highly structure-sensitive reaction. To solve this issue, a metal can be supported on oxides such as La2O3 and CeO2, in which the support type influences catalytic parameters, including active-phase dispersion and nickel particle size [119]. Also, the characteristics of the metal-support interface have a tremendous impact not only on nickel particle stability but also on reactant adsorption, thereby influencing the probability of coke formation. Several researchers have sought to overcome the carbon-deposition problem with Ni-based catalysts. For example, in a study reported by Tian et al. [176], $LaNiO_x$/ZSM-5 was prepared and applied in the CDRM reaction. They compared its performance with that of La_2NiO_4/MCM-41 and La_2NiO_4/γ-Al_2O_3 catalysts to examine differences in catalytic activity. They showed that $LaNiO_x$/ZSM-5 exhibited less coke deposition (5%) over 100 h of reaction. This

behavior, attributed to the formation of La-Ni active species in the ZSM-5 channel or on its surface, was observed as La_2O_3-NiO due to the strong interaction between ZSM-5 and the metal ions (Ni^{2+} and La^{3+}). Hence, choosing the appropriate support is an important consideration during catalyst preparation [176]. La-Ni-based perovskite catalysts show potential for dry methane reforming (CDRM), but carbon deposition remains a challenge. In which carbon deposition rises at higher temperatures [177]. The high temperatures during the CDRM reaction lead to carbon accumulation on Ni-based catalysts, as reported by Buasuk et al. [178]. They conducted a study to examine the effects of different operating parameters associated with the coking process on 5 wt% Ni/Al_2O_3. The results showed that an operating temperature of 600 ℃ led to the production of a large amount of coke. Additionally, at 800 ℃, coke production was higher because the conversion was lower. Thus, an operating temperature of 700 ℃ was the optimum one because no coke production was found [178]. However, the most significant aspect of developing a dry reforming system is producing a catalyst with high resistance to carbon deposition, and perovskite-type oxides have been employed as catalyst precursors for dry reforming because they are known to limit carbon formation. Several studies proved the good performance of perovskite catalysts. An important study was conducted by Moogi et al. [99], prepared $LaCoO_3$ and $LaNiO_3$ catalysts. These catalysts showed strong anti-coking performance due to the formation of the $La_2O_2CO_3$ phase, which can oxidize deposited carbon and act as a self-regenerator, as well as to the high nickel dispersion [99]. Singh et al. [179] prepared a shape-controlled $LaNiO_3$ perovskite catalyst by the modified hydrothermal and precipitation methods. Resulting in three shapes (cubes, spheres, and rods), they aimed to study the effect of $LaNiO_3$ shape on coke deposition. They found that Ni/La_2O_3 depended on the shape and structure of $LaNiO_3$ nanoparticles. Also, after 100 hr of reforming reaction, catalysts derived from $LaNiO_3$ spheres and rods were free of carbon deposition, while the catalysts in cube shape had significant carbon deposition. As a result, active and stable catalysts can be formed by modifying the shape and structure of perovskite catalysts [179]. In summary, cooking is still a major problem, particularly at high temperatures. Deactivation of the La-Ni-perovskite catalyst may result from carbon buildup on the catalyst surface, blocking active sites. Thus, it will be necessary to address carbon deposition by implementing anti-coking methods, such as adjusting the perovskite structure and introducing Ba, which can enhance resistance to deactivation [175]. In addition, catalyst regeneration via reversible segregation of Ni from the perovskite structure during the reduction and oxidation phases enables catalyst regeneration after the coking process [174]. Some strategies are needed to improve the performance of La-Ni-based perovskites. These strategies include altering the A and B sites, designing supported and porous structures to address low surface area, and enhancing metal-support interactions [180].

6.2.Sintering

In many catalytic processes that require high temperatures, metal nanoparticles in a catalyst tend to sinter, growing into larger particles and reducing the catalyst's specific surface area. Hence, catalyst sintering is a thermal process that deactivates catalysts and reduces their surface area by promoting the growth of metal particles. Sintering can also promote pore collapse on active-phase metals. It comes from the kinetically preferred crystallites' surface energy reduction and size-dependent migration on the catalyst support. Generally, sintering occurs when crystallites minimize their surface energy, which is a thermodynamically favorable process. Furthermore, the size-dependent mobility of crystals on different supports plays a key role in sintering [181]. During CDRM at high temperatures, active metal crystallite sintering occurred via two mechanisms on support, as shown in the schematic diagram in Fig. 19 [182]. Crystallite migration in a type of coalescence, and Ostwald ripening [183]. The coalescence mechanism involves two or more metal nanoparticles moving across the surface of a catalyst support by Brownian-like motion until they collide and coalesce into a larger particle. Particles diffuse faster when metal-support interactions are weak, and coalescence is faster when particles are closer together. In the Ostwald ripening mechanism, single metal atoms leave the surface of one nanoparticle and join another nanoparticle via surface diffusion on the support or by moving through the vapor or solution phase. For supported catalysts, the metal atoms move over the support surface rather than through the vapor phase, unless volatile compounds are involved. The active component can lose mass by transferring the metal atoms across the vapor phase. Because larger particles have a lower chemical potential, they are more likely to grow at the expense of smaller particles, which shrink and eventually disappear. However, Ostwald ripening often leads to sintering of supported metal nanoparticles [182].

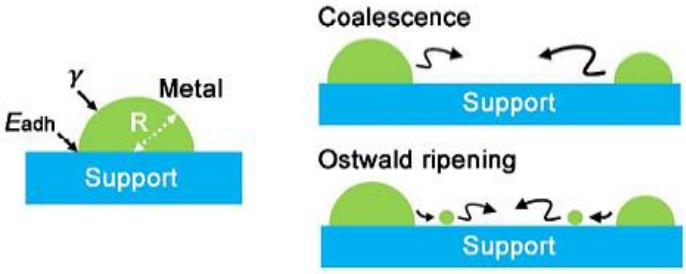

Fig. 19 Ostwald Ripening and Crystallite Migration in Type of Coalescence [182].

The sintering of La-Ni-perovskite catalysts during methane dry reforming (DRM) is a major concern since it affects catalytic performance. Sintering reduces active surface area and catalytic activity, which is principally determined by structural characteristics and the production of metallic nickel during the process [22]. For example, Shahnazi et al. [102] synthesized $LaNiO_3$ perovskite catalysts and used them in the CDRM reaction. The catalyst sintered after 10 hrs of reaction due to its small pore sizes [102]. Du et al. [184] prepared a $LaNiO_3$ perovskite catalyst using the Pechini method and tested its performance in the catalytic dry-reforming reaction. The catalyst underwent sintering during the high-temperature reaction at 700 ℃. Therefore, the high CDRM reaction temperature is the primary cause of sintering, particularly during long reaction times [182]. Various approaches have been studied to improve sintering resistance, such as partial substitution of A or B sites in the perovskite structure [51]. The researchers investigated the partial substitution of Ni by Zn in $LaNiO_3$. This leads to a lower reduction temperature for $LaNiO_3$, resulting in a more stable structure under severe reaction conditions that can inhibit Ni sintering. Because of this property, $LaNi_{1-x}Zn_xO_3$ samples ($x \leq 0.4$) displayed an improvement in catalytic activity and stability in the CDRM reaction compared to $LaNiO_3$. Other researchers stated that La-Ni-derived catalysts produce oxycarbonate species ($La_2O_2CO_3$) during the CDRM reaction, which result from CO2 reacting with La2O3 and can electronically stabilize Ni particles, thereby preventing metal sintering [185]. Su et al. [132] prepared $LaNiO_3$ and $La_{1-x}Ce_xNiO_3$ ($x \leq 0.5$). The catalysts showed good resistance to sintering due to the formation of $La_2O_2CO_3$, which can inhibit sintering through the CDRM reaction [132]. Using appropriate support is one effective way to develop catalysts with improved catalytic activity and resistance to sintering and coking for the CDRM process. Recently, an approach was offered to achieve the goal, utilizing the strong metal-support interaction. Also known as SMSI, it increases the catalyst's resistance to sintering, which requires proper support and appropriate methods to achieve it [186]. For example, Ruan et al. [187] successfully prepared $LaAl_{0.25}Ni_{0.75}O_3$ perovskite catalyst with SBA-15 as a templating agent. The catalyst showed high resistance to sintering due to enhanced interaction between the Ni metal and the support, leading to strong alkalinity and an increase in the number of strong basic sites [187]. Jing et al. [188] prepared $La_{0.8}Ca_{0.2}FeO_3$ and dispersed it on $MgAl_2O_4$ spinel (MgAl) support. The catalyst exhibited improved sintering resistance due to chemical modification of $La_{0.8}Ca_{0.2}FeO_3$ active sites by MgAl [188]. Zhang et al. [189] reported a study on Ni-SBA-15, Ni-KIT-6, and Ni-MCM-41 catalysts that demonstrated high stability, attributed to improved nickel dispersion and metal-support interactions. These results are attributed to the hexagonal arrangement of the large pore size of the mesoporous supports [189]. To conclude, support addition alters the reaction's thermal dynamics, leading to sinter inhibition. Preparing bimetallic catalysts is also an effective way to reduce catalyst sintering compared to monometallic catalysts. Bimetallic catalysts usually show higher activity and improved anti-sintering properties after the addition of a second metal species. Zhang et al. [190] prepared Ni–Me–Al–Mg–O composite, Ni–Me (Me = Co, Fe, Cu, or Mn) bimetallic catalysts. They showed that bimetallic catalysts exhibited superior performance for CDRM compared with monometallic catalysts due to high metal dispersion, strong metal-support interactions, and the formation of stable solid solutions. This enhancement is related to the good interaction between metals, which can reduce the likelihood of metal oxidation. Also, they indicated that the formed MgO phase in the Ni-Mg catalyst has good resistance to sintering due to its high melting point of 3073℃ [190]. The same is true for La-Ni-based perovskite catalysts; the sintering process can be reduced by using a bimetallic perovskite.

6.3.Poisoning

Another major challenge for the CDRM process is the influence of sulfur compounds on catalyst activity. The poisoning of catalysts by sulfur compounds results from strong chemisorption of reactants, products, and contaminants, which can alter the catalyst surface structure and affect catalytic activity. Poisoning has an operating meaning: when a species serves as a poison, its influence on catalyst activity is determined by its adsorption strength in

comparison to the other species [191]. The methane sources are natural gas and biogas, which contain small amounts of H_2S. Catalyst poisoning due to impurity chemisorption on catalyst active sites is unavoidable in methane reforming operations. The surface coverage results from the adsorption of H_2S molecules onto a metal surface. The H_2S subsequently dissociates, forming a bulk sulfide phase that inhibits reactant access to the metal particles' active sites, thereby suppressing surface reactions [167]. Metal sulfides are formed through the chemisorption of sulfur with the active metal of a catalyst, such as nickel, via this equation: $H_2S + Ni \rightarrow Ni\text{-}S + H_2$ [192]. Nickel has been discovered to be more sensitive to sulfur poisoning than other metals. The established mechanism of sulphur poisoning (the chemisorption of sulfur on the Ni surface) means that the catalyst deactivates by sulfidation of the active Ni particles and the creation of Ni-S species that do not participate in the reforming processes [193]. Depending on the poison source, whether it is derived from feed or created during the reaction, mitigation techniques vary greatly. For feed poisons, pre-treatment of the feed solution could be essential before the reaction. For instance, sulfur removal and similar sulfur species (e.g., H_2S, CS_2, SO_4^{2-}, and $S_2O_3^{2-}$) from the feed are common in petrochemical processes. This gives these species the ability to irreversibly poison metal-based catalysts [194]. In the same manner, the presence of specific dissolved cations, such as Na^+, K^+, and Ca^{2+}, can readily contaminate [195] or deplete Brønsted acid sites via ion exchange. In this situation, the feed could be pre-treated with ion-exchange materials to remove these impurities [137]. The high level of H_2S in the feed has also been found to accelerate coke formation on the catalyst by affecting coke gasification reactions. Thus, both the chemisorption of sulfur on metal sites and fouling due to increased coke deposition lead to rapid catalyst deactivation in the CDRM reaction [196]. Generally, Ni-based catalysts are rapidly poisoned and deactivated due to the presence of trace sulfur found in the feed gas, such as natural gas or biogas, the two most prevalent methane sources, with concentrations of H_2S up to 200 ppm. More accurately, the intense chemisorption of sulfur on the nickel-based catalyst in the CDRM will significantly affect the electronic structure around metal atoms, thus affecting the original capacity to dissociate or adsorb molecules. Even when exposed to a low sulfur content, the catalyst can be totally deactivated. Meanwhile, the coverage of nickel-based catalyst by sulfur is a function of both temperature and partial pressure, represented by a ratio of H_2S to H_2 ($P_{(H_2S)}/P_{(H_2)}$), since low temperature and low H_2 partial pressure will speed up the deactivation process [197]. Numerous variables influence the catalyst poisoning during the actual reaction process, including reaction temperature, gas composition, reactor parameters, H_2S concentration, and catalyst type. Thus, due to the exothermic and theoretical reversibility of the sulfur chemisorption process, surface Ni–S can be regenerated by either stopping H2S feeding or elevating the temperature. Spinel Ni catalysts are frequently regenerated via self-regeneration (removal of H_2S from the stream) or calcination at elevated temperatures (>700 °C) in the presence of air. Furthermore, it has been found that at lower temperatures (<700 °C), Ni catalysts poisoned with H_2S are typically not recovered through self-regeneration. However, at higher temperatures, recovery can be achieved simply by eliminating H_2S from the feed stream [198]. An important study on the effect of sulfur concentration in the feed was reported by Gallego et al. They prepared a $LaNiO_3$ perovskite catalyst precursor and tested its tendency to H2S poisoning by subjecting the catalyst to multiple H_2S poisoning processes before and after reduction, during the CDRM reaction, at different H_2S concentrations (0-250 ppm). X-ray diffraction was used to characterize the materials' textural properties [199], and [200] reported that both the metal and the support were deactivated in all cases. Three types of sulfides were observed: lanthanum oxysulfide (La_2O_2S), lanthanum sulfide (LaS_y), and nickel sulfides with varying stoichiometry (Ni_xS_y). The experiments indicated that the catalyst's catalytic activity was affected by H2S poisoning, as higher H2S concentrations increased the deactivation rate [200]. To understand the poisoning mechanism, a noteworthy study reported by Zhu et al. [201] investigated the reaction mechanism and the SO_2 poisoning on the $LaCoO_3/Al_2O_3$ catalyst. They concluded that some sulfates, such as $La2(SO_4)_3$, formed on the catalyst surface. The mechanism represented SO_2 diffusion into $LaCoO_3$ film and reacted with $LaCoO_3$ to produce $La_2(SO_4)_3$, $La_2(SO_3)_3$, $La_2O_2SO_4$, and CoO composites in the internal layer of $LaCoO_3$. The poisoning process destroyed the $LaCoO_3$ structure, leading to a decrease in the catalytic activity. They tested catalyst poisoning at high temperatures and found that high temperatures facilitate the decomposition of sulfates and sulfite species, but the perovskite $LaCoO_3$ phase was destroyed [201]. In addition to H_2S, the poisoning by SO_2 gained special attention due to the residual sulfur present in the fuels, which is unavoidable, and perovskite-type oxide catalysts are affected by SO_2 due to their basic properties, leading to sulfate formation, which could prevent reactants from reaching the perovskite surface and cause a change in the surface properties. Even though, according to current research, SO2 poisoning is still not

addressed, some reports indicate that partial substitution of perovskite cations, such as the incorporation of Ce or noble metals (e.g., Pt, Pd), would inhibit or slow the poisoning process [202]. As well as for poisoning by H_2S, substitution in the B-site or A-site of the $LaNiO_3$ perovskite leads to the creation of a bimetallic catalyst in order to alter its reactivity to H_2S without affecting the CDRM reaction. For example, Gallego et al. [108] investigated the effect of Pr and Ce substitution to obtain $La_{1-x}Ce_xNiO_3$ and $La_{1-x}Pr_xNiO_3$ perovskites. The $La_{0.9}Pr_{0.1}NiO_3$ showed higher catalytic activity and stability with no carbon deposits observed over 100 h of reaction. The reason behind such limited poisoning is the presence of small nickel particles, and the redox chemistry of the Pr_2O_3 produced after reduction treatment [108]. To conclude, the deactivation problems (carbon/coke formation, sintering, and poisoning) observed in Ni-based catalysts, particularly in La-Ni-based perovskite catalysts, during the CDRM reaction are significant challenges that should be addressed to enhance catalytic performance. As the investigation into La-Ni perovskite catalysts for catalytic dry methane reformation (CDRM) is advancing, several promising future directions have been proposed. These include improving catalytic performance through structural alterations, such as partial substitution of Ni or La by various metals, including Mn, which has been demonstrated to enhance structural stability and reduce carbon deposition, thereby improving catalytic performance [102]. And designing supported and porous perovskite catalysts to overcome low surface area issues, as well as investigating innovative perovskite compositions for better catalytic performance in CDRM [53]. In addition, optimizing synthesis processes, such as the co-precipitation method, can yield mesoporous structures that enhance catalyst resistance to coke formation and sintering [203]. CDRM's potential for resource efficiency and CO_2 utilization is one of its main benefits. The method has the potential to reduce climate change by converting two greenhouse gases into beneficial products [204]. Furthermore, CDRM can generate syngas with an H_2/CO ratio of 1, which is challenging to achieve with other techniques and has industrial relevance [205]. Nonetheless, additional research is required in several areas to advance CDRM technology. For example, development is needed to create highly active and stable catalysts capable of withstanding the high temperatures required for CDRM and resisting coking [116].

7.CONCLUSIONS

To achieve the goal of commercializing and applying CDRM for industrial syngas production, it is essential to develop a catalyst system that exhibits superior stability and catalytic performance. According to this review, La-Ni-based perovskite catalysts exhibit notable performance in the CDRM reaction, with both catalytic activity and stability. $LaNiO_3$ perovskites exhibit strong metal-support interactions and a strong affinity to produce $La_2O_2CO_3$ by reacting La_2O_3 with CO_2. The formation of $La_2O_2CO_3$ can enhance carbon removal by providing oxygen species that react with deposited carbon. Partial substitution of A and B sites affects catalytic activity and stability, another benefit of perovskite-type structures.

- Lanthanum-nickel-based perovskite catalysts have demonstrated superior performance in catalytic dry reforming of methane (CDRM) to produce syngas, exhibiting high activity and stability when compared to traditional catalysts.
- Different preparation methods can influence La-Ni-based perovskite surface area and porosity. Higher surface area and appropriate porosity enhance activity by providing more active sites. The hydrothermal and co-precipitation methods yielded the best characteristics for La-Ni-based perovskite catalysts, including high surface area and catalytic performance.
- For A-site partial substitution with alkaline earth metals such as (Ba, Mg, and Ca) gives a perovskite structure with better catalytic activity and stability, as well as lower coke formation than the bulk $LaNiO_3$, and this can be attributed to the presence of oxygen vacancies and the fast movement of lattice oxygen from the bulk toward the surface of the particle. The presence of Ba influences Ni dispersion and accessibility, resulting in a slight increase in particle size. As the alkaline earth components move from higher to lower positions on the periodic table, the concentrations of La_2NiO_4 and NiO phases increase. In some cases, A-site substitution can yield undesirable results, as observed with Zr-doped perovskite, due to difficulties in the reduction process, which may be attributed to the presence of oxides in forms other than perovskite.
- B-site partial substitution increases metal-support interactions; thus, smaller particle sizes can enhance the surface area, crystallinity, and nickel dispersion. B-site substitution with alkaline earth metals (Mg, Sr, Ba, and Ca) yields high methane conversion, especially with Ba, due to the formation of La_2NiO_4 and NiO phases. On the other hand, B-site substitution with other elements (e.g., Fe, Co, Ru, Mn) makes the reduction process more difficult but yields higher activity, as with Ru and Co. The latter was due to the creation of Ni^0-Co^0 particles on the $La_2O_2CO_3$ matrix, which prevents coke formation even under severe conditions. Fe substitution results in

decreased catalytic activity and increased coke resistance compared to Mn-substituted perovskite, which the presence of an Fe-Ni alloy and strong metal-support interactions can explain.

- The support addition plays a key role in producing active perovskite catalysts with high surface area, in which silica-based materials are the best choice as supporting materials for La-Ni-based perovskite catalysts, which can influence their catalytic performance.
- The deactivation challenges reported in La-Ni-based perovskite catalysts during the CDRM process underscore a crucial need for different solutions. Several approaches involve catalyst modification, reaction condition optimization, the addition of a support, or the use of a bimetallic catalyst.

However, numerous challenges remain to be addressed, and more studies are needed to gain a deeper understanding of how to produce a perovskite catalyst with superior activity and stability before considering whether this structure is suitable for industrial DRM applications.

ACKNOWLEDGMENT

The authors confirm that they solely support this manuscript without external sponsorship.

NOMENCLATURE

T	Temperature, °C, k
P	Pressure, atm
GHSV	Gas Hourly Space Velocity, $L.g^{-1}.h^{-1}$, h^{-1}
WHSV	Water Hourly Space Velocity ,$L.g^{-1}.h^{-1}$
ΔH°_{298}	Standard Enthalpy of Formation at 298 °C, kJ/mol
Greek symbols	
C_{α}	Carbolic carbon, $g/g_{cat.}$
C_{β}	Amorphous carbon, $g/g_{cat.}$
C_{γ}	Graphitic carbon, $g/g_{cat.}$
δ	Oxygen deficiency, mol

REFERENCES

[1] Wang J, Azam W. **Natural Resource Scarcity, Fossil Fuel Energy Consumption, and Total Greenhouse Gas Emissions in Top Emitting Countries.** *Geoscience Frontiers* 2024; **15**(2): 101757.

[2] Al-Ali M, Aljbory A, Abdullah GH. **Kinetic Analysis of Catalytic Dry Reforming of Methane Using Ni-ZrO2/MCM-41 Catalyst.** *Tikrit Journal of Engineering Sciences* 2024; **31**(1): 236–250.

[3] Li G, Cheng Z, Huang J, Cui P, Wang H, Wang J. **Dry Reforming of Methane over Ni/Al2O3 Catalysts: Support Morphological Effect on the Coke Resistance.** *Fuel* 2024; **362**: 130855.

[4] Alagha SM, Rushdi S, Al-Sharify ZT, Onyeaka H. **Production of Biodiesel from Caster Oil: Experimental and Optimization Study.** *Tikrit Journal of Engineering Sciences* 2024; **31**(1): 251–261.

[5] Ali AA, Mohammed HN, Ahmed S. **Evaluation of the Performance of CO2 Absorption Using Nanofluid in a Continuous Oscillatory Baffled Column.** *SSRN Electronic Journal* 2024; 4897177.

[6] Yolcan OO. **World Energy Outlook and State of Renewable Energy: 10-Year Evaluation.** *Innovation and Green Development* 2023; **2**(4): 100070.

[7] Dechamps P. **The IEA World Energy Outlook 2022–a Brief Analysis and Implications.** *European Energy & Climate Journal* 2023; **11**(3): 100–103.

[8] Raimi D, Zhu Y, Newell RG, Prest BC, Bergman A. **Global Energy Outlook 2023: Sowing the Seeds of an Energy Transition.** *Resources for the Future* 2023.

[9] Chava R, Snytnikov PV, Amosov YI, Fedorova YV, Snytnikov VY, Parmon VN. **Effect of Calcination Time on the Catalytic Activity of Ni/γ-Al2O3 Cordierite Monolith for Dry Reforming of Biogas.** *International Journal of Hydrogen Energy* 2021; **46**(9): 6341–6357.

[10] Chong CC, Cheng YW, Khaleel M, Jalil AA, Setiabudi HD. **Dry Reforming of Methane over Ni/Dendritic Fibrous SBA-15 (Ni/DFSBA-15): Optimization, Mechanism, and Regeneration Studies.** *International Journal of Hydrogen Energy* 2020; **45**(15): 8507–8525.

[11] Akiki E, Alenazey F, Al-Fatesh AS, Singh SK, Al-Otaibi RL, Al-Zahrani AA, Fakeeha AH. **Production of Hydrogen by Methane Dry Reforming: A Study on the Effect of Cerium and Lanthanum on Ni/MgAl2O4 Catalyst Performance.** *International Journal of Hydrogen Energy* 2020; **45**(41): 21392–21408.

[12] Ranjekar AM, Yadav GD. **Dry Reforming of Methane for Syngas Production: A Review and Assessment of Catalyst Development and Efficacy.** *Journal of the Indian Chemical Society* 2021; **98**(1): 100002.

[13] Hambali HU, Siang TJ, Al-Fatesh AS, Fakeeha AH, Ibrahim AA, Rosid HM, Vo DVN. **Fibrous Spherical Ni-M/ZSM-5 (M: Mg, Ca, Ta, Ga) Catalysts for Methane Dry Reforming: The Interplay between Surface Acidity-Basicity and Coking Resistance.** *International Journal of Energy Research* 2020; **44**(7): 5696–5712.

[14] Li L, Wang S, Sun H, Yan G, Han J. **Methane Dry Reforming over Activated Carbon Supported Ni-Catalysts Prepared by Solid Phase**

Synthesis. *Journal of Cleaner Production* 2020; **274**: 122256.

[15] Jin B, Li S, Liang X. **Enhanced Activity and Stability of MgO-Promoted Ni/Al2O3 Catalyst for Dry Reforming of Methane: Role of MgO.** *Fuel* 2021; **284**: 119082.

[16] Pantaleo G, Parola VL, Testa ML, Venezia AM. **CO2 Reforming of CH4 over SiO2-Supported Ni Catalyst: Effect of Sn as Support and Metal Promoter.** *Industrial & Engineering Chemistry Research* 2021; **60**(51): 18684–18694.

[17] Gürsan C, de Gooyert V. **The Systemic Impact of a Transition Fuel: Does Natural Gas Help or Hinder the Energy Transition?** *Renewable and Sustainable Energy Reviews* 2021; **138**: 110552.

[18] Mehmood I, Ahmad S, Kanwal S, Abbasi J, Hussain M, Jamil M, Al-Fatesh AS, Abasaeed AE. **Carbon Cycle in Response to Global Warming.** *Environment, Climate, Plant and Vegetation Growth* 2020; 1–15.

[19] Saleh SR, Wiheeb AD. **Kinetic Study of Carbon Dioxide Reaction with Binding Organic Liquids.** *Tikrit Journal of Engineering Sciences* 2019; **26**(1): 26–32.

[20] Jassim MN, Mohammed TJ, Karim AMeA. **Experimental Investigation of CO2 Solubility in New Amine-Based Deep Eutectic Solvents.** *Tikrit Journal of Engineering Sciences* 2024; **31**(1): 262–277.

[21] Ali AA, Mohammed H, Ahmed S. **A Comprehensive Review of the Impact of CO2 Emissions on Global Warming and the Potential Using Solar Energy Mitigation.** *Al-Rafidain Journal of Engineering Sciences* 2024; **2**(2): 319–340.

[22] Hussien AG, Polychronopoulou K. **A Review on the Different Aspects and Challenges of the Dry Reforming of Methane (DRM) Reaction.** *Nanomaterials* 2022; **12**(19): 3400.

[23] Dawood F, Anda M, Shafiullah G. **Hydrogen Production for Energy: An Overview.** *International Journal of Hydrogen Energy* 2020; **45**(7): 3847–3869.

[24] Xiong H, Han C, Tang J, Li J, He S, Zhao Y, Zhang J, Li J. **Highly Efficient and Selective Light-Driven Dry Reforming of Methane by a Carbon Exchange Mechanism.** *Journal of the American Chemical Society* 2024; **146**(13): 9465–9475.

[25] Parsapur RK, Chatterjee S, Huang K-W. **The Insignificant Role of Dry Reforming of Methane in CO2 Emission Relief.** *ACS Energy Letters* 2020; **5**(9): 2881–2885.

[26] Grim RG, Huang Z, Guarnieri MT, Ferrell CS, Tao L, Schaidle JA. **Transforming the Carbon Economy: Challenges and Opportunities in the Convergence of Low-Cost Electricity and Reductive CO2 Utilization.** *Energy & Environmental Science* 2020; **13**(2): 472–494.

[27] Abdel-Rahman ZA, Abdullah ZA. **Utilization of CO2 in Flue Gas for Sodium Bicarbonate Production in a Bubble Column.** *Tikrit Journal of Engineering Sciences* 2019; **26**(2): 28–38.

[28] Le Saché E, Reina T. **Analysis of Dry Reforming as Direct Route for Gas Phase CO2 Conversion. The Past, the Present and Future of Catalytic DRM Technologies.** *Progress in Energy and Combustion Science* 2022; **89**: 100970.

[29] Giles A, Valera-Medina A, Marsh R. **Ammonia Sprays for Combustion: A Review.** *Johnson Matthey Technology Review* 2024; **68**(4): 435–451.

[30] Yentekakis IV, Panagiotopoulou P, Artemakis G. **A Review of Recent Efforts to Promote Dry Reforming of Methane (DRM) to Syngas Production Via Bimetallic Catalyst Formulations.** *Applied Catalysis B: Environmental* 2021; **296**: 120210.

[31] Yusuf M, Farooqi AS, Keong LK, Hellgardt K, Abdullah B. **Contemporary Trends in Composite Ni-Based Catalysts for CO2 Reforming of Methane.** *Chemical Engineering Science* 2021; **229**: 116072.

[32] Araiza DG, Arcos DG, Gómez-Cortés A, Díaz G. **Dry Reforming of Methane over Pt-Ni/CeO2 Catalysts: Effect of the Metal Composition on the Stability.** *Catalysis Today* 2021; **360**: 46–54.

[33] de Araújo Moreira TG, de Souza MB, Rodrigues CP, de Lima GF, Santos JVP, Mattos IC, Silva AM. **Highly Stable Low Noble Metal Content Rhodium-Based Catalyst for the Dry Reforming of Methane.** *Fuel* 2021; **287**: 119536.

[34] Gamal A, Eid K, Abdullah AM. **Engineering of Pt-Based Nanostructures for Efficient Dry (CO2) Reforming: Strategy and Mechanism for Rich-Hydrogen Production.** *International Journal of Hydrogen Energy* 2022; **47**(9): 5901–5928.

[35] Wei Y, Zhang W, Gao J. **Trash or Treasure? Sustainable Noble Metal**

Recovery. *Green Chemistry* 2024; **26**(10): 5684–5707.

[36] Chen H, Gao J, Jiang Y, Wang Y, Hu P, Lin Z, Zhang J. **Self-Regenerative Noble Metal Catalysts Supported on High-Entropy Oxides.** *Chemical Communications* 2020; **56**(95): 15056–15059.

[37] Pakhare D, Spivey J. **A Review of Dry (CO2) Reforming of Methane over Noble Metal Catalysts.** *Chemical Society Reviews* 2014; **43**(22): 7813–7837.

[38] Sungmin K, Lee S, Kim J, Kim J, Kim H, Choi M. **Structural Insight into an Atomic Layer Deposition (ALD) Grown Al2O3 Layer on Ni/SiO2: Impact on Catalytic Activity and Stability in Dry Reforming of Methane.** *Journal of CO2 Utilization* 2021; **51**: 101625.

[39] Chaudhary PK, Deo G. **Influence of Particle Size and Metal-Support Interaction on the Catalytic Performance of Ni-Al2O3 Catalysts for the Dry and Oxidative-Dry Reforming of Methane.** *Colloids and Surfaces A: Physicochemical and Engineering Aspects* 2022; **646**: 128973.

[40] Bhalothia D, Tsai TH, Wang CW, Yan C, Chang LY, Lee JF, Chen TY. **Recent Advancements and Future Prospects of Noble Metal-Based Heterogeneous Nanocatalysts for Oxygen Reduction and Hydrogen Evolution Reactions.** *Applied Sciences* 2020; **10**(21): 7708.

[41] Al-Fatesh AS, Fakeeha AH, Ibrahim AA, Khan WY, Khan SU, Al-Otaibi RL, Abasaeed AE. **Reforming of Methane: Effects of Active Metals, Supports, and Promoters.** *Catalysis Reviews* 2023; **65**: 1–99.

[42] Nguyen T, Luu CL, Phan HP, Nguyen PA, Van Nguyen TT. **Methane Dry Reforming over Nickel-Based Catalysts: Insight into the Support Effect and Reaction Kinetics.** *Reaction Kinetics, Mechanisms and Catalysis* 2020; **131**(2): 707–735.

[43] Vogt ET, Fu D, Weckhuysen BM. **Carbon Deposit Analysis in Catalyst Deactivation, Regeneration, and Rejuvenation.** *Angewandte Chemie International Edition* 2023; **62**(29): e202300319.

[44] Nirmal Kumar S, Appari S, Kuncharam BVR. **Techniques for Overcoming Sulfur Poisoning of Catalyst Employed in Hydrocarbon Reforming.** *Catalysis Surveys from Asia* 2021; **25**(4): 362–388.

[45] Yuan B, Yang H, Han J, Wang S, Yan G. **Deactivation Mechanism and Anti-Deactivation Measures of Metal Catalyst in the Dry Reforming of Methane: A Review.** *Atmosphere* 2023; **14**(5): 770.

[46] Zheng J, Impeng S, Liu J, Deng J, Zhang D. **Mo Promoting Ni-Based Catalysts Confined by Halloysite Nanotubes for Dry Reforming of Methane: Insight of Coking and H2S Poisoning Resistance.** *Applied Catalysis B: Environmental* 2024; **342**: 123369.

[47] Ruh T, Schrenk F, Berger T, Rameshan C. **Perovskite-Type Oxides as Exsolution Catalysts in CO2 Utilization.** *Encyclopedia* 2023; **3**(4): 1461–1473.

[48] Sheshko T, Serov A, Kryuchkova T, Sheshko N, Kapokova L, Zvereva I. **Gd-Co-Fe Perovskite Mixed Oxides as Catalysts for Dry Reforming of Methane.** *Sustainable Chemistry and Pharmacy* 2022; **30**: 100897.

[49] Shao Z, Huang Y, Chen H, Mao X, Wu H, Xu Z. **Synthesis, Characterization, and Methanol Steam Reforming Performance for Hydrogen Production on Perovskite-Type Oxides SrCo1-xCuxO3-δ.** *Ceramics International* 2022; **48**(8): 11836–11848.

[50] Cao Y, Lin H, Lin J, Lin S, Lin W, Xu J. **Recent Advances in Perovskite Oxides as Electrode Materials for Supercapacitors.** *Chemical Communications* 2021; **57**(19): 2343–2355.

[51] Georgiadis AG, Charisiou ND, Goula MA. **A Mini-Review on Lanthanum–Nickel-Based Perovskite-Derived Catalysts for Hydrogen Production Via the Dry Reforming of Methane (DRM).** *Catalysts* 2023; **13**(10): 1357.

[52] Muñoz H, Korili S, Gil A. **Recent Advances in the Application of Ni-Perovskite-Based Catalysts for the Dry Reforming of Methane.** *Catalysis Reviews* 2024; **66**: 1–53.

[53] Bian Z, Das S, Kawi S. **A Review on Perovskite Catalysts for Reforming of Methane to Hydrogen Production.** *Renewable and Sustainable Energy Reviews* 2020; **134**: 110291.

[54] Goto Y, Morikawa A, Tanabe T, Iwasaki M. **Effect of Al Substitution on Structural Stability and Topotactic Oxygen Release Rate of LaNi1–xAlxO3 with Perovskite Structure.** *ACS Applied Energy Materials* 2019; **2**(11): 7943–7952.

[55] Spennati E, Riani P, Garbarino G. **A Perspective of Lanthanide Promoted Ni-Catalysts for CO2 Hydrogenation to Methane:**

Catalytic Activity and Open Challenges. *Catalysis Today* 2023; **418**: 114131.

[56] Lider A, Kudiiarov V, Elman R, Pushilina N, Belykh S, Bordulev Y. **Materials and Techniques for Hydrogen Separation from Methane-Containing Gas Mixtures.** *International Journal of Hydrogen Energy* 2023; **48**(73): 28390–28411.

[57] Volkova N, Baklanova Y, Tarakina N, Chupakhina L, Gorshkov V, Baklanov M. **Influence of A- and B-Site Substitutions on Crystal Structure and Oxygen Content in Air-Prepared Ba1−xPrxFe1−yCoyO3−δ Perovskites.** *Journal of Alloys and Compounds* 2021; **860**: 158438.

[58] Nguyen DL, Van Huy N, Van Nguyen TT, Nguyen T. **Methane Dry Reforming: A Catalyst Challenge Awaits.** *Journal of Industrial and Engineering Chemistry* 2024; **131**: 1–18.

[59] Georgiadis AG, Siakavelas G, Charisiou ND, Baklavaridis A, Polychronopoulou K, Goula MA. **An Experimental and Theoretical Approach for the Biogas Dry Reforming Reaction Using Perovskite-Derived La0.8X0.2NiO3-δ Catalysts (X= Sm, Pr, Ce).** *Renewable Energy* 2024; **227**: 120511.

[60] Wang K, Chen H, Xu X, Shao Z, Wang W. **Perovskite Oxide Catalysts for Advanced Oxidation Reactions.** *Advanced Functional Materials* 2021; **31**(30): 2102089.

[61] Ahmad N, Wahab R, Manoharadas S, Alrayes BF, Alharthi F. **Utilization of Greenhouse Gases for Syngas Production by Dry Reforming Process Using Reduced BaNiO3 Perovskite as a Catalyst.** *Sustainability* 2021; **13**(24): 13855.

[62] Ahmad N, Fakeeha AH, Al-Fatesh AS, Al-Otaibi RL, Alharthi FA, Abasaeed AE. **Syngas Production Via CO2 Reforming of Methane over SrNiO3 and CeNiO3 Perovskites.** *Energies* 2021; **14**(10): 2928.

[63] Osazuwa OU, Setiabudi HD, Rasid RA, Cheng CK. **Syngas Production Via Methane Dry Reforming: A Novel Application of SmCoO3 Perovskite Catalyst.** *Journal of Natural Gas Science and Engineering* 2017; **37**: 435–448.

[64] Johansson T, Gracia JM, van Vegten N, Baiker A, Niemantsverdriet JW. **Characterization of LaRhO3 Perovskites for Dry (CO2) Reforming of Methane (DRM).** *Chemical Papers* 2014; **68**(9): 1208–1218.

[65] Kapokova L, Pavlova S, Bunina RV, Alikina GE, Sadykov VA, Krieger TA, Mirodatos C. **Dry Reforming of Methane over LnFe0.7Ni0.3O3-δ Perovskites: Influence of Ln Nature.** *Catalysis Today* 2011; **164**(1): 227–233.

[66] Gallego GS, Mondragón F, Barrault J, Tatibouët J-M, Batiot-Dupeyrat C. **CO2 Reforming of CH4 over La–Ni Based Perovskite Precursors.** *Applied Catalysis A: General* 2006; **311**: 164–171.

[67] Choudhary VR, Mondal KC, Mamman AS, Joshi UA. **Carbon-Free Dry Reforming of Methane to Syngas over NdCoO3 Perovskite-Type Mixed Metal Oxide Catalyst.** *Catalysis Letters* 2005; **100**(3-4): 271–276.

[68] Batiot-Dupeyrat C, Gallego GAS, Mondragon F, Barrault J, Tatibouët J-M. **CO2 Reforming of Methane over LaNiO3 as Precursor Material.** *Catalysis Today* 2005; **107**: 474–480.

[69] Pino L, Italiano C, Laganà M, Vita A, Recupero V. **Kinetic Study of the Methane Dry (CO2) Reforming Reaction over the Ce0.70La0.20Ni0.10O2−δ Catalyst.** *Catalysis Science & Technology* 2020; **10**(8): 2652–2662.

[70] Zhang T, Liu Q. **Perovskite LaNiO3 Nanocrystals inside Mesostructured Cellular Foam Silica: High Catalytic Activity and Stability for CO2 Methanation.** *Energy Technology* 2020; **8**(3): 1901164.

[71] Pérez-Camacho MN, Abu-Dahrieh J, Goguet A, Sun K, Rooney D. **Self-Cleaning Perovskite Type Catalysts for the Dry Reforming of Methane.** *Chinese Journal of Catalysis* 2014; **35**(8): 1337–1346.

[72] Allabergenova R, Serov AY, Kapokova L, Serova V, Zvereva I. **Synthesis, Characterization, and Catalytic Properties of GdCoO3 for Dry Reforming of Methane.** *Journal of the Serbian Chemical Society* 2024; **89**(1): 51–61.

[73] Lanre MS, Al-Fatesh AS, Ibrahim AA, Singh S, Abasaeed AE, Fakeeha AH. **Modification of CeNi0.9Zr0.1O3 Perovskite Catalyst by Partially Substituting Yttrium with Zirconia in Dry Reforming of Methane.** *Materials* 2022; **15**(10): 3564.

[74] Alenazey F, Akiki E, Al-Fatesh AS, Al-Zahrani AA, Abasaeed AE, Fakeeha AH. **A Novel Carbon-Resistant Perovskite Catalyst for Hydrogen Production Using Methane Dry Reforming.** *Topics in Catalysis* 2021; **64**(5-6): 348–356.

[75] Anil C, Modak JM, Madras G. **Syngas Production Via CO2 Reforming of Methane over Noble Metal (Ru, Pt, and Pd) Doped LaAlO3 Perovskite Catalyst.** *Molecular Catalysis* 2020; **484**: 110805.

[76] Yafarova LV, Silyukov OI, Kryuchkova TA, Sheshko TF, Zvereva IA. **The Influence of Fe Substitution in GdFeO3 on Redox and Catalytic Properties.** *Russian Journal of Physical Chemistry A* 2020; **94**(13): 2679–2684.

[77] Oh JH, Baek SW, Hayat MA, Kim J, Kim H, Choi M. **Importance of Exsolution in Transition-Metal (Co, Rh, and Ir)-Doped LaCrO3 Perovskite Catalysts for Boosting Dry Reforming of CH4 Using CO2 for Hydrogen Production.** *Industrial & Engineering Chemistry Research* 2019; **58**(16): 6385–6393.

[78] Yafarova LV, Silyukov OI, Sheshko TF, Zvereva IA. **Sol–Gel Synthesis and Investigation of Catalysts on the Basis of Perovskite-Type Oxides GdMO3 (M = Fe, Co).** *Journal of Sol-Gel Science and Technology* 2019; **92**(2): 264–272.

[79] De Caprariis B, De Filippis P, Hernandez AD, Scarsella M, Verdone N. **Rh, Ru and Pt Ternary Perovskites Type Oxides BaZr(1-X)MexO3 for Methane Dry Reforming.** *Applied Catalysis A: General* 2016; **517**: 47–55.

[80] Gurav HR, Bobade R, Das VL, Chilukuri S. **Carbon Dioxide Reforming of Methane over Ruthenium Substituted Strontium Titanate Perovskite Catalysts.** *Applied Catalysis A: General* 2012; **421**: 130–136.

[81] Khalesi A, Arandiyan HR, Parvari M. **Effects of Lanthanum Substitution by Strontium and Calcium in La-Ni-Al Perovskite Oxides in Dry Reforming of Methane.** *Chinese Journal of Catalysis* 2008; **29**(10): 960–968.

[82] Zhang Z, Zhang Y, Liu L. **Role and Mechanism of Calcium-Based Catalysts for Methane Dry Reforming: A Review.** *Fuel* 2024; **355**: 129329.

[83] Wang N, Yu X, Wang Y, Chu W, Liu M. **A Comparison Study on Methane Dry Reforming with Carbon Dioxide over LaNiO3 Perovskite Catalysts Supported on Mesoporous SBA-15, MCM-41 and Silica Carrier.** *Catalysis Today* 2013; **212**: 98–107.

[84] Shahnazi A, Firoozi S. **Improving the Catalytic Performance of LaNiO3 Perovskite by Manganese Substitution Via Ultrasonic Spray Pyrolysis for Dry Reforming of Methane.** *Journal of CO2 Utilization* 2021; **45**: 101455.

[85] Omari E, Makhloufi S, Omari M. **Preparation by Sol–Gel Method and Characterization of Co-Doped LaNiO3 Perovskite.** *Journal of Inorganic and Organometallic Polymers and Materials* 2017; **27**(5): 1466–1472.

[86] Özbay N, Şahin RZ. **Preparation and Characterization of LaMnO3 and LaNiO3 Perovskite Type Oxides by the Hydrothermal Synthesis Method.** *AIP Conference Proceedings* 2017; **1833**: 020050.

[87] Touahra F, Halliche D, Bachari K, Saadi A. **Enhanced Catalytic Behaviour of Surface Dispersed Nickel on LaCuO3 Perovskite in the Production of Syngas: An Expedient Approach to Carbon Resistance During CO2 Reforming of Methane.** *International Journal of Hydrogen Energy* 2016; **41**(4): 2477–2486.

[88] Sagar TV, Lingaiah N, Sai Prasad PS, Tušar NN, Štangar UL. **Influence of Method of Preparation on the Activity of La–Ni–Ce Mixed Oxide Catalysts for Dry Reforming of Methane.** *RSC Advances* 2014; **4**(91): 50226–50232.

[89] Chawla SK, George M, Patel F, Patel S. **Production of Synthesis Gas by Carbon Dioxide Reforming of Methane over Nickel Based and Perovskite Catalysts.** *Procedia Engineering* 2013; **51**: 461–466.

[90] Pereñiguez R, Gonzalez-delaCruz VM, Caballero A, Holgado JP. **LaNiO3 as a Precursor of Ni/La2O3 for CO2 Reforming of CH4: Effect of the Presence of an Amorphous NiO Phase.** *Applied Catalysis B: Environmental* 2012; **123**: 324–332.

[91] Rivas ME, Fierro JLG, Peña MA, Griboval-Constant A. **Structural Features and Performance of LaNi1-xRhxO3 System for the Dry Reforming of Methane.** *Applied Catalysis A: General* 2008; **344**(1-2): 10–19.

[92] Ramadhan HA, Al-Ali M. **Optimizing Catalyst Performance: A Study of Support Addition Effects on La-Ni-Mn in Catalytic Dry Reforming of Methane.** *Kufa Journal of Engineering* 2025; **16**(4).

[93] Navas D, Fuentes S, Castro-Alvarez A, Chavez-Angel E. **Review on Sol-Gel Synthesis of Perovskite and Oxide Nanomaterials.** *Gels* 2021; **7**(4): 275.

[94] Muñoz HJ, Korili SA, Gil A. **Progress and Recent Strategies in the Synthesis and Catalytic**

Applications of Perovskites Based on Lanthanum and Aluminum. *Materials* 2022; **15**(9): 3288.

[95] Singh S, Zubenko D, Rosen BA. **Influence of LaNiO3 Shape on Its Solid-Phase Crystallization into Coke-Free Reforming Catalysts.** *ACS Catalysis* 2016; **6**(7): 4199–4205.

[96] Wang X, Zhu L, Zhuo Y, Zhu Y, Wang S. **Enhancement of CO2 Methanation over La-Modified Ni/SBA-15 Catalysts Prepared by Different Doping Methods.** *ACS Sustainable Chemistry & Engineering* 2019; **7**(17): 14647–14660.

[97] Mosinska M, Maniukiewicz W, Szynkowska-Jozwik MI, Mierczynski P. **Influence of NiO/La2O3 Catalyst Preparation Method on Its Reactivity in the Oxy-Steam Reforming of LNG Process.** *Catalysts* 2021; **11**(10): 1174.

[98] Silva P, Soares AB. **Lanthanum Based High Surface Area Perovskite-Type Oxide and Application in CO and Propane Combustion.** *Eclética Química* 2009; **34**: 31–38.

[99] Moogi S, Moogi S, Lingaiah N, Lee S, Tušar NN, Štangar UL. **Influence of Catalyst Synthesis Methods on Anti-Coking Strength of Perovskites Derived Catalysts in Biogas Dry Reforming for Syngas Production.** *Chemical Engineering Journal* 2022; **437**: 135348.

[100] Barros BS, Kulesza J, Melo DMdA, Kienneman A. **Nickel-Based Catalyst Precursor Prepared Via Microwave-Induced Combustion Method: Thermodynamics of Synthesis and Performance in Dry Reforming of CH4.** *Materials Research* 2015; **18**(4): 732–739.

[101] Osti A, Rizzato L, Cavazzani J, Glisenti A. **Optimizing Citrate Combustion Synthesis of A-Site-Deficient La, Mn-Based Perovskites: Application for Catalytic CH4 Combustion in Stoichiometric Conditions.** *Catalysts* 2023; **13**(8): 1177.

[102] Shahnazi A, Firoozi S. **Mesoporous LaNi1-xMnxO3 Perovskite with Enhanced Catalytic Performance and Coke Resistance Synthesized Via Glycine-Assisted Spray Pyrolysis for Methane Dry Reforming.** *Molecular Catalysis* 2023; **547**: 113320.

[103] Lovell EC, Scott J, Amal R. **Ni-SiO2 Catalysts for the Carbon Dioxide Reforming of Methane: Varying Support Properties by Flame Spray Pyrolysis.** *Molecules* 2015; **20**(3): 4594–4609.

[104] Sagar TV, Lingaiah N, Sai Prasad PS, Tušar NN, Štangar UL. **Phase Transformation of Zr-Modified LaNiO3 Perovskite Materials: Effect of CO2 Reforming of Methane to Syngas.** *Catalysts* 2024; **14**(1): 91.

[105] Jahangiri A, Pahlavanzadeh H, Aghabozorg H. **Synthesis, Characterization and Catalytic Study of Sm Doped LaNiO3 Nanoparticles in Reforming of Methane with CO2 and O2.** *International Journal of Hydrogen Energy* 2012; **37**(13): 9977–9984.

[106] Rivas ME, Fierro JLG, Peña MA, Griboval-Constant A. **Structural Features and Performance of LaNi1-xRhxO3 System for the Dry Reforming of Methane.** *Applied Catalysis A: General* 2008; **344**(1-2): 10–19.

[107] Provendier H, Petit C, Estournes C, Libs S, Kiennemann A. **Stabilisation of Active Nickel Catalysts in Partial Oxidation of Methane to Synthesis Gas by Iron Addition.** *Applied Catalysis A: General* 1999; **180**(1-2): 163–173.

[108] Gallego GS, Marín JG, Batiot-Dupeyrat C, Barrault J, Mondragón F. **Influence of Pr and Ce in Dry Methane Reforming Catalysts Produced from La1-XAxNiO3-δ Perovskites.** *Applied Catalysis A: General* 2009; **369**(1-2): 97–103.

[109] Lima SMd, Assaf JM. **Synthesis and Characterization of LaNiO3, LaNi (1-x) Fe xO3 and LaNi (1-x) Co xO3 Perovskite Oxides for Catalysis Application.** *Materials Research* 2002; **5**: 329–335.

[110] Blasco J, Garcia J, de Teresa JM, Ibarra MR, Perez J, Algarabel PA, Marquina C, Ritter C. **Synthesis and Structural Study of LaNi1-xMnxO3+δ Perovskites.** *Journal of Physics and Chemistry of Solids* 2002; **63**(5): 781–792.

[111] Mousavi M, Pour AN. **Performance and Structural Features of LaNi0.5Co0.5O3 Perovskite Oxides for the Dry Reforming of Methane: Influence of the Preparation Method.** *New Journal of Chemistry* 2019; **43**(27): 10763–10773.

[112] Moradi G, Hemmati H, Rahmanzadeh M. **Preparation of a LaNiO3/γ-Al2O3 Catalyst and Its Performance in Dry Reforming of**

Methane. *Chemical Engineering & Technology* 2013; **36**(4): 575–580.

[113] Moradi P, Parvari M. **Preparation of Lanthanum-Nickel-Aluminium Perovskite Systems and Their Application in Methane-Reforming Reactions.** *Applied Catalysis A: General* 2006; **304**: 120–128.

[114] Grabchenko M, Pantaleo G, Puleo F, Vodyankina O, Liotta LF. **Ni/La2O3 Catalysts for Dry Reforming of Methane: Effect of La2O3 Synthesis Conditions on the Structural Properties and Catalytic Performances.** *International Journal of Hydrogen Energy* 2021; **46**(11): 7939–7953.

[115] Ramon AP, Gonçalves RV, Zanchet D, Bueno JM. **In Situ Study of Low-Temperature Dry Reforming of Methane over La2Ce2O7 and LaNiO3 Mixed Oxides.** *Applied Catalysis B: Environmental* 2022; **315**: 121528.

[116] Cao D, Li K, Wu Y, Zhu Y, Wang S, Chen S. **Dry Reforming of Methane by La2NiO4 Perovskite Oxide, Part I: Preparation and Characterization of the Samples.** *Fuel Processing Technology* 2023; **247**: 107765.

[117] Trevisani SAC, Batista MdS. **CO2 Reforming of CH4 over M (Ca, Ba, Sr)xLa1-xNiO3 Perovskites Used as Coke Resistant Catalyst Precursor.** *Chemical Industry and Chemical Engineering Quarterly* 2021; **27**(3): 215–221.

[118] Abasaeed AE, Ibrahim AA, Fakeeha AH, Al-Fatesh AS. **The Influence of Ni Stability, Redox, and Lattice Oxygen Capacity on Catalytic Hydrogen Production Via Methane Dry Reforming in Innovative Metal Oxide Systems.** *Energy Science & Engineering* 2023; **11**(4): 1436–1450.

[119] da Silva BC, Lima JGS, Santos JCP, Melo DMA, Barros BS, Melo MAF. **Perovskite-Type Catalysts Based on Nickel Applied in the Oxy-CO2 Reforming of CH4: Effect of Catalyst Nature and Operative Conditions.** *Catalysis Today* 2021; **369**: 19–30.

[120] Li K, Wang H, Wang S, Zhu Y, Chen S, Wu Y. **Ordered Mesoporous Ni/La2O3 Catalysts with Interfacial Synergism Towards CO2 Activation in Dry Reforming of Methane.** *Applied Catalysis B: Environmental* 2019; **259**: 118092.

[121] Oliveira AAS, Barros BS, Melo DMdA, Melo MAF. **One-Step Synthesis of LaNiO3 with Chitosan for Dry Reforming of Methane.** *International Journal of Hydrogen Energy* 2018; **43**(20): 9696–9704.

[122] Dacquin JP, Dujardin C, Granger P, Dhainaut J. **Efficient and Robust Reforming Catalyst in Severe Reaction Conditions by Nanoprecursor Reduction in Confined Space.** *ChemSusChem* 2014; **7**(2): 631–637.

[123] de Araujo GC, de Lima SM, Assaf JM, Peña MA, Garcia-Fierro JL. **Catalytic Evaluation of Perovskite-Type Oxide LaNi1-xRuxO3 in Methane Dry Reforming.** *Catalysis Today* 2008; **133**: 129–135.

[124] Lima SM, Assaf JM, Peña MA, Fierro JLG. **Structural Features of La1-xCexNiO3 Mixed Oxides and Performance for the Dry Reforming of Methane.** *Applied Catalysis A: General* 2006; **311**: 94–104.

[125] Dhillon GS, Cao G, Yi N. **The Role of Fe in Ni-Fe/TiO2 Catalysts for the Dry Reforming of Methane.** *Catalysts* 2023; **13**(8): 1171.

[126] Gonzalez-Delacruz VM, Ternero F, Pereñíguez R, Caballero A, Holgado JP. **Study of Nanostructured Ni/CeO2 Catalysts Prepared by Combustion Synthesis in Dry Reforming of Methane.** *Applied Catalysis A: General* 2010; **384**(1-2): 1–9.

[127] Zhang Z, Verykios XE, MacDonald SM, Affrossman S. **Comparative Study of Carbon Dioxide Reforming of Methane to Synthesis Gas over Ni/La2O3 and Conventional Nickel-Based Catalysts.** *The Journal of Physical Chemistry* 1996; **100**(2): 744–754.

[128] de Caprariis B, De Filippis P, Petrullo A, Scarsella M. **Methane Dry Reforming over Nickel Perovsikite Catalysts.** *Chemical Engineering Transactions* 2015; **43**: 991–996.

[129] Touahra F, Chebout R, Lerari D, Halliche D, Bachari K. **Role of the Nanoparticles of Cu-Co Alloy Derived from Perovskite in Dry Reforming of Methane.** *Energy* 2019; **171**: 465–474.

[130] Nair MM, Kaliaguine S. **Structured Catalysts for Dry Reforming of Methane.** *New Journal of Chemistry* 2016; **40**(5): 4049–4060.

[131] Moradi GR, Rahmanzadeh M, Khosravian F. **The Effects of Partial Substitution of Ni by Zn in LaNiO3 Perovskite Catalyst for Methane Dry Reforming.** *Journal of CO2 Utilization* 2014; **6**: 7–11.

[132] Su Y-J, Pan K-L, Chang M-B. **Modifying Perovskite-Type Oxide Catalyst LaNiO3 with Ce for Carbon Dioxide Reforming of Methane.** *International Journal of Hydrogen Energy* 2014; **39**(10): 4917–4925.

[133] Lima S, Assaf J, Peña M, Fierro J. **Structural Features of La1−xCexNiO3 Mixed Oxides and Performance for the Dry Reforming of Methane.** *Applied Catalysis A: General* 2006; **311**: 94–104.

[134] Dezvareh P, Aghabozorg H, Sadr MH, Zare K. **Synthesis, Characterization, and Catalytic Performance of La1-xCexNi1-yZryO3 Perovskite Nanocatalysts in Dry Reforming of Methane.** *Oriental Journal of Chemistry* 2018; **34**(3): 1469–1478.

[135] Gomes R, Santos JVP, Mattos IC, Silva AM. **Dry Reforming of Methane over NiLa-Based Catalysts: Influence of Synthesis Method and Ba Addition on Catalytic Properties and Stability.** *Catalysts* 2019; **9**(4): 313.

[136] De Lima SM, Peña MA, Fierro JLG, Assaf JM. **La1−x Cax NiO3 Perovskite Oxides: Characterization and Catalytic Reactivity in Dry Reforming of Methane.** *Catalysis Letters* 2008; **124**(3-4): 195–203.

[137] Talaie N, Sadr MH, Aghabozorg H, Zare K. **Synthesis and Application of LaNiO3 Perovskite-Type Nanocatalyst with Zr for Carbon Dioxide Reforming of Methane.** *Oriental Journal of Chemistry* 2016; **32**(5): 2723–2731.

[138] Moradi GR, Rahmanzadeh M. **The Influence of Partial Substitution of Alkaline Earth with La in the LaNiO3 Perovskite Catalyst.** *Catalysis Communications* 2012; **26**: 169–172.

[139] Bhavani AG, Wani TA. **Synthesis of Single Phase LaMn1-xNixO3 Perovskite Material.** *Materials Letters: X* 2021; **12**: 100107.

[140] Messaoudi H, Thomas S, Slyemi S, Djaidja A, Barama A. **Syngas Production Via Methane Dry Reforming over La-Ni-Co and La-Ni-Cu Catalysts with Spinel and Perovskite Structures.** *Bulletin of Chemical Reaction Engineering & Catalysis* 2020; **15**(3): 885–897.

[141] Valderrama G, Kiennemann A, Goldwasser MR. **Dry Reforming of CH4 over Solid Solutions of LaNi1-xCoxO3.** *Catalysis Today* 2008; **133**: 142–148.

[142] Song X, Ma L, Ma S, Xu L, Dong H. **Effects of Fe Partial Substitution of La2NiO4/LaNiO3 Catalyst Precursors Prepared by Wet Impregnation Method for the Dry Reforming of Methane.** *Applied Catalysis A: General* 2016; **526**: 132–138.

[143] Jahangiri A, Aghabozorg H, Pahlavanzadeh H. **Effects of Fe Substitutions by Ni in La–Ni–O Perovskite-Type Oxides in Reforming of Methane with CO2 and O2.** *International Journal of Hydrogen Energy* 2013; **38**(25): 10407–10416.

[144] De Lima SM, Assaf JM. **Ni–Fe Catalysts Based on Perovskite-Type Oxides for Dry Reforming of Methane to Syngas.** *Catalysis Letters* 2006; **108**(1-2): 63–70.

[145] Zhao T, Xie S, Chen Y, Fu L, Liu Y, Zhang J. **Influences of Ni Content on the Microstructural and Catalytic Properties of Perovskite LaNixCr1-xO3 for Dry Reforming of Methane.** *Catalysts* 2022; **12**(10): 1143.

[146] Komarala EP, Komissarov I, Rosen BA. **Effect of Fe and Mn Substitution in LaNiO3 on Exsolution, Activity, and Stability for Methane Dry Reforming.** *Catalysts* 2019; **10**(1): 27.

[147] Kim WY, Moon DJ, Lim SS, Noh Y-s, Yang E-h. **Reduced Perovskite LaNiO3 Catalysts Modified with Co and Mn for Low Coke Formation in Dry Reforming of Methane.** *Applied Catalysis A: General* 2019; **575**: 198–203.

[148] Nuvula S, Sagar TV, Valluri DK, Prasad PSS. **Selective Substitution of Ni by Ti in LaNiO3 Perovskites: A Parameter Governing the Oxy-Carbon Dioxide Reforming of Methane.** *International Journal of Hydrogen Energy* 2018; **43**(8): 4136–4142.

[149] Das S, Das S, Das S, Kawi S. **Effect of Partial Fe Substitution in La0.9Sr0.1NiO3 Perovskite-Derived Catalysts on the Reaction Mechanism of Methane Dry Reforming.** *ACS Catalysis* 2020; **10**(21): 12466–12486.

[150] Dezvareh P, Sadr MH, Aghabozorg H, Zare K. **Dry Reforming of Methane over Various Doping Level of Ce on La1-xCexNi0.4Fe0.6O3 Perovskite Nano Catalyst.** *Oriental Journal of Chemistry* 2016; **32**(5): 2549–2558.

[151] Yang E-h, Noh Y-s, Ramesh S, Lim SS, Moon DJ. **The Effect of Promoters in La0.9M0.1Ni0.5Fe0.5O3 (M= Sr, Ca) Perovskite Catalysts on Dry Reforming of Methane.** *Fuel Processing Technology* 2015; **134**: 404–413.

[152] Sutthiumporn K, Maneerung T, Kathiraser Y, Kawi S. **CO2 Dry-Reforming of Methane over La0.8Sr0.2Ni0.8M0.2O3 Perovskite (M= Bi, Co, Cr, Cu, Fe): Roles of Lattice Oxygen on C–H Activation and Carbon Suppression.** *International Journal of Hydrogen Energy* 2012; **37**(15): 11195–11207.

[153] da Silva PRN, Zanoteli K. **Evaluation of Nickel Catalysts Supported in Dry Methane Reform Aiming at Hydrogen Production/Case of Supports: SiO2, La2O3 MCM-41, and Al2O3.** *Orbital: The Electronic Journal of Chemistry* 2020; **12**(3): 140–147.

[154] Liu C, Gao J, Zhang Z, Wang Y, Hu P, Lin Z. **Catalytic Steam Reforming of in-Situ Tar from Rice Husk over MCM-41 Supported LaNiO3 to Produce Hydrogen Rich Syngas.** *Renewable Energy* 2020; **161**: 408–418.

[155] Han Y, Wen B, Zhu M, Dai B. **Lanthanum Incorporated in MCM-41 and Its Application as a Support for a Stable Ni-Based Methanation Catalyst.** *Journal of Rare Earths* 2018; **36**(4): 367–373.

[156] Messaoudi H, Thomas S, Djaidja A, Slyemi S, Barama A. **Study of LaxNiOy and LaxNiOy/MgAl2O4 Catalysts in Dry Reforming of Methane.** *Journal of CO2 Utilization* 2018; **24**: 40–49.

[157] Yan X, Zhang X, Han S, Zhang J, Li Y, Zhao Y. **A Comparison of Al2O3 and SiO2 Supported Ni-Based Catalysts in Their Performance for the Dry Reforming of Methane.** *Journal of Fuel Chemistry and Technology* 2019; **47**(2): 199–208.

[158] Zhang Z, Zhao G, Bi G, Guo Y, Xie J. **Monolithic SiC-Foam Supported Ni-La2O3 Composites for Dry Reforming of Methane with Enhanced Carbon Resistance.** *Fuel Processing Technology* 2021; **212**: 106627.

[159] Zhang T, Liu Q. **Mesostructured Cellular Foam Silica Supported Bimetallic LaNi1-xCoxO3 Catalyst for CO2 Methanation.** *International Journal of Hydrogen Energy* 2020; **45**(7): 4417–4426.

[160] Sellam D, Sellam D, Siari A. **CO2 Reforming of Methane over LaNiO3 Perovskite Supported Catalysts: Influence of Silica Support.** *Bulletin of Chemical Reaction Engineering & Catalysis* 2019; **14**(3): 568–578.

[161] Rivas I, Alvarez J, Pietri E, Pérez-Zurita MJ, Goldwasser MR. **Perovskite-Type Oxides in Methane Dry Reforming: Effect of Their Incorporation into a Mesoporous SBA-15 Silica-Host.** *Catalysis Today* 2010; **149**(3-4): 388–393.

[162] Yadav PK, Das T. **Production of Syngas from Carbon Dioxide Reforming of Methane by Using LaNixFe1-xO3 Perovskite Type Catalysts.** *International Journal of Hydrogen Energy* 2019; **44**(3): 1659–1670.

[163] Rabelo-Neto RC, Rabelo-Neto RC, Barros BS. **CO2 Reforming of Methane over Supported LaNiO3 Perovskite-Type Oxides.** *Applied Catalysis B: Environmental* 2018; **221**: 349–361.

[164] Meloni E, Martino M, Palma V. **A Short Review on Ni Based Catalysts and Related Engineering Issues for Methane Steam Reforming.** *Catalysts* 2020; **10**(3): 352.

[165] Argyle MD, Bartholomew CH. **Heterogeneous Catalyst Deactivation and Regeneration: A Review.** *Catalysts* 2015; **5**(1): 145–269.

[166] Seo HO. **Recent Scientific Progress on Developing Supported Ni Catalysts for Dry (CO2) Reforming of Methane.** *Catalysts* 2018; **8**(3): 110.

[167] Minh DP, Pham X-H, Siang TJ, Vo D-VN. **Review on the Catalytic Tri-Reforming of Methane-Part I: Impact of Operating Conditions, Catalyst Deactivation and Regeneration.** *Applied Catalysis A: General* 2021; **621**: 118202.

[168] Ye G, Zhou X, Chen D, Yuan W, Ye G. **Optimizing Catalyst Pore Network Structure in the Presence of Deactivation by Coking.** *AIChE Journal* 2019; **65**(10): e16687.

[169] Lin X, Fan Y, Shi G, Liu H, Bao X. **Coking and Deactivation Behavior of HZSM-5 Zeolite-Based FCC Gasoline Hydro-Upgrading Catalyst.** *Energy & Fuels* 2007; **21**(5): 2517–2524.

[170] Bitters JS, Gunasooriya GTT, Saavedra J, Beswick RR, Savara A, Chorkendorff I, Jaramillo TF, Nørskov JK **Utilizing Bimetallic Catalysts to Mitigate Coke Formation in Dry Reforming**

of Methane *Journal of Energy Chemistry* 2022;**68**:124-142

[171] Dipu AL **Methane Decomposition into Cox-Free Hydrogen over a Ni-Based Catalyst: An Overview** *International Journal of Energy Research* 2021;**45**(7):9858-9877

[172] de Araujo GC, de Souza Sarmento R, da Silva MAC, de Oliveira FJ Santos, Rodrigues MG **Catalytic Evaluation of Perovskite-Type Oxide Lani1–Xruxo3 in Methane Dry Reforming** *Catalysis Today* 2008;**133**:129-135

[173] Károlyi J, Németh M, Evangelisti C, Somodi F, Baán K, Varga T, Sáfrán G, Paszti Z, Tompos A, Pápai I **Carbon Dioxide Reforming of Methane over Ni–in/Sio2 Catalyst without Coke Formation** *Journal of Industrial and Engineering Chemistry* 2018;**58**:189-201

[174] Steiger P, Nachtegaal M, Kröcher O, Ferri D **Reversible Segregation of Ni in Lafeo. 8nio. 2o3±Δ During Coke Removal** *ChemCatChem* 2018;**10**(19):4456-4464

[175] Umar A, Thotyl MO **Perovskite Modified Catalysts with Improved Coke Resistance for Steam Reforming of Glycerol to Renewable Hydrogen Fuel** *GCB Bioenergy* 2023;**15**(6):791-804

[176] Tian L, Zhao XH, Liu BS, Zhang WD **Preparation of an Industrial Ni-Based Catalyst and Investigation on Ch4 /Co2 Reforming to Syngas** *Energy & Fuels* 2009;**23**(2):607-612

[177] Cao D, Wen J, Wang M, Li J, Luo J, Jiang L **Carbon Deposition Properties and Regeneration Performance of La2nio4 Perovskite Oxide for Dry Reforming of Methane** *Journal of Environmental Chemical Engineering* 2023;**11**(5):111022

[178] Buasuk N, Ngamcharussrivichai C, Chollier MJ, Faungnawakij K, Powell J, Wittayakun J **Deactivating and Non-Deactivating Coking Found on Ni-Based Catalysts During Combined Steam-Dry Reforming of Methane** *Topics in Catalysis* 2021;**64**(5-6):357-370

[179] Singh S, Zubenko D, Rosen BA **Influence of Lanio3 Shape on Its Solid-Phase Crystallization into Coke-Free Reforming Catalysts** *ACS Catalysis* 2016;**6**(7):4199-4205

[180] Li S, Gong J **Strategies for Improving the Performance and Stability of Ni-Based Catalysts for Reforming Reactions** *Chemical Society Reviews* 2014;**43**(21):7245-7256

[181] Tsakoumis NE, Rønning M, Borg Ø, Rytter E, Holmen A **Deactivation of Cobalt Based Fischer–Tropsch Catalysts: A Review** *Catalysis Today* 2010;**154**(3-4):162-182

[182] Dai Y, Lu P, Cao Z, Campbell CT, Xia Y **The Physical Chemistry and Materials Science Behind Sinter-Resistant Catalysts** *Chemical Society Reviews* 2018;**47**(12):4314-4331

[183] Abdulrasheed A, Jalil AA, Gambo Y, Ibrahim M, Hambali HU, Shahul Hamid MY **A Review on Catalyst Development for Dry Reforming of Methane to Syngas: Recent Advances** *Renewable and Sustainable Energy Reviews* 2019;**108**:175-193

[184] Du Z, Cui H, Zhang K, Cheng Y, Chen J, Gong X, Qin Q **Development of Stable Lao. 9ceo. 1nio3 Perovskite Catalyst for Enhanced Photothermochemical Dry Reforming of Methane** *Journal of CO2 Utilization* 2023;**67**:102317

[185] Toniolo FS, Schmal M **Improvement of Catalytic Performance of Perovskites by Partial Substitution of Cations and Supporting on High Surface Area Materials** *Perovskite Materials-Synthesis, Characterisation, Properties, and Applications: IntechOpen* 2016;167-184

[186] Han C, Zhu X, Chen B, Wang X **A Strategy of Constructing the Ni@ Silicalite-1 Catalyst Structure with High Activity and Resistance to Sintering and Carbon Deposition for Dry Reforming of Methane** *Fuel* 2024;**355**:129548

[187] Ruan Y, Du J, Lu L, Wang J, He J, Chen L, Tian Z **Mesoporous Laalo. 25nio. 7503 Perovskite Catalyst Using Sba-15 as Templating Agent for Methane Dry Reforming** *Microporous and Mesoporous Materials* 2020;**303**:110278

[188] Jing Z, Li H, Jiang Z **The Chemical Interaction of Support and Active Phase in Sintering Resistant Lao. 8cao. 2feo3 Perovskite Catalysts** *Fuel* 2019;**243**:322-331

[189] Zhang Q, Zhang T, Shi Y, Zhao B, Wang M, Liu Q, Jiao Z, Zhang P, Shao G **A Sintering and Carbon-Resistant Ni-Sba-15 Catalyst Prepared by Solid-State Grinding Method for Dry Reforming of Methane** *Journal of CO2 Utilization* 2017;**17**:10-19

[190] Zhang J, Wang H, Dalai AK **Development of Stable Bimetallic Catalysts for Carbon Dioxide**

Reforming of Methane *Journal of Catalysis* 2007;**249**(2):300-310

[191] Rodríguez E, Félix G, Ancheyta J, Trejo F **Modeling of Hydrotreating Catalyst Deactivation for Heavy Oil Hydrocarbons** *Fuel* 2018;**225**:118-133

[192] Chen X, Li S, Ho S, City B, Wu J, Wang S, Gong J **Dry Reforming of Model Biogas on a Ni/Sio2 Catalyst: Overall Performance and Mechanisms of Sulfur Poisoning and Regeneration** *ACS Sustainable Chemistry & Engineering* 2017;**5**(11):10248-10257

[193] Capa A, Maroño M, Sánchez-Hervás JM, Lopez-Velasco A, Rodriguez JJ **Effect of H2s on Biogas Sorption Enhanced Steam Reforming Using a Pd/Ni-Co Catalyst and Dolomite as a Sorbent** *Chemical Engineering Journal* 2023;**476**:146803

[194] Hammond C **Intensification Studies of Heterogeneous Catalysts: Probing and Overcoming Catalyst Deactivation During Liquid Phase Operation** *Green Chemistry* 2017;**19**(12):2711-2728

[195] Al-Ali MI, Abdullah AI, Mohammad AM, Al-Ali KI **Estimating and Modelling the Interrelationships between Physicochemical Pollutants of Samara Drug Factory Wastewater** *European Journal of Scientific Research* 2011;**61**(2):230-241

[196] Das S, Lim KH, Gani TZ, Aksari S, Kawi S **Bi-Functional Ceo2 Coated Nico-Mgal Core-Shell Catalyst with High Activity and Resistance to Coke and H2s Poisoning in Methane Dry Reforming** *Applied Catalysis B: Environmental* 2023;**323**:122141

[197] Li D, Zhu Q, Bao Z, Jin L, Hu H **New Insight and Countermeasure for Sulfur Poisoning on Nickel-Based Catalysts During Dry Reforming of Methane** *Fuel* 2024;**363**:131045

[198] Dega FB, Abatzoglou N **H2s Poisoning and Regeneration of a Nickel Spinellized Catalyst Prepared from Waste Metallurgical Residues, During Dry Autothermal Methane Reforming** *Catalysis Letters* 2019;**149**(6):1730-1742

[199] Al-Ali M, Alsamarrae A, Salih KI, Pairsamy S, Parthasarathy R **Impacts of the High Moisture Wet Granulation and Novel Microwave Drying on the Textural Characteristics of Pharmaceutical Particles** *IOP Conference Series: Materials Science and Engineering* 2018;**454**(1):012056

[200] Gallego J, Batiot-Dupeyrat C, Barrault J, Mondragón F **Severe Deactivation of a Lanio3 Perovskite-Type Catalyst Precursor with H2S During Methane Dry Reforming** *Energy & Fuels* 2009;**23**(10):4883-4886

[201] Zhu Y, Tan R, Feng J, Ji S, Cao L **The Reaction and Poisoning Mechanism of So2 and Perovskite Lacoo3 Film Model Catalysts** *Applied Catalysis A: General* 2001;**209**(1-2):71-77

[202] Zhu J, Li H, Zhong L, Xiao P, Xu X, Yang X, Wei Z, Luo J **Perovskite Oxides: Preparation, Characterizations, and Applications in Heterogeneous Catalysis** *ACS Catalysis* 2014;**4**(9):2917-2940

[203] Shah M, Al Mesfer MK, Danish M **Design and Optimization of Ni–Fe–La Based Catalytic System for Co2 Utilization for Sustainable Syngas Production Via Dry Reforming of Methane** *Journal of the Energy Institute* 2023;**110**:101346

[204] Lei Y, Ye J, García-Antón J, Liu H **Recent Advances in the Built-in Electric-Field-Assisted Photocatalytic Dry Reforming of Methane** *Chinese Journal of Catalysis* 2023;**53**:72-101

[205] Sandoval-Diaz LE, Schlögl R, Lunkenbein T **Quo Vadis Dry Reforming of Methane?—a Review on Its Chemical, Environmental, and Industrial Prospects** *Catalysts* 2022;**12**(5):465